THE SYNTHESIS AND CHARACTERIZATION OF NEW HIGHER NUCLEARITY ARENE-RUTHENIUM-SULFUR CLUSTERS

A thesis presented in partial
fulfillment of the requirements
for the degree of
Master of Science
in Chemistry
at

Massey University
New Zealand

Libei Guo
1999

ACKNOLEDGEMENT

I sincerely thank my supervisor Dr. A. H. Wright for his encouragement, guidance and assistance in many ways and for his many hours spent on reading and modifying my thesis. I also thank him for helping me with my papers and many other things in my life. He is not only a very good supervisor in my research work, but also a very good friend of mine.

Thank you very much:

Professor A. M. Brodie and Associate Professor D. R. K. Harding for encouraging me to continue my study and research work.

Dr. A. H. Wright and Dr. A. K. Burrell for their assistance with calculations on quantum study and X ray crystallography.
Dr. P. Edward for his assistance with ^{1}H NMR spectrometry.

Members of the Chemistry Department with help and advice; in particular Mr. W. Campbell, Mr. G. H. Freeman and Mr. T. W. G. Canton.

ABBREVIATION

cymene	1-isopropyl-4-methylcymene
en	ethylenediamine
NMR	nuclear magnetic resonance
$NNEt_2en$	N,N-diethylethylenediamine
DBU	1,8-diazabicyclo[5.4.0]undec-7-ene
IR	infra red
THF	tetrahydrofurane
DMSO	dimethylsulphoxide
TLC	thin layer chromatography
Me	methyl
Cp	cyclopentadiene
Cp'	$CH_3C_5H_5$ (MeCp)
Cp*	Me_5Cp
Ph	phenyl
Triphos	$MeC(CH_2PPh_2)_3$
Cod	cycloocta-1,5-diene
'S_4'	1,2-bis((2-mercaptophenyl)thiol)ethane(2-))
Cl_4-cat	tetrachlorocatecholate
^iPr	isopropyl

ABSTRACT

This thesis describes a project investigating the synthesis and characterization of new higher nuclearity arene-ruthenium-sulfur clusters and arene-ruthenium-nitrogen complexes.

The thesis is divided into four chapters, with the introduction in Chapter One. The synthesis and characterization of new higher nuclearity arene-ruthenium-sulfur clusters are described in Chapter Two. These include two novel clusters, $[Ru_5S_4(cymene)_4](PF_6)_2$, $[Ru_4(S_2)(SO)(cymene)_4](PF_6)_2$ and one known cluster, $[Ru_3S_2(cymene)_3](PF_6)_2$. The X-ray crystallographic structures of these three arene-ruthenium-sulfur clusters are discussed in detail including how the number of valence electrons influences the structure, how the solid state structure and single crystal structure effect each other and how the structures determine the chemical shifts and other characters of the clusters. The unusual signals of these three clusters on ^1H NMR spectra are discussed carefully. The mechanisms of formation of arene-ruthenium-sulfur clusters are described in detail. Some electrochemistry and calculations (quantum chemistry) are also involved.

The synthesis and characterization of arene-ruthenium-nitrogen complexes are described in Chapter Three. These include two new mono-nuclear complexes, $[RuCl_2(NH_3)(cymene)]$, $[Ru(NH_3)_3(cymene)](PF_6)_2$, one novel amide dimer $[RuCl(NH_2)(cymene)]_2$ and one known complex, $[RuCl(NH_3)_2(cymene)]PF_6$. The mechanisms of reactions in which they are formed are also discussed. In Chapter Four, the experimental data is presented.

The X ray crystallography of $[Ru_5S_4(cymene)_4](PF_6)_2$, $[Ru_4(S_2)(SO)(cymene)_4](PF_6)_2$, $[RuCl_2(NH_3)(cymene)]$ and $[RuCl(NH_2)(cymene)]_2$ is described in detail.

INDEX

LIST OF TABLES AND SCHEMES

LIST OF FIGURES

CHAPTER ONE INTRODUCTION

1.1. Transition metal compounds

This thesis is about the synthesis and characterization of high nuclearity ruthenium clusters. The underlying motivations for examining these clusters include:

The first involves industrial catalysis and the multi-electron redox reactions such as Haber-Bosch process (nitrogen reduction) and fuel processing (hydrodesulfurization, dehydration and hydrocracking).

Catalysts lie at the heart of many industrial processes. The more efficient the catalysts used, the more energy can be saved in the processes of production. A major task of industrial chemistry is to discover new efficient catalysts. Transition metals and their clusters are one of the main choices for catalysts in industries.

The second involves modeling catalysis either in industrial or biological systems such as nitrogen reduction, hydrogenation and other reductions of small molecules.

Insights into the mechanisms of catalytic processes offer the prospect of improved efficiency. In multi- component heterogeneous sulfide catalysts, many phases are present and more than one active site or reaction channel may be present, and it is not always clear which phase catalyses a given channel.

The chemistry of transition metal clusters has helped the study of heterogeneous catalysts and catalysis in several ways: modes of ligands binding to multi-metallic sites are often the same on metal surfaces and clusters. Ligand transformations on clusters may be used as guides to similar reaction pathways on the heterogeneous catalysts. Clusters may be adsorbed on surfaces and their surface reactions may then be followed by various spectroscopic techniques. The surface structure formed in these reactions are often catalytically active and comparison of the activity of catalysts prepared from organometallic cluster precursors with that of conventionally prepared catalysts can give useful information on active site structures and reaction mechanisms.

In biochemical systems, the exact mechanisms of nitrogenases and hydrogenases are still not yet clear after almost one century of study. Many scientists have tried to mimic and model these processes using synthesized transition metal clusters in vitro, and a lot of progress has been made particularly during the last forty years. It both benefits the mechanisms that are studied in biological and chemical systems at the same time.

1.1.1. Transition metal clusters

Transition metal clusters are complexes that contain a group of transition metal atoms joined by metal-metal bonds. A cluster usually contains a metal core surrounded by ligands.

Sometimes, this definition is not very strict. Compounds without metal-metal bonds but with metals joined together by ligands as bridges are also called clusters. For example, iron-sulfur cubane cluster, $[Fe_4S_4]$ is the basic component of many metalloproteins, in which iron atoms are joined together by sulfur atoms as bridges. (Figure 1)

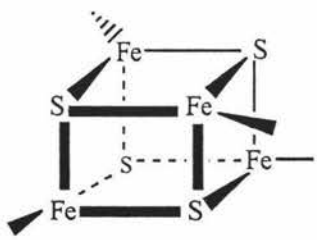

Fe_4S_4 cluster

Figure 1 Structure of cubane cluster $[Fe_4S_4]$

There are several aspects that effect the characters of the cluster:

- The type of the metal atoms

Ruthenium and iron are both group eight transition metals, and it is well known that ruthenium has a greater catalytic ability than iron. For example, ruthenium has been

known to be 45 times as catalytically active as its equivalent weight of iron as promoters in Haber-Bosch process [1].

New complexes of lanthanide and actinide series are providing new insights. Early in 1992, Evans et al. found that a mononuclear η^2-hydrazine samarium complex could be synthesized by protonation of an $[N_2H_2]^{2-}$ complex, which is an interesting models for the mechanism of dinitrogen reduction [2].

- The number of the metal atoms

The number of the metal atoms in the cluster may influence the ability of the electron storing and transferring, and hence the ability of catalysis. Poly-nuclear clusters usually have more ability of catalysis than corresponding mono- or bi-nuclear complexes. For example, in a recent quantum chemical study, Siegbahn et.al suggested that N_2 is four-coordinated in the $[Fe_8S_9]^{2-}$ cluster rather than two-coordinated in the dimer model. Add two hydrogen atoms on the bridging sulfur between the cubanes, making all iron atoms Fe^{2+}, opens up the cavity for easy access of N_2. Hence N_2 is activated with N-N distance of 1.21 Å in the cluster model rather than 1.19 Å in the dimer model [3], which indicates that N_2 is more activated in the cluster model.

- The way that metal atoms joined together

It is different in characters of metal-metal multiple bonds compared to metal-metal single bonds. For example, $[Os_3(CO)_{12}]$ is more stable comparing to its unsaturated derivative $[H_2Os_3(CO)_{10}]$ that contains one Os=Os double bond in it [97].

- The type of the ligands and the mode of coordination

Complexes with sulfur-containing ligands have different properties to those with other element containing ligands, such as oxygen and nitrogen. For example, $[(benzene)_4Ru_4(OH)_4]^{4+}$ (Figure 2a) decomposes with hydroxide ion to corresponding bi-nuclear complexes [4], while $[(p\text{-cymene})_3Ru_3S_2]^{2+}$ just opens one of its metal-metal bond when it gains two electrons giving $[(p\text{-cymene})_3Ru_3S_2]$ (Scheme 1) [5].

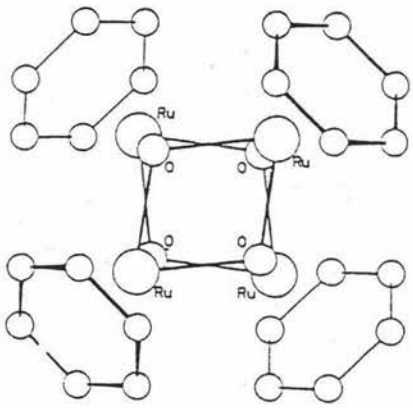

a

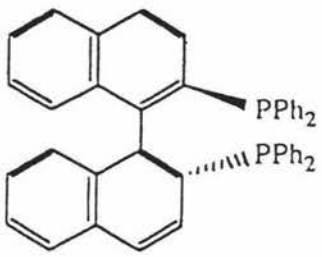

(S)-(-)BINAP

b

Figure 2 Structures of $[(benzene)_4Ru_4(OH)]^{4+}$ and a stereo ligand (S)-(-)BINAP

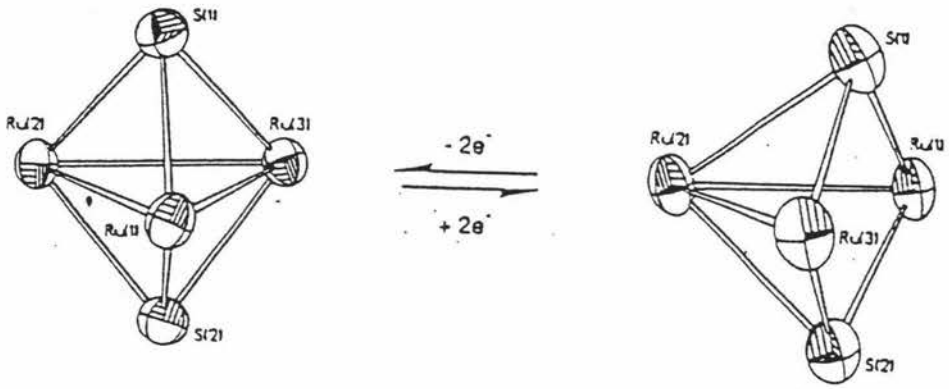

Scheme 1 Structure change from $[Ru_3S_2(cymene)_3]^{2+}$ to $[Ru_3S_2(cymene)_3]$

Some complexes have been known with stereo-ligands, which have been designed for special use of catalysts. For example, BINAP-Ru(2+) [6] that produced by treatment of $[RuCl_2(\eta^6\text{-benzene})]_2$ with (R)- or (S)-BINAP (Figure 2b) can catalyze the highly enantioselective hydrogenation of functionalized ketones [6] and β-substituted (E)-β-(acylamino)acrylic acid [7].

This project has been targeted at the synthesis and characterization of ruthenium sulfur (also some nitrogen) arene clusters with the underlying aim of modeling catalysis and testing for catalytic activity.

1.1.2. Iron-sulfur clusters and their functions

The well known iron sulfur clusters can offer insights that are helpful to design the aim compounds, and one possible role for ruthenium sulfur clusters might be to model the mechanism of iron clusters in biological systems, vise versa.

Models that uncover the mechanistic detail of nitrogen reduction are an attractive target. For example, $[Fe_4S_4]$ cluster is the subunit of all the clusters in the three kinds of nitrogenases. There are also three kinds of hydrogenases and except "iron, nickel free" one, $[Fe_4S_4]$ cluster consists the clusters in the other two kinds of hydrogenases. In sulfite reductase, the $[Fe_4S_4]$ cluster is bridged by a cystine sulfur atom to a heme group [8] (Figure 3 a). In the two distinct clusters of carbon monoxide dehydrogenase, it is bridged by an unknown atom to a nickel center cluster [9] (Figure 3 b).

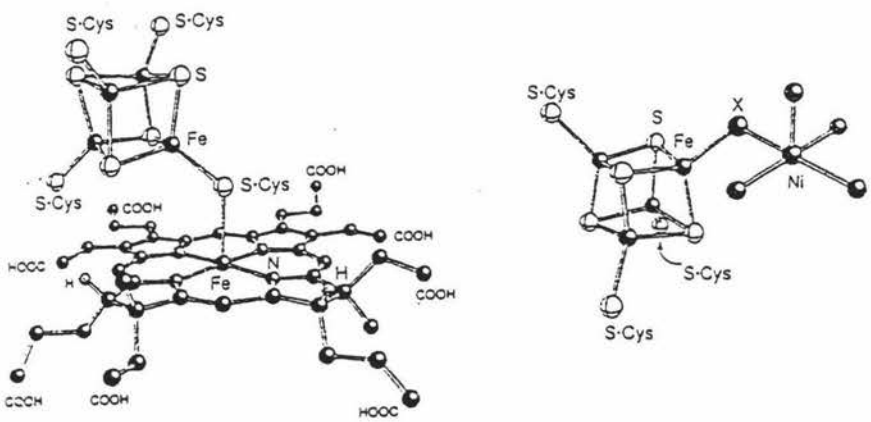

a b

Figure 3 Structures of sulfite reductase and carbon monoxide dehydrogenase

Nature's modular iron-sulfur clusters include $[Fe_2S_2]$, $[Fe_3S_4]$, and $[Fe_4S_4]$ clusters (scheme 2). There are several ways of showing their structural versatility and robustness. They have facility for conversion and interconversion in both the free and protein bound conditions (chemical systems and biological systems, respectively). They also undergo ligand exchange reactions and oxidative degradation [10].

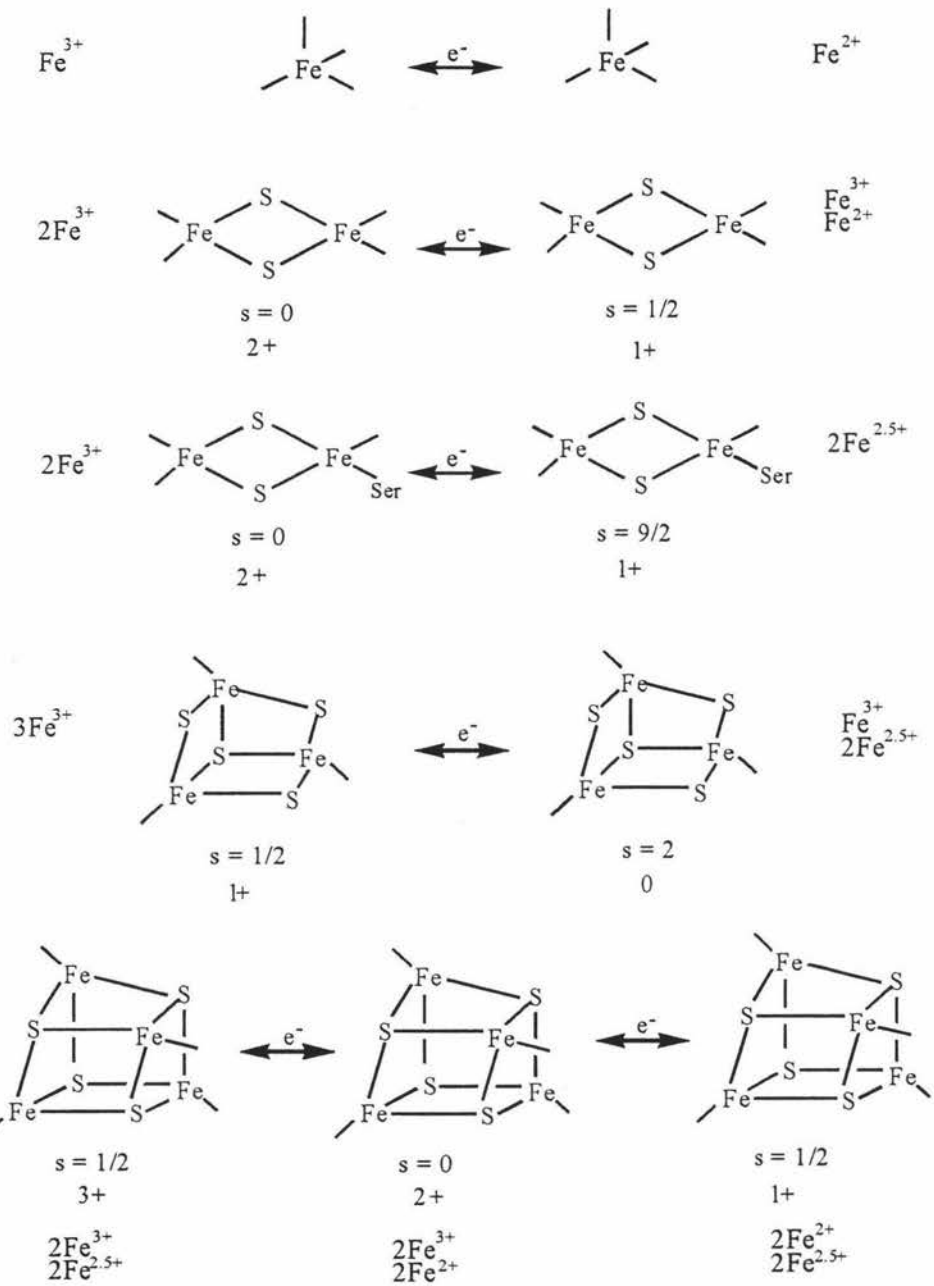

Scheme 2 Localization-delocalization patterns of iron sulfur clusters

Iron-sulfur clusters have functions of electron transferring, accepting, donating, shifting and storing because of their versatility and robustness. Other functions not of a redox nature have also been discovered. These include the binding and activation of

substrates at the unique iron site of $[Fe_4S_4]$ cluster in the catalytic function of actonitase [11] and related enzymes, and apparently stabilizing radicals in reductions occurring by a free-radical pathway. There is evidence that the clusters can function in coupling electron transfer to proton transport [12].

Scheme 2 illustrates the localization-delocalization patterns of iron sulfur clusters. $[Fe_4S_4]$ clusters contain delozalized $Fe^{2.5+}Fe^{2.5+}$ pairs in their most common oxidation states [13]. For $[Fe_2S_2]^{1+}$, only when Cys is mutated to a Ser, the cluster is vanlence-delocalized with S = 9/2 [14]. The $[Fe_3S_4]^0$ clusters provide strong evidence that the delocalized pair has spin S = 9/2 [15]. Spin-state variability depending on cluster environment is considered as a possible control factor for substrate specificity and gated electron transfer [10].

1.1.3. Ruthenium, Haber-Bosch process and hydrodesulfurization (HDS)

The first Haber-Bosch production plant started up at BASF in 1913 [5]. Haber-Bosch process is still the best industrial process for reduction of N_2 with H_2 to form ammonia:

$$3H_2\,(g) + N_2\,(g) \xrightarrow{400\text{-}700^{\circ}C,\ Fe,\ 30000\ kPa} 2NH_3\,(g)$$

The reaction has been running under conditions of high temperature and high pressure. The most widely used catalyst of this process is BASF-developed catalyst that consists of α-iron as the promoter [16].

Great energy savings could be obtained by an improvement in catalytic activity of catalysts allowing for operation at lower temperatures and pressures. Therefore, new efficient catalysts that can be used at much milder conditions need to be found.

Ruthenium is considered to possess great potential in development of new catalysts for the ammonia synthesis. In the early 1970s, Ozaki and co-workers introduced

a carbon-supported ruthenium catalyst promoted by alkali metal [17,18] at 250°C and 80 kPa. Ru/AC-K (AC = activated carbon) exhibited a 10-fold increase in the rate of NH_3 synthesis compared to a conventional promoted iron catalyst under similar conditions. Since then, Ru/AC-K has been developed for industrial use [19]. Recently, a number of papers have reported the adsorption and the activation of dinitrogen and dihydrogen on ruthenium catalysts by Izumi et.al [20,21,22].

Besides this, it is also found that ruthenium has significant ability of catalysis in other processes such as hydrodesulfurization (HDS) process [23,24]. For both heterogeneous and homogeneous catalysts in this process, ruthenium is almost the most active promoters compared to other metals that have been known [25]. (This will be discussed later in section 1.2).

1997-1998, the world production of ammonia is almost 200 million tons, which is still far less than required [26].

1.1.4 Arene as ligands in transition metal clusters

There are several ways in which arene rings coordinate to metal atoms, such as η^2-, η^2-, and η^6- π coordination [27], which implies that clusters with arene rings as ligands have great flexibility and robustness, and therefore, the great ability of electron storing and transferring during catalysis processes. (Scheme 3)

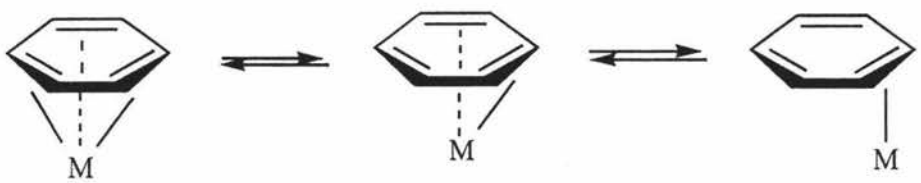

Scheme 3 Ways that arene rings coordinate to metal atoms

Geiger [101], Finke [102] and their co-workers have demonstrated that some cationic metal arene complexes can undergo simultaneous $2e^-$ reduction. These reductions are associated with a η^6-to-η^4 change in the hapticity of the arene (Scheme 19).

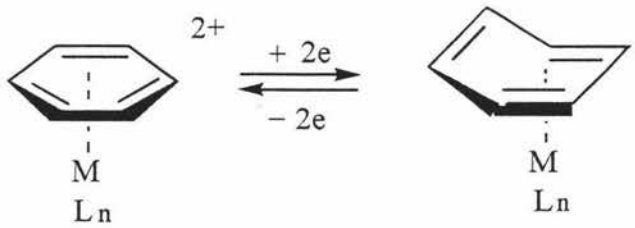

Scheme 19 η^6-to-η^4 change of the arene ring

Depending on this, Rauchfuss et.al [5] suggest an alternative structural possibility for the $50e^-$ cluster $[Ru_3S_2(cymene)_3]$. In this alternative structure the closo Ru_3S_2 core is retained, but one arene adopts the η^4- geometry (Figure 51) rather than the η^6- geometry with one metal-metal bond opened. (The open structure was shown in Figure 11.)

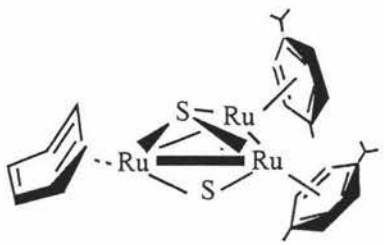

Figure 51 Alternative structure of $[Ru_3S_2(cymene)_3]$

It has also been reported the electrophilic properties of arene rings. Mononuclear systems have been studied quite extensively [107]. For instance the $[Cr(CO)_3]$ fragment shows an electron withdrawing effect on coordinating arene rings, resulting in an activation towards the addition of nucleophiles [108]. The influence of a metal cluster should be even larger. Both η^6 (terminal) and μ_3-η^2:η^2:η^2 (face bridging) coordination modes of

the arene rings have been found in many clusters such as $Os_3(CO)_9(\mu_3\text{-}\eta^2\text{:}\eta^2\text{:}\eta^2\text{-}C_6H_6)$[109], $Ru_6C(CO)_{11}(\mu_3\text{-}\eta^2\text{:}\eta^2\text{:}\eta^2\text{-}C_6H_6)(\eta^6\text{-}C_6H_6)$ [109] and $Ru_6C(CO)_{11}(\eta^6\text{-}C_6H_6)_2$ [110]. Different coordination mode leads to different activation of arene rings. When coordinated to a tri-osmium carbonyl cluster $Os_3(CO)_9(\mu_3\text{-}\eta^2\text{:}\eta^2\text{:}\eta^2\text{-}C_6H_6)$ in the face-capping mode, benzene is activated towards nucleophiles such as H^-, Me^- or Ph^-, which add the ring in the exo position [111]. In contrast, nucleophiles do not appear to add to plain arenes which are coordinated to a tris-(cyclopentadienylcobalt) cluster [112].

Different coordination modes of arene rings also lead to different molecular aggregations. For example, it has been found that there are two different kinds of coordination modes of the arene rings in a pair of isomeric bis-arene clusters $Ru_6C(CO)_{11}(\mu_3\text{-}\eta^2\text{:}\eta^2\text{:}\eta^2\text{-}C_6H_6)(\eta^6\text{-}C_6H_6)$ [109] and $Ru_6C(CO)_{11})(\eta^6\text{-}C_6H_6)_2$ [110]. In both crystals the benzene ligands face each other in graphitic arrangements, causing the formation of molecular "snakes" and "rows", respectively. (Figure 53) [106].

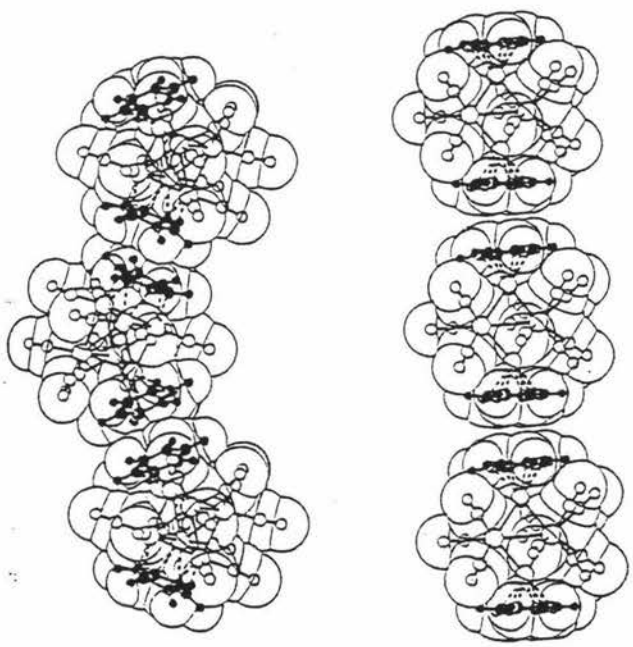

Figure 53 Molecular aggregation of $Ru_6C(CO)_{11}(\mu_3\text{-}\eta^2\text{:}\eta^2\text{:}\eta^2\text{-}C_6H_6)(\eta^6\text{-}C_6H_6)$ and $Ru_6C(CO)_{11}(\eta^6\text{-}C_6H_6)_2$

Central of the arene ruthenium chemistry is the dimeric complex $[(arene)RuCl_2]_2$ prepared from the reaction of cyclohaxadienes and hydrated ruthenium trichloride [28]. The p-cymene derivative of these dimers was selected for this study because of its good solubility compared to the bezene and hexamethylbezene derivatives, ease of synthesis from commercially available α-phellandrene and convenient ^1H NMR characteristics of its derivatives. The chemical shift of hydrogen atoms on the cymene ring, the methyl group and isopropyl group are all easy to recognize, especially the chemical shift of the four hydrogen atoms on the cymene ring are very specific when the ring coordinates to metal atoms. But the chemical shift of hydrogen atoms on the benzene ring is only one single peak, which is more difficult to identify compared to the cymene ring.

Although the work on ruthenium arene clusters has been done for several decades, very few ruthenium arene clusters have been found. In 1975, Stephenson described the characterization of cubane cluster $[Ru_4(OH)_4(benzene)]^{4+}$ (Figure 2 a) formed by the base hydrolysis of $[(bezene)RuCl_2]_2$ [29] . The electron-deficient clusters $[M_4H_4(arene)_4]^{2+}$ (M = Ru, Os) has been briefly reported in 1986 (Figure 4 a) [30], and their properties of activating dihydrogen have been discovered by Suss-Fink et al. in 1993 [31]. The first arene ruthenium sulfur cluster $[(p\text{-cymene})_3Ru_3S_2]^{2+}$ (Figure 4 b) was made by Lockmayer et.al using $[(p\text{-cymene})RuCl_2]_2$ as starting material in 1989 [5]. (This will be discussed in detail later in section 2.2.1.)

$$3/2\ [(p\text{-cymene})RuCl_2]_2 + 2\ S^{2-} \longrightarrow [(p\text{-cymene})_3Ru_3S_2]^{2+} + 6\ Cl^-$$

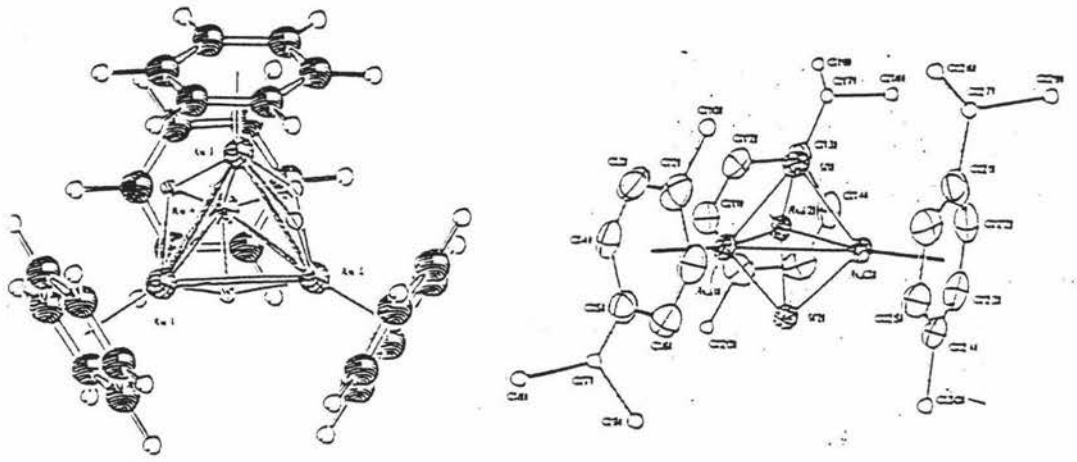

a b

Figure 4 Structures of $[Ru_4H_4(benzene)_4]^{2+}$ and $[Ru_3S_2(cymene)_3]^{2-}$

1.1.5. Sulfur as ligands in transition metal clusters

Sulfur-containing compounds have long been known to act as poisons for noble metal catalysts because of their strong coordinating and adsorptive properties, which cause them to block reactive metal sites [32]. Nevertheless, many transition metal sulfides (S^{2-}) display intriguing catalytic activity in their own way. Sulfide ligands form relatively strong bonds with many transition metals, and the ligands can play an important role in stabilizing di- and poly-nuclear complexes against fragmentation process during catalysis [33]. This gives the cluster a metal core that can catalytically store and transfer electrons and protons to molecules.

Sulfur donor ligands tend to favor lower oxidation states of metal ions. The relatively positive reduction potentials of the sulfide complexes, for example, when compared to relative oxygen or nitrogen donor systems, provide a favorable environment for many catalytic reduction reactions that have been characterized [34]. The redox changes of the sulfide complexes can be attributed by changes in the formal oxidation states of the metal ions. However, the ability of coordinated sulfide ligands to participate in redox chemistry, for example,

$$2\,S^{2-} \xrightarrow{-2\,e^-} S\text{-}S^{2-}$$

has also been proved [35].

It has been found that sulfur can act in an important role in the hydrodesulfurization processes. Dihydrogen is split by metal-sulfur center to metal-hydride and thiol hydride [36].

It is claimed that protonation of the activated dinitrogen proceeds with the aid of the bridging hydrosulfido ligands in the Fe/Mo cluster by several groups recently [37]. Dance gave a model of that the bridging sulfido ligands mediate proton transfer to the coodinated dinitrogen bound to the Fe_4 face of the Fe/Mo sulfido cluster via μ-SH intermediate (Figure 44) [37c-f].

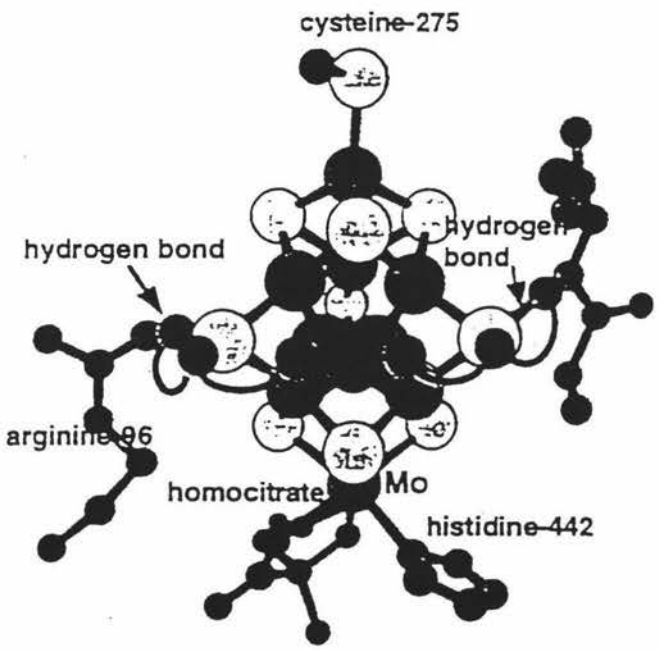

The Fe_7MoS_9(cysteine)(histidine)(homocitrate) cluster, showing hydrogen bonds from behind the S^{2-} atoms flanking the front face, and the postulated transfer of H to bound N_2 by inversion of (S^{2-}–H)

Figure 44 Model of dinitrogen binding to Fe_4 face of Fe/Mo cluster

Recently, Hidai et al. have proved this experimently by investigating the reactivity of dinuclear complexes (Ru, Ir or Rh) containing bridging hydrosulfido ligands toward coordinated dinitrogen on tungsten giving NH_3 [38]. They have given the first example of proton transfer from metal μ-SH complexes to coordinated dinitrogen, especially those μ-SH ligands in cationic dinuclear complexes because they are more acidic than those in corresponding neutral complexes. (Scheme 12)

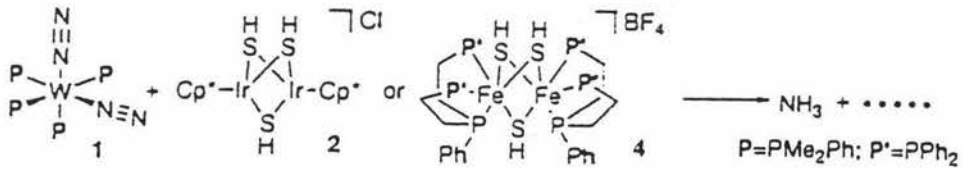

Scheme 12 Proton transfer from metal-SH complexes to coordinated dinitrogen

Some transition metal clusters have been synthesized, which are analogues to the cubane subunit of the clusters in nitrogenases and hydrogenases, such as $(Et_4N)_2[(Cl_4\text{-cat})(CH_3CN)MoFe_3S_4Cl_3]$ [39] (Cl_4-cat = tetrachlorocatecholate), (Figure 5 a) and $[Ru_4S_4Cp^*_4]^{2+}$ [40] (Figure 5 b). It has been proved that $[Fe_4S_4(SR)_4]^{2-}$ (R = Ph, C_6H_4Me) can catalyze the reduction of diphenylacetylene to cis-stilbene by excess sodium borohydride in CH_3CN / MeOH [41]. The $(Et_4N)_2$ $[(Cl_4\text{-cat})(CH_3CN)MoFe_3S_4Cl_3]$ cluster, in which Mo atom has a coordination environment very similar to that in nitrogenases, can catalyze the four-electron reduction of N=N bond of cis-dimethyldiazene giving methylamine.

a b

Figure 5 Structures of $(Et_4N)_2[(Cl_4\text{-cat})(CH_3CN)MoFe_3S_4Cl_3]$ and $[Ru_4S_4Cp^*_4]^{2+}$

Many ruthenium sulfur clusters have been synthesized and characterized. Most of them are CO containing clusters such as $[Ru_6S_3(H)(CO)_{15}]$ [42]. A Ru-Mo cluster $[\{CpMo(CO)_2\}_2SRu(CO)_3]$ that contains a μ_3-sulfide ligand, which has the same mode of coordination as in $[(p\text{-cymene})_3Ru_3S_2]^{2+}$, was found to promote a nonreductive coupling of alkynes [43].

1.2. Transition metal sulfur complexes for catalysis --- hydrodesulfurization (HDS)

Transition metal complexes are widely used for catalysts. Hydrodesulfurization is one of their very important applications.

The hydroprocessing of petroleum represents one of largest scale chemical processes carried out by industries in the world today. In this procedure, crude oil is treated with hydrogen at high pressure (1500-3000 lbf in^{-2}) over a hot heterogeneous catalyst (Co- or Ni- promoted, Mo or W sulfide supported on Al_2O_3) (500 – 825°C) to

remove nitrogen, sulfur and residue metals prior to further processing [44]. The removal of sulfur from residues in oil is commonly referred to as hydrodesulfurization.

On one hand, since new drilling techniques allow the recovery of heavier crude oils that contain higher levels of sulfur, removal of this element is becoming even more important, particularly for those countries that possess very large reserves of heavy crudes. On the other hand, recent environmental pollution regulations require lower amounts of sulfur in fuels, which can not be achieved using known technology. Thus there is increasing interest in developing new catalysts and processes for the removal of sulfur from the organosulfur compounds in petroleum.

1.2.1 Industry catalysts and mechanisms

Many metals are more active as HDS promoters than cobalt or nickel mixture. The active sequence has been proven to be: Ni < Co < Pd < Pt < Re < Ir < Rh < Os ≤ Ru [45]. That is, ruthenium is the most active promoter compared to other metals in HDS processes while cobalt and nickel are still the metals of choice for current industry use. A good heterogeneous catalyst of Co/Mo/S compositions and the related Ni/W/S systems are widely used to catalyze the HDS of fossil fuel feedstocks [46]. The catalyst is conventionally prepared by impregnating a high-sulfur-area alumina with ammonium molybdate and a cobalt salt in an aqueous medium. This pre-catalyst is then treated with hydrogen and a source of sulfur (H_2S, organic sulfur compounds, or the feedstocks) at temperature near 350°C. This sulfidation step converts the molybdenum oxides into a MoS_2-like phase that gives metal-sulfur cores indicating the active sites [47].

Under the reducing atmosphere of high H_2 pressures, the surfaces of these sulfides exhibit coordinatively unsaturated reduced metal sites. A redox HDS mechanism involves binding of thiophene at one of these electron rich sites, oxidative addition, sulfur removal and reduction of the metal [48]. A recently study on soluble transition metal sulfur clusters in homogeneous catalytic systems has proved this. A cluster $[(Cp')_2Mo_2Co_2S_3(CO)_4]$ (Cp'

= $CH_3C_5H_4$) with μ_3- and μ_4-sulfur ligands could remove sulfur directly from thiophene producing a cubane cluster $[(Cp')_2Mo_2Co_2S_4(CO)_2]$ (scheme 14) [49, 47, 50].

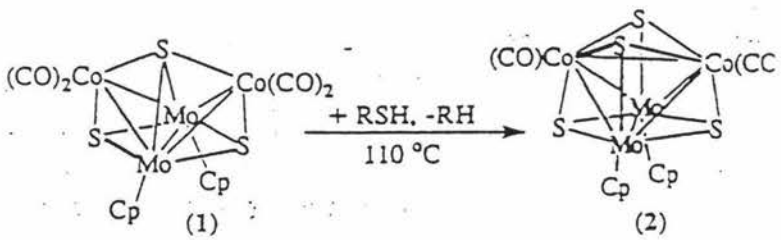

Scheme 14 Sulfur atoms removed by $[(Cp')_2Mo_2Co_2S_3(CO)_4]$

The principal mechanism proposed for the heterogeneous HDS of thiophenes is summarized in Scheme 4 [51].

From the scheme, it can be seen that hydrogenation and hydrogenolysis are the main parts in the HDS process of thiophenes.

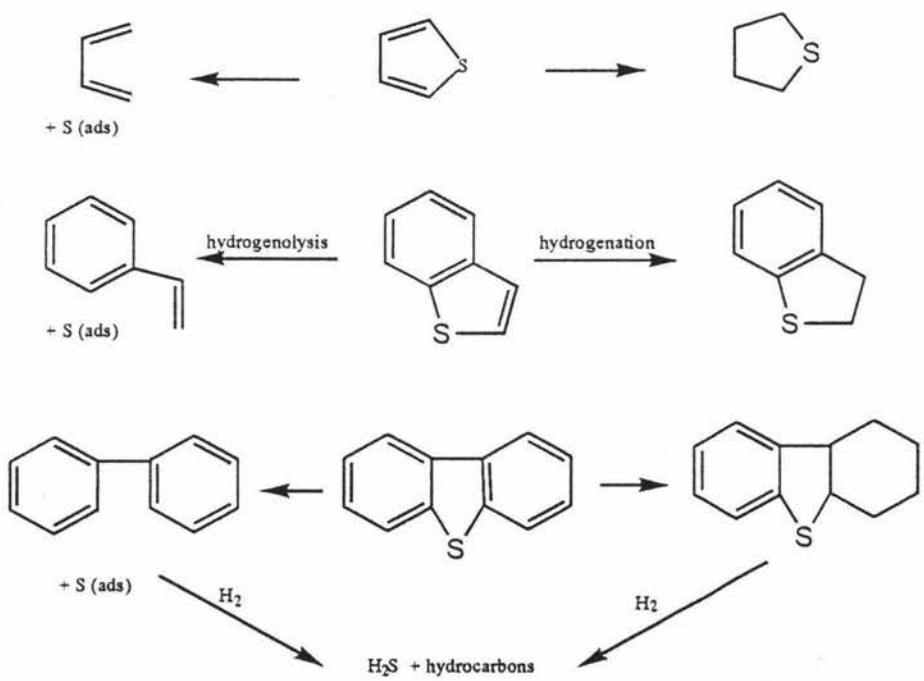

Scheme 4 The principal mechanism for heterogeneous HDS of thiophene

1.2.2 Catalytic hydrogenation reactions

The development of efficient catalysts for plain hydrogenation of thiophenes remains an important goal in HDS chemistry. In fact, the cyclic thioether products can subsequently be desulfurized over conventional HDS catalysts under milder reaction conditions than those necessary to accomplish the hydrodesulfurization of the thiophene precursors. This aspects is particularly important for the benzothiophenes and dibenzothiophenes because the conventional catalysts can desulfurize the corresponding cyclic thioethers, dihydrobenzothiophenes and hexahydrodibenzothiophenes, without affecting the benzene rings, necessary to preserve a high octane number.

Several homogeneous hydrogenation reactions of the model substrate benzothiophene to dihydrobenzothiophene have been carried out over the last fifteen years [52, 53, 54, 55]. Such as $[RuCl_2(PPh_3)_3]$, $[RuH(Cl)(CO)(PPh_3)_3]$ [56] and $[Rh(Cp^*)(MeCN)_3][BF_4]_2$, etc. The proposed mechanism of hydrogenation using $[Rh(cod)(PPh_3)_2]^+$ (cod = cycloocta-1,5-diene) is shown in Scheme 5 [54].

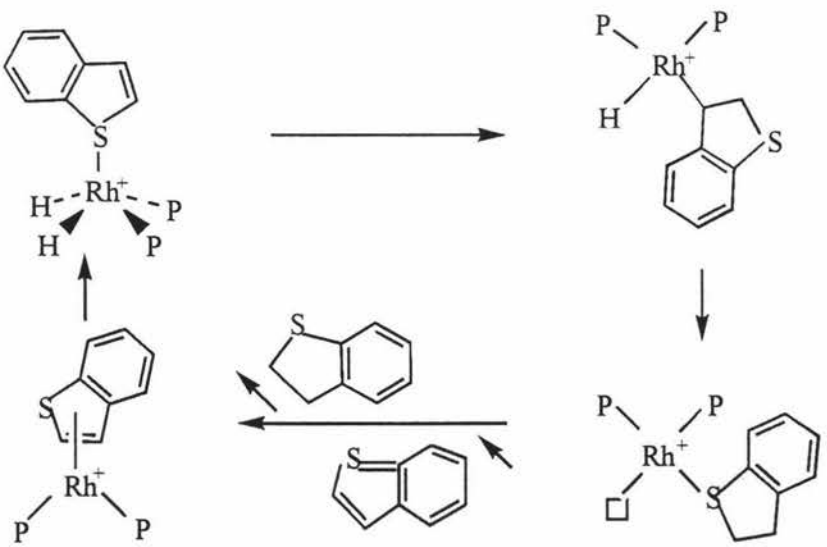

Scheme 5 The proposed mechanism of hydrogenation using $[Rh(cod)(PPh_3)_2]^+$

At comparable donor-atom sets of the catalytic precursor, the hydrogenation activity increases in the order of Ir < Rh < Ru ≤ Os, which is not far away from the trend observed for the heterogeneous HDS of dibenzothiophenes [57]. That is, ruthenium is almost the most active catalytic precursor in these processes.

1.2.3 Catalytic hydrogenolysis reactions

For hydrogenolysis reactions, those metal-mediated transformations of thiophenes that result in the opening and hydrogenation of the substrates to give the corresponding unsaturated thiols, which eventually are reduced to the saturated derivatives.

For the reasons put forward in the case of the hydrogenation, the hydrogenolysis reactions of thiophenes are of great relevance for the conventional heterogeneous catalysts under milder conditions than those required to desulfurize the thiophenes directly.

Ruthenium is also very active in these catalytic processes. A similar trend of activity is shown by the heterogeneous HDS catalysts, which emphasizes the great catalytic ability of ruthenium in these processes [58].

1.2.4.Catalytic desulfurization reaction

Several transition metal cluster based systems have been developed evolving desulfurizing organic compounds. All the desulfurization action reported [59,60,61,62,63,64] involves the concomitant action of two metals, one of which opens or activates the thiophene, while the other one promotes the extrusion of the sulfur atom. The later step can occur either thermally or by treatment with H_2. Soluble clusters such as $[Ru_3(CO)_{12}]$ [65] and $[IrH(\eta^2\text{-}C,S\text{-}C_{12}H_8S)(triphos)]$ (triphos = $MeC(CH_2PPh_2)_3$) [66] are capable of straight

forwardly desulfurizing thiophenes giving catalytic amount of biphenyl and H_2S under relatively mild condition. (Scheme 6)

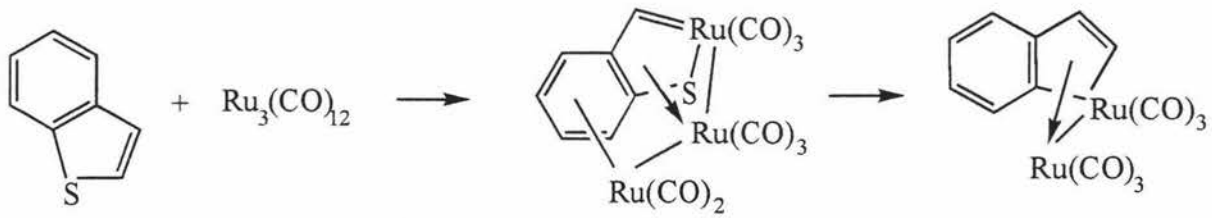

Scheme 6 Desulfurization of thiophenes by $[Ru_3(CO)_{12}]$

1.3. Nitrogenases and dinitrogen reduction

While reduced dinitrogen is an integral component of proteins, nucleic acids and most other biomolecules, dinitrogen is regarded as one of the most inert molecules under laboratory condition because of the large activation energy required to form ammonia. Consequently, acquisition of metabolically usable forms of nitrogen is essential for the growth and survival of all organisms, which implies that dinitrogen reduction is one of the most basic energy sources of human beings. Although elemental dinitrogen is abundant in the earth's atmosphere, the great difficulty of reducing it to a usable form has been known for one century. The tough conditions of dinitrogen reduction in industries have already been shown earlier in Haber-Bosch process.

On the other hand, some bacteria containing nitrogenases can reduce atomospheric dinitrogen to ammonia under ambient condition.

There are three distinct kinds of nitrogenases, each of which consists essentially of two proteins. The most common nitrogenase contains iron and molybdnum but more recently two variants have been characterized. They are based upon iron and vanadium, and upon iron alone, respectively. The first one has been widely studied.

The molybdnum nitrogenase consists of two metalloproteins, the iron (Fe-) sulfur protein and the molybdenum iron (MoFe-) sulfur protein. The two clusters are P-cluster and Mo-cofacter, respectively, which are the active sites in the proteins. (Figure 6) Together, these proteins mediate the ATP-dependent reduction of dinitrogen to ammonia.

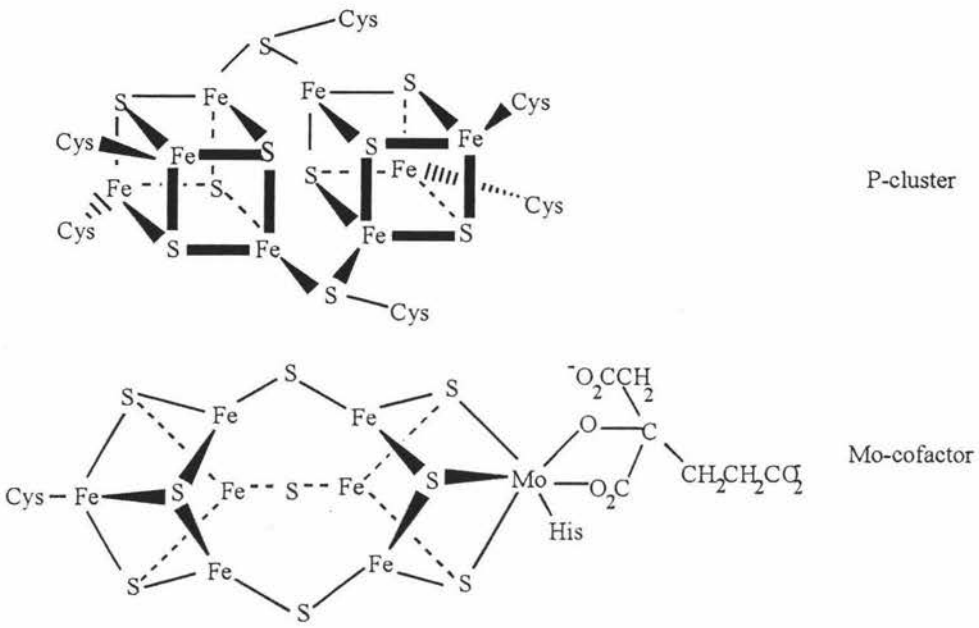

Figure 6 Structure of nitrogenase clusters

Currently, it has been discovered that the molybdenum atom is the dinitrogen binding site. Electrons are transferred from P-cluster to Mo-cofacter to achieve the dinitrogen reduction process.

It has been suggested that sulfur atoms in the clusters act in a key role of activating dinitrogen molecules in redox chemistry. A recent quantum chemical study on nitrogenases showed that the bridging sulfide ligands might be the main factor responsible for the activation of dinitrogen and for the subsequent formation of the N-H bonds. When a hydrogen atom binds onto the bridging sulfur, the way that dinitrogen bind onto the cluster might change from end-on coordination to one of the metal atoms to bridging

coordination between two metal atoms, which might increase the activity of dinitrogen to form ammonia [3] (scheme 7). For example, for the dimeric model, it is calculated that the addition of first hydrogen becomes exothermic by 55.9 kcal / mol for B (with hydrogen atom on the sulfur bridge) rather than 18.5 kcal / mol for A (without hydrogen atom on the sulfur bridge).

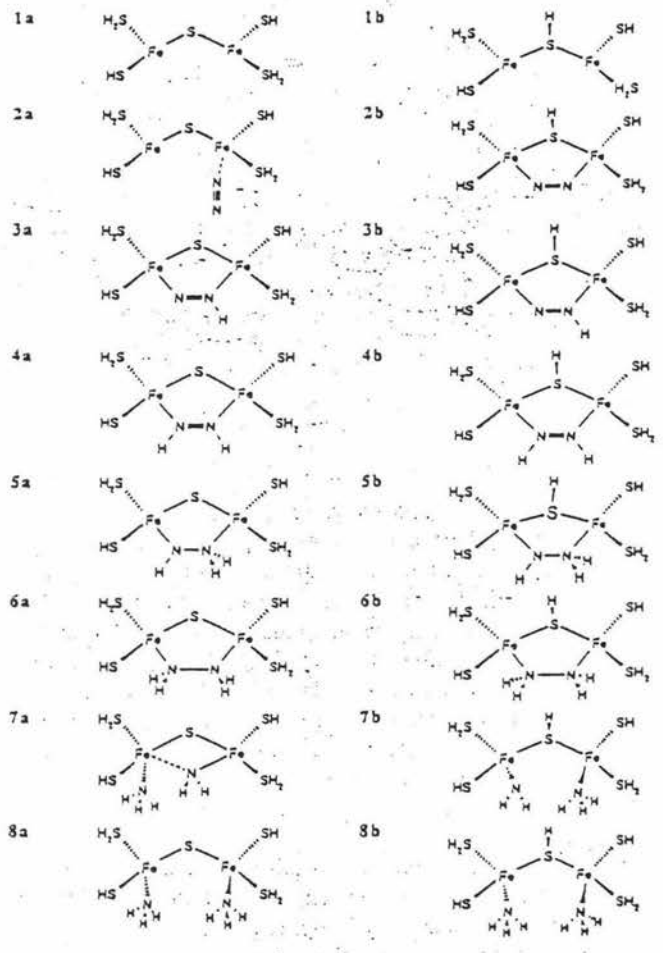

Scheme 7 Activation of dinitrogen by sulfur bridge with hydrogen on it

1.3.1 Transition metal mono- or bi-nuclear complexes in dinitrogen reduction

The existence of biological nitrogen fixation has inspired chemists to research for purely chemical systems capable of fixing dinitrogen catalytically under mild condition. Since 1960s, a lot of work has been done to mimic biological nitrogen fixation using transition metal complexes. Protonation of mono- or binuclear transition metal complexes with coordinating dinitrogens has been the most interesting area during the last three decades. It has been proven that many this kind of complexes can be protonated to give ammonia or other intermediate compounds such as hydrazine in lower temperature and pressure [67].

There are mainly two ways that dinitrogen molecules coordinate to the metal atoms in mono- or bi-nuclear complexes: end-on coordination to one metal atom or bridging coordination between two metal atoms, which have been mainly studied. In $[RuH_2(N_2)(PPh_3)_2]$ [68] and cis-$[Mo(N_2)(PMe_2Ph)_4]$ [69], etc, the end-on coordinating dinitrogen can be reduced to ammonia at fairly mild conditions. In $[\{Zr(C_5Me_5)_2(N_2)\}(N_2)]$ [70] and $[WCp^*Me_2(OC_6F_5)]_2(N_2)$ [71] etc., dinitrogen coordinating between two metal atoms can be reduced indirectly.

Recently Hidai et al. found the first bimetallic catalytic system that tungsten dinitrogen complex cis-$[W(N_2)_2(PMe_2Ph)_4]$ was treated with an equilibrium mixture of $[RuCl(dppp)_2]X$ and trans-$[RuCl(\eta^2\text{-}H_2)(dppp)_2]X$ (X = BF_4, PF_6, or OSO_2CF_3; dppp = 1,3-bis(diphenylphosphino)propane) under 1 atmosphere of dihydrogen at 55 °C giving NH_3 in moderate yield. It has been proven that the coordinating dinitrogen reacted with dihydrogen via the complexes with coordinating dihydrogen [72].

1.3.2. Transition metal clusters in dinitrogen reduction

In dinitrogen reduction, the catalysts are expected to be poly-nuclear clusters with a maximum number of contacts with nitrogen during the catalysis process.

When electrons transfer to dinitrogen in a metal complex, bond formation must compensate for the energy of NN bond loosening. Apparently, the larger the number of metal atoms directly bound to dinitrogen, the easier it is to reach the same extent of NN bond weakening, since each metal provides electrons to NN bond and therefore, is already a reductant at the stage of complex formation. Therefore, it might be expected that a three- or even four-nuclear complex would activate dinitrogen more effectively than mono- or binuclear complexes. It is suggested that when dinitrogen bind on cluster $[V_3(catecholate)_3]$, a tetranuclear intermediate might be formed (Scheme 8) [73].

Besides the way that the dinitrogen binds on the metal atoms, the number of the electrons that the cluster can store and transfer to the dinitrogen molecule for the requiring of breaking the NN bond is also very important in catalytic process. It needs six electrons altogether to reduce the dinitrogen to ammonia, which is difficult to achieve for mono- or bi-nuclear complexes. Sometimes, clusters can open their structures by breaking one metal-metal bond during electron storing and transferring processes, which implies larger abilities of catalysis than mono- or binuclear complexes.

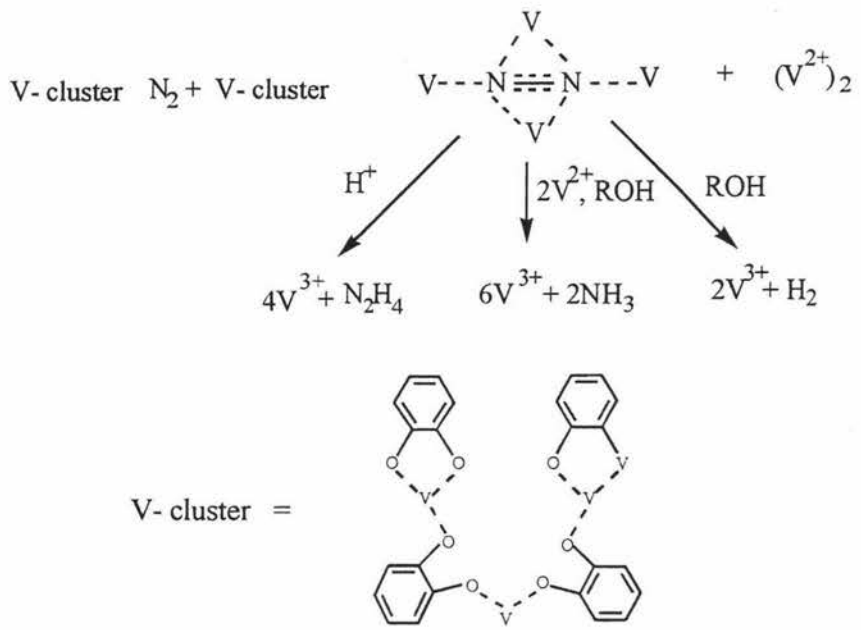

Scheme 8 Tetranuclear intermediate of dinitrogen binding on $[V_3(catcholate)_3]$

1.4. Clusters in hydrogenases and hydrogenation

The formation and consumption of dihydrogen by microorganisms are catalyzed by hydrogenases. Beside the hydrogenases without nickel and iron-sulfur clusters in *methanogenic archaea* [74], the other two types of metal clusters in hydrogenases are [Ni, Fe, S or Se] and [Fe, S]. Both of the clusters exhibit sulfur-rich coordination spheres, which are believed to be the dihydrogen activation sites [75, 76]. On the basis of redox titrations and EPR spectra, it has been suggested that the nickel atom and iron atom are the dihydrogen binding sites in [NiFe] hydrogenases and nickel-free "iron only" hydrogenases, respectively. Both enzymes catalyze the redox equilibrium and the heterolytic cleavage of dihydrogen (Scheme 9) [77]:

$$H_2 \rightleftharpoons 2\,H^+ + 2\,e^-$$

$$H_2 + D_2O \rightleftharpoons HD + HDO$$

Scheme 9 Redox equilibrium catalyzed by hydrogenases

The proposed mechanism is shown in Scheme 10:

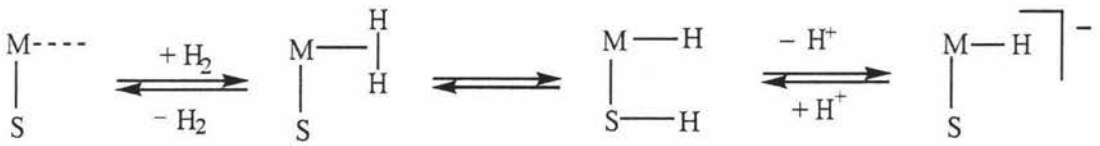

Scheme 10 The proposed mechanism of heterolytic cleavage of dihydrogen

The metal-sulfur sphere cleaves the dihydrogen via formation of η^2-H_2 and thiol species.

Recently, Sellmann et.al found that the dihydrogen molecule can heterolytically be cleaved at ruthenium sulfur sites of cluster [Ru(PCy$_3$)('S$_4$')] ('S$_4$' = 1.2-bis((2-mercaptophenyl)thiol)ethane(2-)) in the presence of NaOMe at very mild condition (Scheme 11) [78].

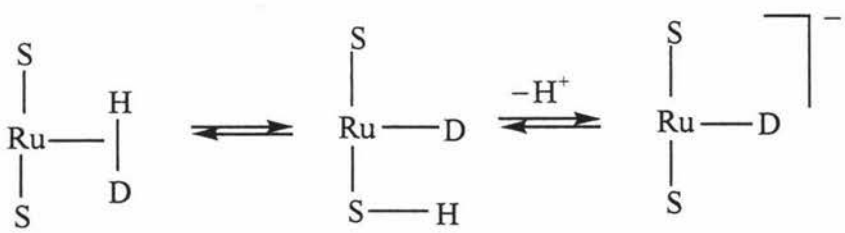

Scheme 11 Dihydrogen cleaved at Ru-S sites of cluster [Ru(PCy$_3$)('S$_4$')]

In this case, thiol hydride species could not yet be detected. However, an experiment on analogue rhodium cluster has been proven [79]. They both yield model compounds that combine structural and functional feature of the active centers in hydrogenases.

1.5. New arene ruthenium sulfur clusters

It has been shown that transition metal sulfur compounds play very important roles in a range of biological and industrial processes.

The potential for insights into these processes from sulfur containing clusters is large. The next chapter of this thesis explores the synthesis and characterization of the new high nuclearity arene-ruthenium-sulfur clusters

CHAPTER TWO SYNTHESIS OF ARENE-RUTHENIUM- SULFUR CLUSTERS

2.1. Synthetic strategy

The only reported arene-ruthenium-sulfur clusters, $[Ru_3S_2(cymene)_3]^{2+}$ and $[Ru_3S_2(cymene)_3]$ are interesting because the cationic cluster and its reduced cluster can be interconverted in the reversible redox processes [5]. When the cationic cluster gains two electrons to form the neutral cluster, the structure opens one metal-metal bond. When the neutral cluster loses two electrons to re-form the cationic cluster, the metal-metal bond is re-formed (Scheme 1, see Chapter One). (The cationic cluster $[Ru_3S_2(cymene)_3]^{2+}$ could be reduced giving the neutral cluster $[Ru_3S_2(cymene)_3]$ by CpCo complex [5].)

The plausible target for this project was synthesis of high nuclearity arene-ruthenium-sulfur clusters using the neutral cluster as starting material. One widely used strategy involves adding mono-nuclear complexes to a neutral cluster. The mono-nuclear complex usually has labile ligands coordinating to the metal atom such as acetonitrile and acetone [115]. The proposed reaction of $[Ru_3S_2(cymene)_3]$ and $[(cymene)Ru(NCMe)_3]^{2+}$ would be:

$$[Ru_3S_2(cymene)_3]^0 + [(cymene)Ru(NCMe)_3]^{2+} \rightarrow [Ru_4S_2(cymene)_4]^{2+} + 3\ NCMe$$

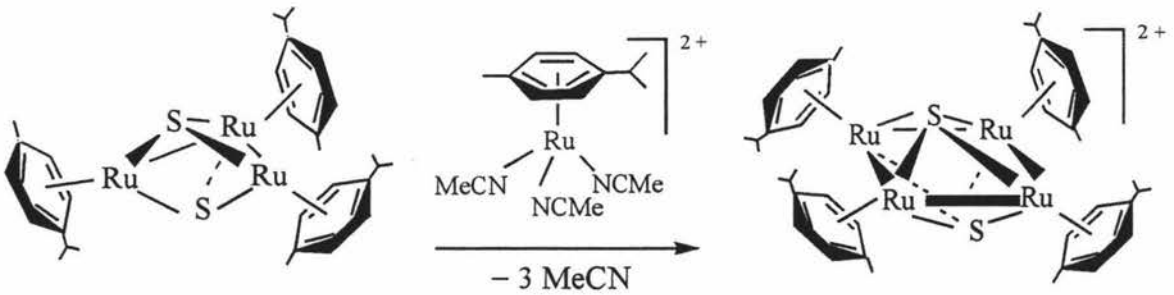

A further aim was to investigate the reactivities of these clusters with some substrates such as dinitrogen, dihydrogen, CO and some organic molecules as well as an investigation of the electrochemistry of any new clusters.

Early in 1989, Rauchfuss et.al reported the synthesis of the $[Ru_3S_2(cymene)_3]^{2+}$ cluster using Na_2S, NaSH or $(SiMe_3)_2S$ as a sulfur source and $[RuCl_2(cymene)]_2$ as the arene ruthenium source [5].

The reaction in aqueous Na_2S is:

$$3/2\ [RuCl_2(cymene)]_2 + 2\ S^{2-} \longrightarrow [Ru_3S_2(cymene)_3]^{2+} + 6\ Cl^-$$

In the first stage of this project this reaction was investigated to develop a convenient synthesis of the cationic cluster. Initially the three sulfur sources were compared to choose the best one. As a sulfur source, Na_2S is the easiest to use. However the yield from the aqueous solution of Na_2S was 44% [5]. Besides the lower yield, purification of the product of this reaction in water was the most complicated because it needed several steps to get rid of the water [5]. NaSH dissolves in methanol to give SH^-. In this case the yield was 58% that was higher than the former one. The purification of the product from the reaction was much easier than the aqueous Na_2S one [5]. $(Me_3Si)_2S$ in THF is the mildest reagent for the three sulfur-source compounds, and gave the $[Ru_3S_2(cymene)_3]^{2+}$ in reasonable high yield (77%). But it needed to be pre-made and the reactants were not very soluble in the solvent [5].

H_2O and MeOH were chosen not only because of the good solubility of the starting materials, but also releasing of SH^- that might play an important role in the reaction [5]. (This will be discussed later in mechanism section.)

$$H_2O \rightleftharpoons HO^- + H^+$$

$$S^{2-} + H_2O \rightleftharpoons HO^- + SH^-$$

$$MeOH + S^{2-} \rightleftharpoons MeO^- + SH^-$$

In order to avoid the complicated purification of the product, the reaction was repeated in various conditions, especially in methanolic Na_2S.

Since this reaction forms the basis for most of the synthetic work described in this chapter, the results of the study will be considered in detail. The structures of three arene-ruthenium-sulfur clusters will be discussed in detail including how the number of valence electrons influences the structure, how the solid state structure and single crystal structure effect each other and how the structures determine the chemical shifts and other characters of the clusters. The mechanisms of formation of arene-ruthenium-sulfur clusters will also be described in detail. Some electrochemistry and calculations (quantum chemistry) will be also involved.

2.2. Synthesis of arene-ruthenium-sulfur clusters

Initially the reaction to make the $[Ru_3S_2(cymene)_3]^{2+}$ cluster was examined. For the reasons described above, the reaction was not exactly repeated as that Rauchfuss and coworkers did. The method used mainly combined the reactions of using Na_2S and NaSH. It was a big surprise that this reaction was very different with original reactions and was much more interesting than original ones. (The differences will be discussed in the mechanism section in detail).

A mixture of Na_2S in MeOH and $[RuCl_2(cymene)]_2$ in MeOH was stirred at room temperature for one hour and then solid NH_4PF_6 was added. After a further 30 minutes stirring, the solvent was removed in vacuo using a rotary-evaporator. The resulting dark brown solid was extracted into a solvent mixture in the ratio of CH_2Cl_2 : $CHCl_3$: acetone : MeOH = 20 : 10 : 5 : 1. TLC gave three spots ranging in colour from orange-brown, red brown to purple-brown. Using the same solvent, the three products corresponding to the three spots on TLC were separated using a silica gel column. The three solids were crystallized using Et_2O.

2.2.1 Formation of $[Ru_3S_2(cymene)_3](PF_6)_2$

The compound with the highest R_f was shown to be $[Ru_3S_2(cymene)_3](PF_6)_2$. The reaction for the formation of the $[Ru_3S_2(cymene)]^{2+}$ cluster is:

$$3\ [RuCl_2(cymene)]_2 + 4\ Na_2S \longrightarrow 2\ [Ru_3S_2(cymene)_3]Cl_2 + 8\ NaCl$$

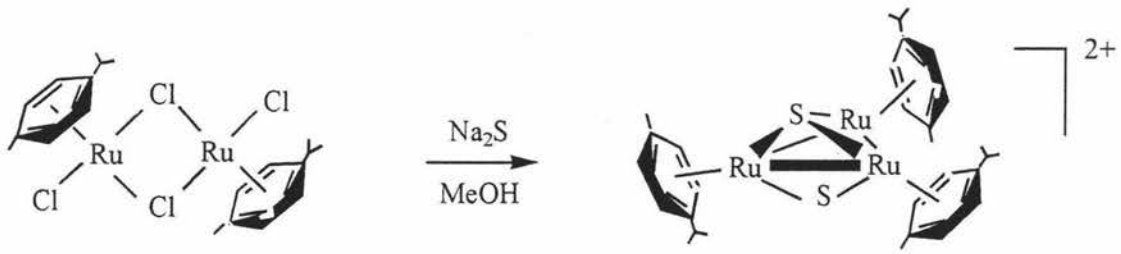

The solid had very bright orange brown colour. Because the method used was similar to that used by Rauchfuss et.al, it was likely that the $[Ru_3S_2(cymene)_3](PF_6)_2$ cluster might be one of the three products. But the three products were all different shades of brown, so it was difficult to judge which was the known compound based on the color alone.

^{1}H NMR spectra of $[Ru_3S_2(cymene)_3]^{2+}$ The absorptions due to the aromatic hydrogen atoms of the cymene rings can provide a convenient and sensitive probe of the nature of the compounds. The critical chemical shift on ^{1}H NMR for cymene-ruthenium compounds is the chemical shift of the four hydrogen atoms on cymene rings.

There are two chemically equivalent pairs of hydrogen atoms on the cymene ring (Figure 54, two H_a and two H_b). So two H_a atoms and two H_b atoms are isochronous which give the same chemical shift, respectively. If the cymene ring can move freely enough, they might be magnetic equivalent. That is, they are equally coupled to any one of the remaining nuclei. So that two H_a atoms couple with two H_b atoms giving a four doublet-of-doublet peaks as they do in many other mono- or di-nuclear complexes with cymene ligands, such as $[Ru_2Cl_2(N_3)_2(cymene)_2]^{2+}$ [103] and those arene-ruthenium-nitrogen complexes described in Chapter Three. This is another important reason for using cymene

instead of benzene besides the solubility of the compounds. Benzene ring only gives one single peak that is more difficult to recognize compared to the four doublet-of-doublet peaks.

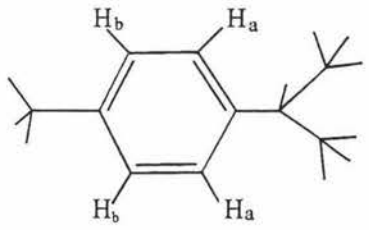

Figure 54 The two pairs of chemically equivalent hydrogen atoms on the cymene ring

Sometimes the two pairs of peaks might not be separated clearly because of coincidence. The two pairs of peaks might be close enough to give three peaks with the biggest one in the middle and two little peaks on each side. If the resolution of the ^1H NMR machine was not high enough to show the two little peaks (the one used in this experiment is 270 MHz), there would be only one peak shown on the spectrum. The $[Ru_3S_2(cymene)_3]^{2+}$ cluster might be in this case. (The $[Ru_5S_4(cymene)_4]^{2+}$ cluster is similar to the $[Ru_3S_2(cymene)_3]^{2+}$ cluster and this will be discussed in section 2.2.2)

But if the ring can not move very freely for steric reasons in a specific molecule, the two H_a atoms and the two H_b atoms might not be isochronous, respectively. Then they might couple in different ways giving different kinds of peaks from normal. (The big cluster and the $[Ru_4S_2(SO)(cymene)_4]^{2+}$ cluster might be in this case. This will be discussed in section 2.2.3).

^1H NMR spectrum for the reaction mixture gave only two single peaks at around 6 ppm and some multiple peaks at about 6-7 ppm which were not the four doublet-of-doublet peaks as it was expected. It was not reported what kind of peak obtained in the literature. Only an average chemical shift was given at 5.80 ppm. These made the identification more complicated. The multiple peaks seemed too far away from the literature. So the only possibility might be one of the two single peaks. But it was really unusual that the peak appeared without splitting into four peaks.

There were always two peaks on ^1H NMR spectra together and the chemical shifts changed in different solvents since the orange brown compound and the red brown compound are co-crystallized. Both of these made it more difficult to determine the compounds. The sample was always a mixture no matter how hard it was tried to pure the crystals. On the other hand, the two peaks gave different chemical shifts in different solvents such as $CDCl_3$ and D_6-acetone that are normally used. It was not clear what caused the differences, the different reaction condition or the different solvents.

There was also a third single peak on the spectrum. It was this single peak that gave the idea of solvent dependence of the chemical shifts for these compounds. This single peak did not appear every time. It appears at 5.60 ppm in D_6-acetone and 5.30 ppm in $CDCl_3$ (Figure 8, peak 2; Figure 7, peak 22).

The third single peak indicated a brown coloured oil-like compound. Because it was very difficult to obtain the crystal, it was still not clear what this compound was. This compound was supposed to be a mono-cationic cluster with hydride or SH as ligands. So a sample was run after 10 minutes of D_2O shaking. But no change was observed on that peak. On the other hand, the reactions of $[Ru_3S_2(cymene)_3]^{2+}$ and $[Ru_5S_4(cymene)_4]^{2+}$ with H_2, N_2 with reductants existing also gave some ideas of what this compound was. It appeared very often and had much more proportion comparing to the original clusters in the reaction. This suggested that it might be one neutral cluster of those three clusters or a polymer made of $[Ru_2S_2(cymene)_2]$ fragment. (This will be discussed later in mechanism section).

Chemical shift of the $[Ru_3S_2(cymene)_3](PF_6)_2$ cluster was solvent dependent. ^1H NMR spectra gave the different chemical shifts of the $[Ru_3S_2(cymene)_3](PF_6)_2$ cluster in different solvents. Spectrum obtained in $CDCl_3$ gave the chemical shift of hydrogen atoms on cymene rings at 5.92 ppm as double peaks (or four doublet-of doublet peaks) (Figure 7, peak 11). In D_6-acetone, a single peak was obtained at 6.13 ppm (Figure 8, peak one). Then the spectrum was run in CD_2Cl_2 giving four doublet-of-doublet peaks at average of 5.80 ppm which matched the chemical shift of $[Ru_3S_2(cymene)_3](PF_6)_2$ given in the literature very well (Figure 9, peak 1 and 2). Only in CD_2Cl_2, the spectrum could tell the difference between the two kinds of hydrogen atoms on cymene rings giving the four doublet-of-doublet peaks. (The sample in $CDCl_3$ was too dilute to tell the detail). That

might be because dichloromethane is less polar than chloroform and acetone, in which the resonance of two different kinds of hydrogen atoms on cymene rings is slow enough to be identifiable.

From Figure 9, it is also can be seen that the two peaks in the middle are very close. If the solvent changed to be more polar (or because of some other reasons), then the two middle peaks might join together giving one big peak in the middle coincidentally. This also supported the explanation why the $[Ru_3S_2(cymene)_3]^{2+}$ cluster (and the $[Ru_5S_4(cymene)_4]^{2+}$ cluster) only gave one single peak in $CDCl_3$ and D_6-acetone. (This will be discussed in section 2.2.2.)

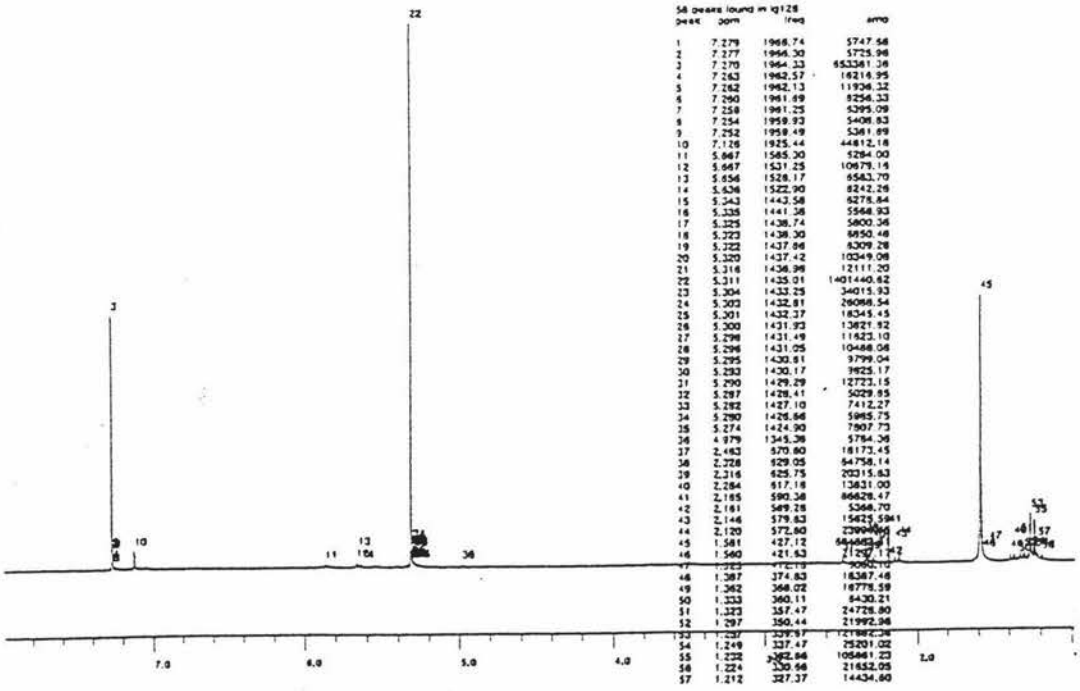

Figure 7 ^1H NMR spectrum of $[Ru_3S_2(cymene)_3]^{2+}$ in $CDCl_3$

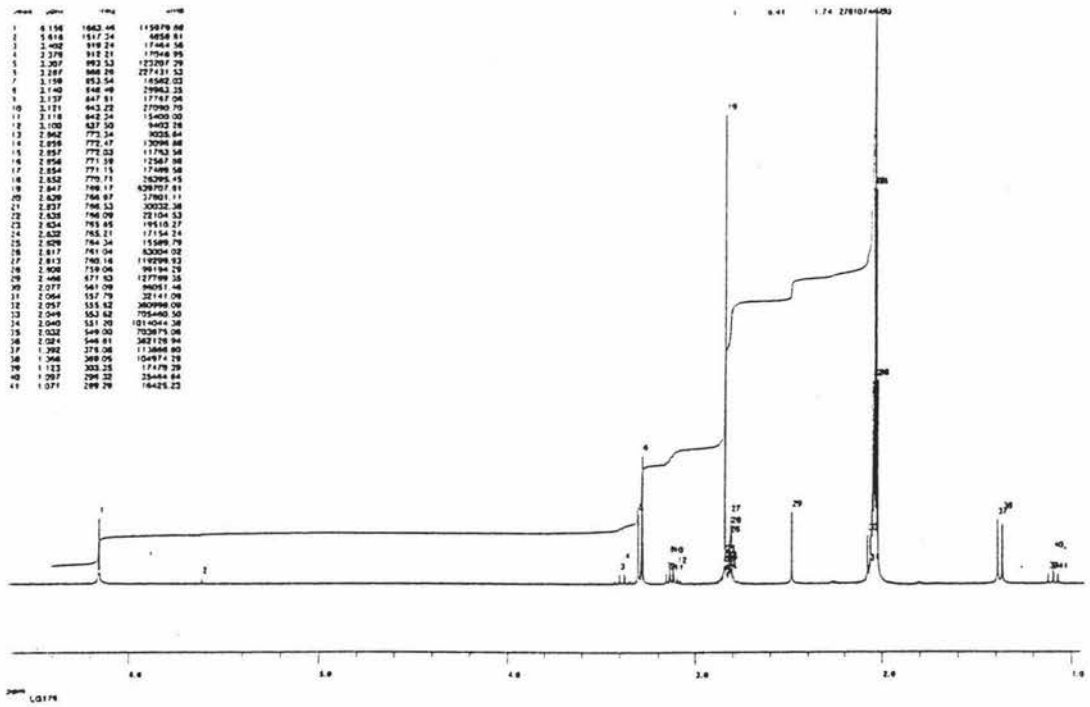

Figure 8 ^{1}H NMR spectrum of $[Ru_3S_2(cymene)_3]^{2+}$ in D_6-acetone

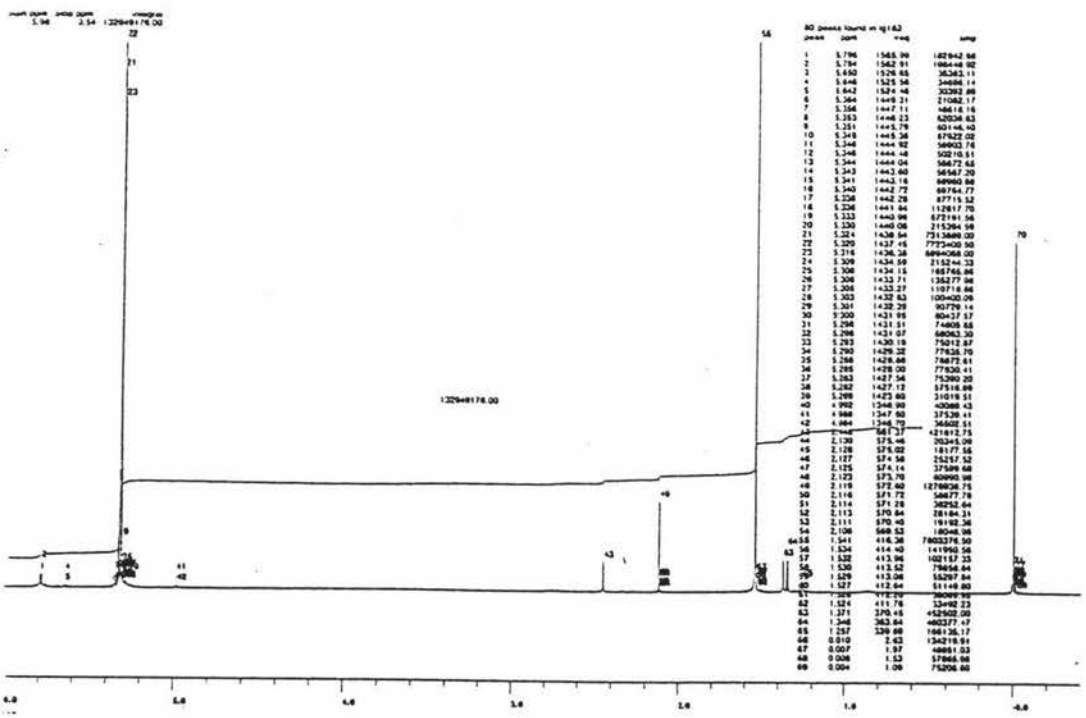

Figure 9 ^{1}H NMR spectrum of $[Ru_3S_2(cymene)_3]^{2+}$ in CD_2Cl_2

Electrospray mass spectrum of $[Ru_3S_2(cymene)_3](PF_6)_2$ The electrospray mass spectrum in acetone confirmed that the orange-brown compound was $[Ru_3S_2(cymene)_3](PF_6)_2$ giving a molecular ion peak at about 767 mass units (Figure 10). It is only 2 mass units deviation from the molecular weight of $[Ru_3S_2(cymene)_3]^{2+}$ (molecular weight for it is 769 mass units with ^{12}C, ^{1}H, ^{101}Ru, ^{32}S).

Electrospray mass spectrometry has been widely used for testing the molecular weight of large biological molecules such as proteins. It does not give the exact distribution of abundance, as does a FAB mass spectrometry but only the biggest peak. However it is much more convenient to use. Since the molecular weights of proteins are usually very big (at least 10,000 mass units), it is convenient to use electrospray mass spectrometry to tell the range of their molecular weights. But it is still relatively unusual to use it for organometallic compounds. For the three arene-ruthenium-sulfur clusters described in this chapter, electrospray mass spectrometry was used to differentiate between the clusters.

The peak at 916 mass units might be $[Ru_3S_2(cymene)_3(PF_6)]^+$. Usually molecular ion peak appears at the highest field. But in this case the highest peak could not be the molecular ion peak. There are two possibilities that fragment falls off making the weight less than 100 mass units, the weight for cymene fragment is about 134 mass units (^{12}C and ^{1}H mostly). For one ruthenium atom and one sulfur atom fragment, the weight is around 133 mass units (^{101}Ru and ^{32}S mostly). They are both at least 15 mass units less than 149 mass units that is the difference between the highest weight peak (916 mass units) and molecular ion peak (767 mass units). The highest peak indicated a one plus cation. Since the cluster is a two plus cation, it might combine an anion to form a one plus cation during the process. The anion might come from the anion of the cluster salt (PF_6^-) or from the solvent (acetone, CH_3CO^-). The weight of PF_6^- fragment (145 mass units) is close to the difference (149 mass units) and it seems reasonable that one PF_6^- fragment might combined the two plus cationic cluster giving the one plus cationic cluster $[Ru_3S_2(cymene)_3(PF_6)]^+$.

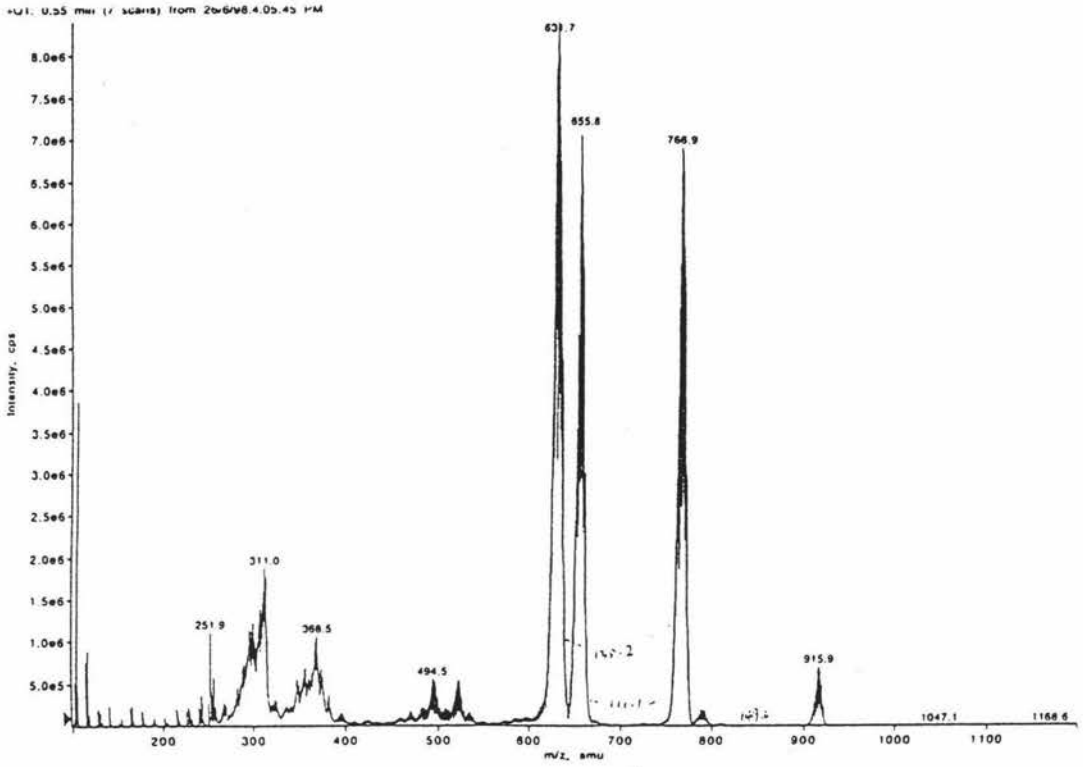

Figure 10 Electrospray mass spectrum of $[Ru_3S_2(cymene)_3]^{2+}$

The structure of the $[Ru_3S_2(cymene)_3](PF_6)_2$ cluster Rauchfuss et.al have reported the crystal structure of the $[Ru_3S_2(cymene)_3](PF_6)_2$ cluster. The ruthenium-sulfur core had a closo structure with two μ_3-sulfur atoms capping the two faces of the ruthenium triangle (Figure 4 b).[5]

As it was described before, the interesting aspect of the structures of the two clusters was that one of the metal-metal bonds opened when the cationic cluster $[Ru_3S_2(cymene)_3]^{2+}$ gained two electrons giving the reduced cluster $[Ru_3S_2(cymene)_3]^0$ (Figure 11). The distance of Ru(1)-Ru(3) changed from 2.763(1) Å in the cationic cluster to 3.612(1) Å in the neutral cluster, which fell into non-bonding range. The bond angle of Ru(1)-Ru(2)-Ru(3) also changed from $59.5(1)^0$ in the cationic cluster to $83.1(1)^0$ in the neutral cluster. This strongly supported that sulfur-bridged ruthenium cluster could provide a relatively robust metal-sulfur framework retaining its original nuclearity without falling apart during the reactions. The prospect of useful catalytic applications stimulated the work described in this study.

Some selected bond lengths and bond angles are listed in table 11 [5].

	$[Ru_3S_2(cymene)_3]^{2+}$	$[Ru_3S_2(cymene)_3]^{0}$
Bond lengths / Å		
Ru1-Ru2	2.775 (1)	2.733 (1)
Ru2-Ru3	2.796 (1)	2.712 (1)
Ru3-Ru1	2.763 (1)	3.612 (1)
Ru1-S1	2.266 (2)	2.329 (2)
Ru2-S1	2.267 (2)	2.351 (2)
Ru3-S1	2.265 (1)	2.340 (2)
Ru1-S2	2.272 (1)	2.235 (2)
Ru2-S2	2.271 (2)	2.348 (2)
Ru3-S2	2.263 (2)	2.328 (2)
Bond angles / ^{0}		
Ru1-Ru2-Ru3	59.5 (1)	83.1 (1)
Ru2-Ru3-Ru1	59.9	
Ru3-Ru1-Ru2	60.6 (1)	
Ru1-S1-Ru2	75.5 (1)	71.5 (1)
Ru1-S1-Ru3	75.1 (5)	101.4 (1)
Ru1-S2-Ru2	75.3 (1)	74.1 (1)
Ru1-S2-Ru3	75.1 (1)	101.6 (1)
Ru2-S2-Ru3	76.2 (1)	70.9 (1)
S1-Ru1-S2	89.9 (1)	77.7 (1)

Table 11 Data of X-ray crystallography for $[Ru_3S_2(cymene)_3]^{2+}$ and $[Ru_3S_2(cymene)_3]$

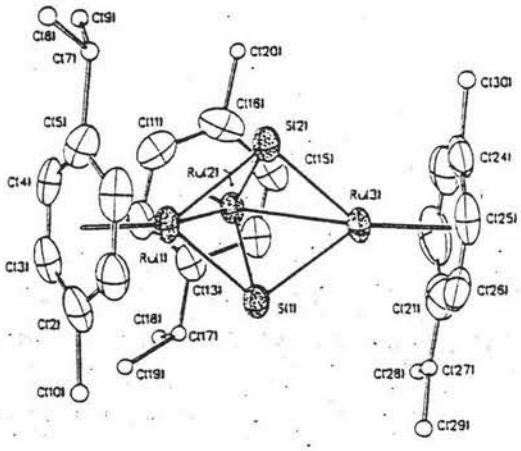

Figure 11 Structure of $[Ru_3S_2(cymene)_3]$

2.2.2. Formation of $[Ru_5S_4(cymene)_4](PF_6)_2$

The compound with the second highest R_f was shown to be the novel high nuclearity $[Ru_5S_4(cymene)_4](PF_6)_2$ cluster.

The reaction of formation of the $[Ru_5S_4(cymene)_4]^{2+}$ cluster is:

$$5\ [RuCl_2(cymene)]_2 + 8\ Na_2S \longrightarrow 2\ [Ru_5S_4(cymene)_4]Cl_2 + 16\ NaCl + 2\ cymene$$

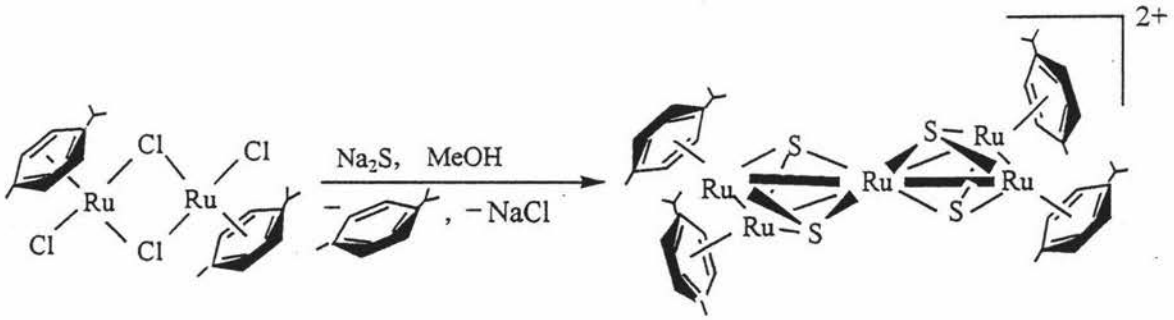

After chromatographic separation, the red-brown solid was crystallized using Et_2O. The $[Ru_5S_4(cymene)_4](PF_6)_2$ cluster and the $[Ru_3S_2(cymene)_3](PF_6)_2$ cluster were still hard to be absolutely pure. Even during recrystallization, they always crystallized under the similar condition and at same time, which meant that they co-crystallized. Therefore, it was always a mixture on the ^1H NMR spectra, even when the crystals were chosen one by one. Only the ratio could tell which one is which.

The chemical shift of this cluster was solvent dependent as well as the $[Ru_3S_2(cymene)_3]^{2+}$ cluster. The ^1H NMR spectrum of red-brown crystals was run in $CDCl_3$. Two double peaks (or four doublet-of-doublet peaks, because the sample was too dilute to give a clear spectrum) at 5.66 ppm were observed for the chemical shift of hydrogen atoms on cymene rings (Figure 12). In D_6-acetone, the single peak appeared at 5.92 ppm (Figure 13). ^1H NMR spectrum was also run in CD_2Cl_2 giving still one single peak at 5.61 ppm (Figure 14), which did not split into four doublet-of-doublet peaks as did the $[Ru_3S_2(cymene)_3]^{2+}$ cluster because of coincidence.

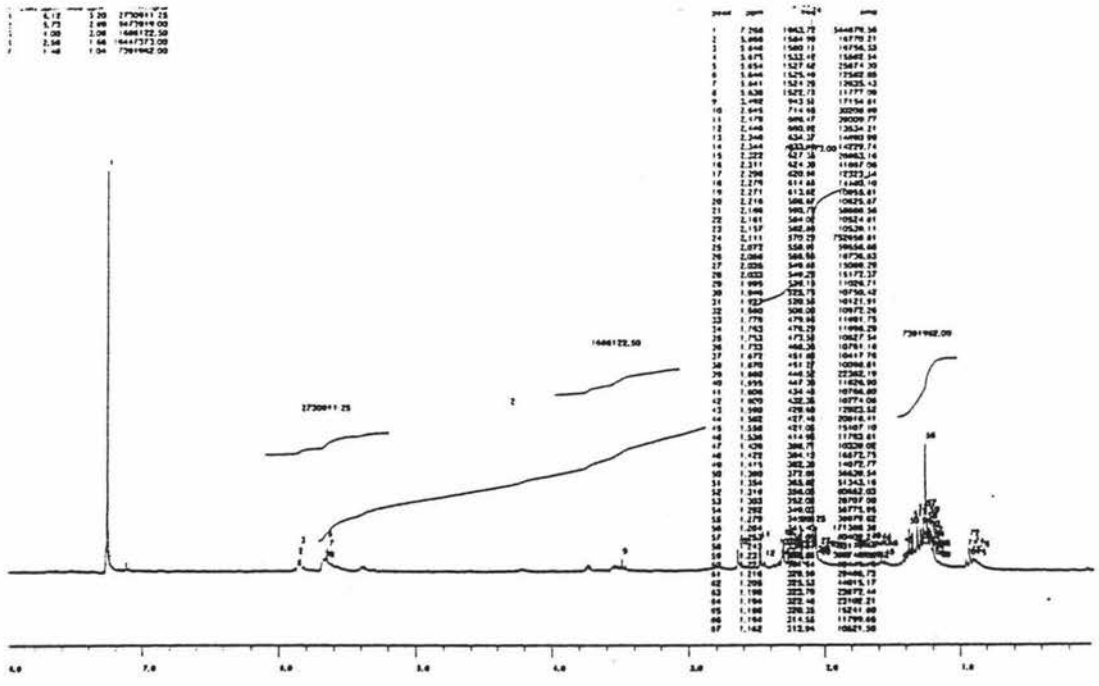

Figure 12 ^1H NMR spectrum of $[Ru_5S_4(cymene)_4]^{2+}$ in $CDCl_3$

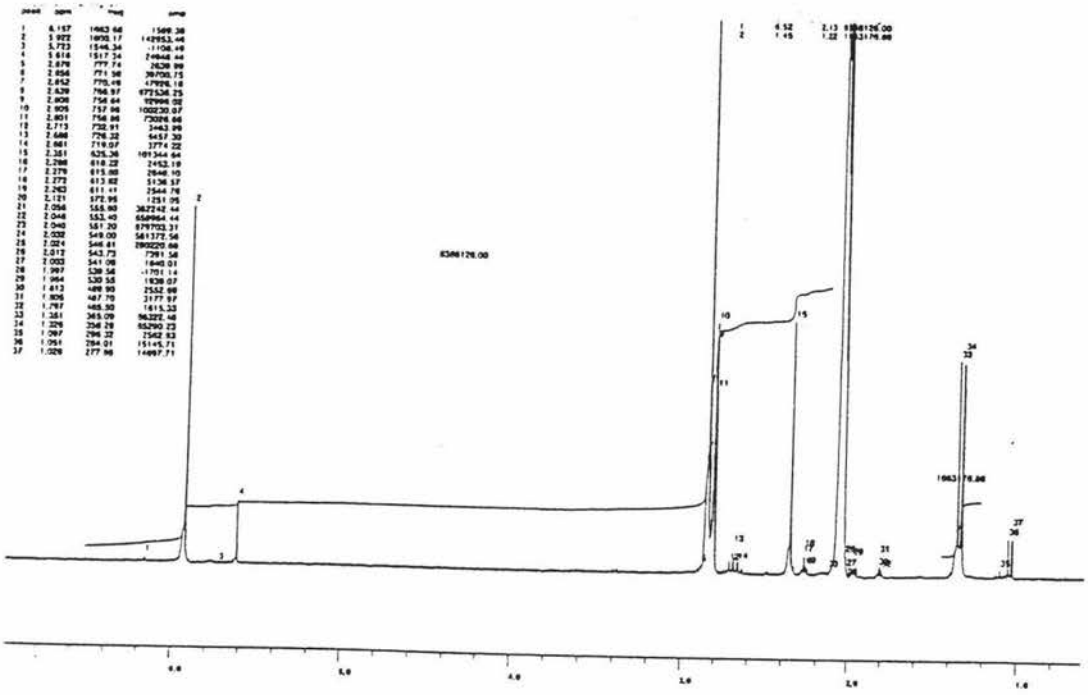

Figure 13 ^{1}H NMR spectrum of $[Ru_5S_4(cymene)_4]^{2+}$ in D_6-acetone

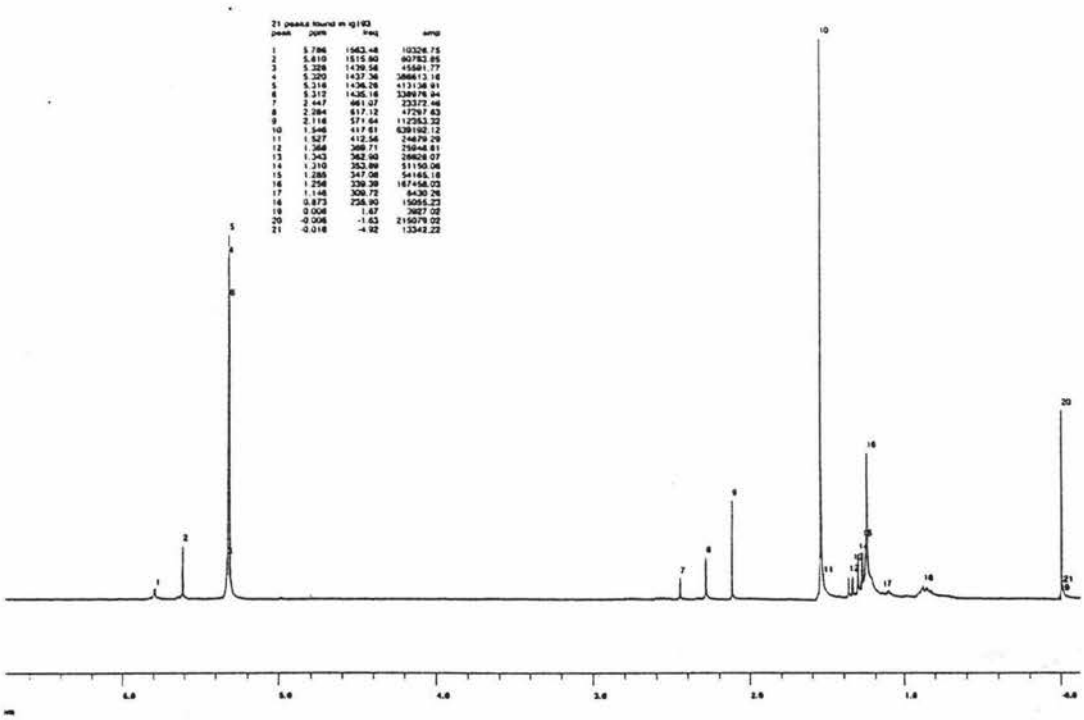

Figure 14 ^{1}H NMR spectrum of $[Ru_5S_4(cymene)_4]^{2+}$ in CD_2Cl_2

The FAB mass spectrum (Figure 15 a) gave the molecular ion peak at 1170 mass units showing that the red-brown compound was a high nuclearity ruthenium cluster matching the formula of $Ru_5S_4(cymene)_4$ or $Ru_6S_5(cymene)_3$. The isotopic distribution (Figure 15 b) given on the spectrum matched the corresponding calculation for $[Ru_5S_4(cymene)_4]^+$ very well. As with the case of the $[Ru_3S_2(cymene)_3]^{2+}$ cluster, there was another peak at higher field, 1317 mass units. The difference between 1317 and 1170 mass units was 147 mass units that was close to the weight of the PF_6^- fragment (145 mass units). So the peak at 1317 mass units might be $[Ru_5S_4(cymene)_4](PF_6)]^+$. (This is similar to the discussion on the $[Ru_3S_2(cymene)_3]^{2+}$ cluster in section 2.2.1).

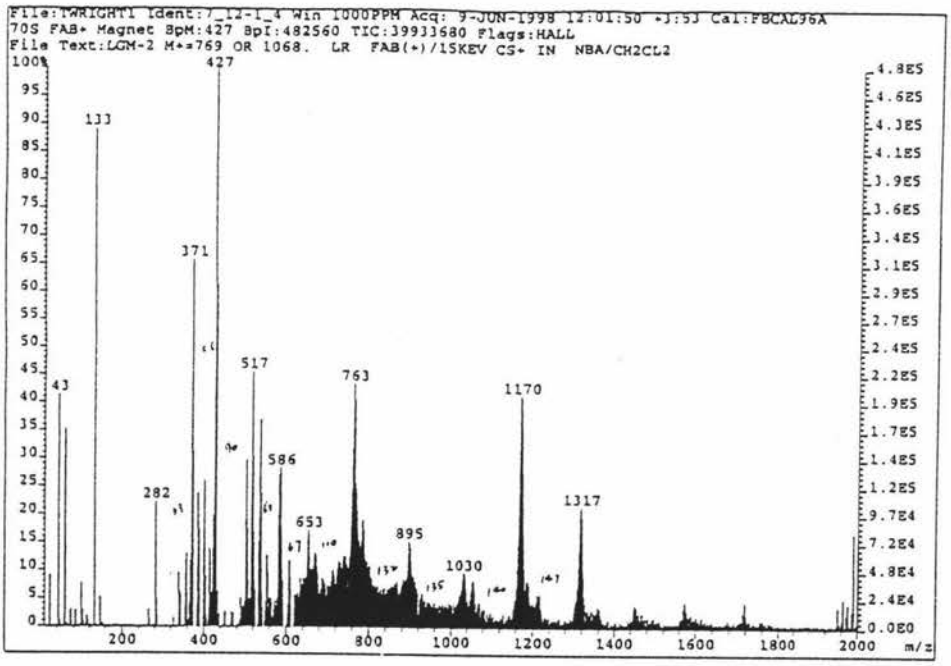

Figure 15a FAB mass spectrum of $[Ru_5S_4(cymene)_4]^{2+}$

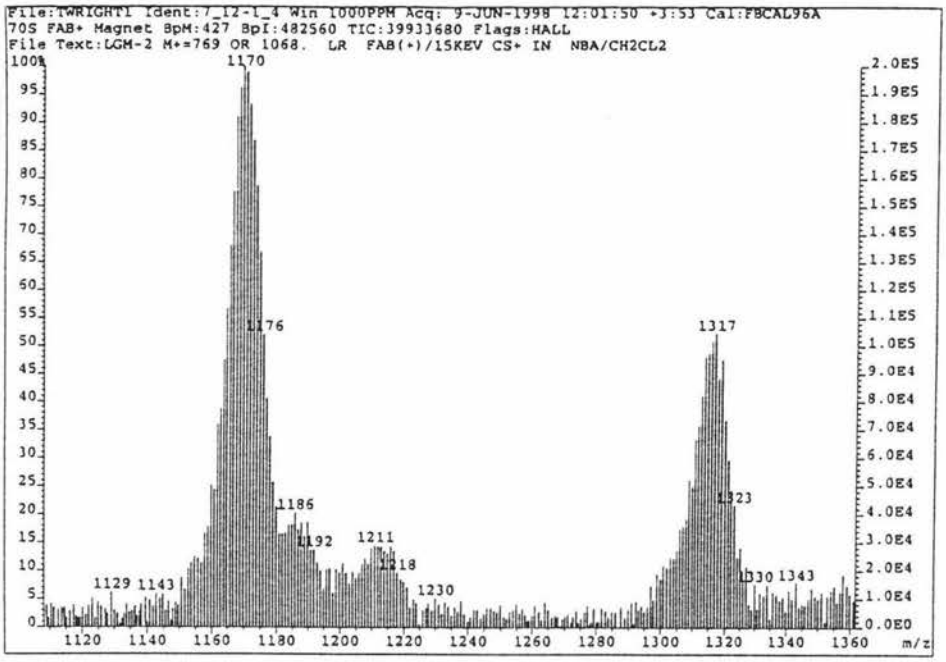

Figure 15b Isotopic distribution of FAB mass spectrum of $[Ru_5S_4(cymene)_4]^{2+}$

Structure of $[Ru_5S_4(cymene)_4](PF_6)_2$ The red brown solid was recrystallized using the isobestic method. Several kinds of crystals of this cluster were obtained in CH_2Cl_2 / Et_2O solution, rectangular thin black crystals (sometimes the red-brown color could be seen when the crystal was thin enough), black flower-like crystals and red-brown crystals with ill-defined shapes. X-ray crystallography for a black thin crystal with two diamond-like faces capped on the rectangular face gave the structure of the cluster. The ORTEP view of the structure of this cluster is given in Figure 16. The selected data is listed in Table 6.

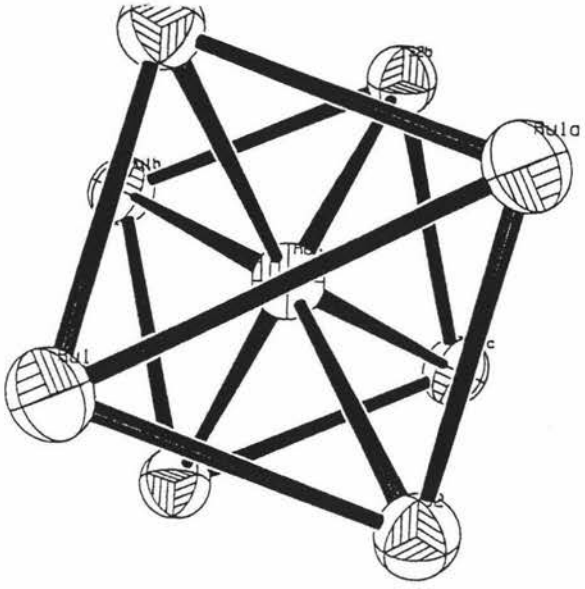

Figure 16 ORTEP structure of $[Ru_5S_4(cymene)_4]^{2+}$

Cluster X		Cluster Y	
Bond lengths / Å		Bond lengths / Å	
Ru1-S1	2.2848(8)	Ru3-S2	2.3230 (9)
Ru1-Ru2	2.6953 (4)	Ru3-Ru4	2.7310 (4)
Ru1-Ru1a	2.7904 (6)	Ru3-Ru3a	2.7375 (6)
Ru1-S1a	2.3185 (9)	Ru3-S2a	2.2491 (9)
Ru2-S1	2.2565 (8)	Ru4-S2	2.2766 (8)
Ru2-Ru1a	2.6953 (5)	Ru4-Ru3a	2.7310 (6)
Bond angles (°)		Bond angles (°)	
S1-Ru1-Ru2	53.1 (2)	S2-Ru3-Ru4	52.80 (2)
S1-Ru1-Ru1a	52.14 (2)	S2-Ru3-Ru3a	51.99 (2)
Ru2-Ru1-Ru1a	58.825 (8)	Ru4-Ru3-Ru3a	59.921 (7)
Ru1a-Ru2-Ru1	62.350(15)	Ru3a-Ru4-Ru3	60.157 (15)
S1a-Ru2-S1	94.59 (4)	S2a-Ru4-S2	92.90 (4)
Ru1b-Ru2-Ru1	125.626(15)	Ru3b-Ru4-Ru3	127.803 (15)
S1-Ru2-Ru1a	54.98 (2)	S2-Ru4-Ru3a	52.42 (2)

Table 6 X-ray crystallographic data of $[Ru_5S_4(cymene)_4](PF_6)_2$

The ruthenium sulfur core is a twisted bowtie with a ruthenium atom in the center. Thus two Ru_3S_2 are joined together at one ruthenium atom. The metal-sulfur framework has high symmetry with the space group of F_{ddd}, so only parts of the data are given. There are two cluster molecules in the asymmetric unit of the unit cell and the crystal contains two clusters with slightly different bond lengths and angles (Figure 60).

The average bond length of Ru-Ru for the $[Ru_5S_4(cymene)_4]^{2+}$ cluster is about 2.71 Å (for cluster X is 2.70 Å and for cluster Y is 2.73 Å) while the average bond length of Ru-Ru for the $[Ru_3S_2(cymene)_3](PF_6)_2$ cluster is 2.78 Å that is 0.06 Å longer than the former cluster. It might be because that in the $[Ru_3S_2(cymene)_3](PF_6)_2$ cluster cymene rings are so close that they push against each other in order to stabilize the cluster.

In the same molecule, the bond length between side ruthenium atoms and the central ruthenium atom and those between two side ruthenium atoms are slightly different. For cluster X, bond length of Ru1-Ru2 is 2.6953(4) Å while that of Ru1-Ru1a is 2.7904(6) Å, which is 0.0051 Å different. For cluster Y, bond length of Ru3-Ru4 is 2.7310 Å while that of Ru3-Ru3a is 2.7375 Å, which is 0.0065 Å different. It means that the two triangles in both clusters are not exactly equilateral, the two wing sides are slightly longer since the cymene rings on these four ruthenium atoms push against each other to keep enough distance between them.

The bond angle of Ru2-Ru1-Ru1a (in cluster X) and Ru4-Ru3-Ru3a (in cluster Y) are $58.825(8)^0$ and $59.921(7)^0$, respectively, that are less than 60^0. But in the $[Ru_3S_2(cymene)_3](PF_6)_2$ cluster the bond angles of the three ruthenium atoms are $59.5(1)^0$, $59.9(1)^0$ and $60.6(1)^0$, respectively. The average of them is 60.0^0, in which the triangle is almost equilateral since those three ruthenium atoms of the triangle are almost the same.

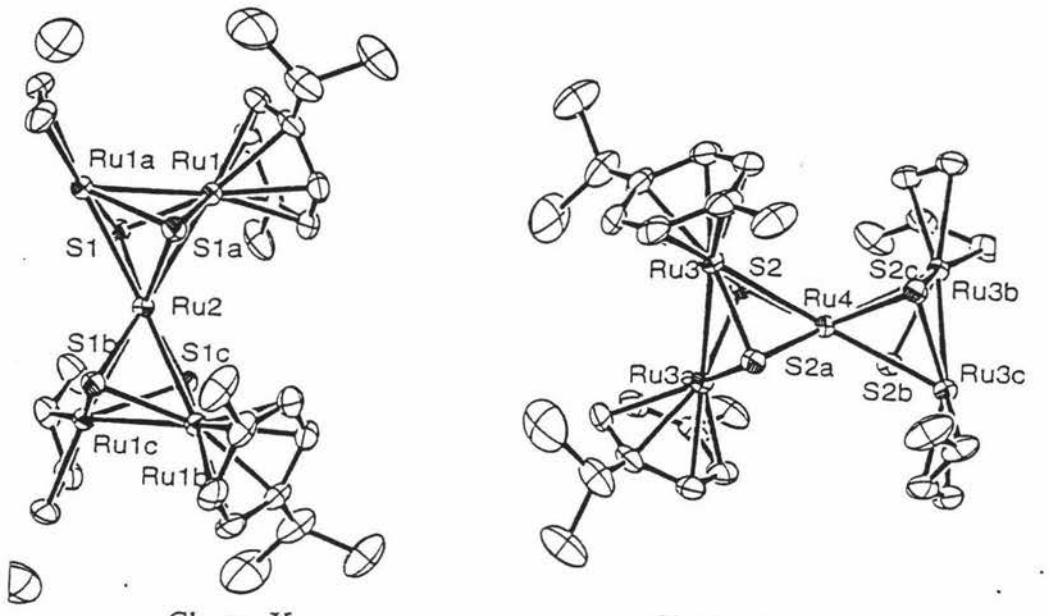

Cluster X Cluster Y

Figure 60 X ray crystallographic structure of $[Ru_5S_4(cymene)_4](PF_6)_2$

The central ruthenium atom The four side ruthenium atoms in the $[Ru_5S_4(cymene)_4](PF_6)_2$ cluster are almost the same, but they are different from the central ruthenium atom without coordinating cymene ring.

The central ruthenium atom has eight-coordination, which is rare for group eight transition metals except some hydride clusters. The only precedent is the iron atom in the hetero-metal cluster $[(Cp^*Ir)_2(\mu_3\text{-}S)_2Fe(Cp^*Ir)_2]Cl$ [80] that has the same bowtie structure as does the $[Ru_5S_4(cymene)_4](PF_6)_2$ cluster.

To examine how different the central ruthenium atom was compared with the side ruthenium atoms, both semi-emperical and Hartree-Fock calculations were carried out. The calculation of electrostatic charges tells the difference between side ruthenium atoms and the central ruthenium atom (Table 7). These data are fairly reasonable, but much less than Ru^{2+} from oxidation state. Sulfur atoms pull electrons from ruthenium atoms while the cymene rings push electrons to them, so the side ruthenium atoms are almost neutral (-0.05 or 0.05). The central ruthenium atom without coordinating cymene ligands has positive charges (0.43 or 0.26).

	Ru (1) (side)	Ru (2) (central)	S
Semi-emperical	-0.05	0.43	-0.27
Hartree-Fock	0.05	0.26	-0.24

Table 7 Electrostatic charges of Ru atoms in $[Ru_5S_4(cymene)_4](PF_6)_2$

The reactivity of this cluster needs further research, especially the reactivity of the central ruthenium atom, which is the critical difference between $[Ru_5S_4(cymene)_4](PF_6)_2$ and $[Ru_3S_2(cymene)_3](PF_6)_2$ clusters. The central ruthenium atom might act very important role in catalytic reaction. It just likes a bridge that might spread the charges on the whole molecule. The cluster would be relatively stable when it gains or loses electrons during the reaction. Therefore the ability of transferring and storing electrons should increase compared to the $[Ru_3S_2(cymene)_3](PF_6)_2$ cluster.

Cymene loss It needs to be mentioned that there were cymene rings falling off during the reaction. It was really unusual that it happened under such a mild condition with only stirring at room temperature. Usually cymene rings can coordinate to the metal atoms stably under 130^0C in reactions. Firstly, The original cymene-ruthenium-chloride dimer, $[RuCl_2(cymene)]_2$ was obtained by refluxing trichlororuthenium with cyclohexadiene at about 90^0C [105]. Secondly, organometallic compounds with cymene ligands usually give up cymene rings at above 130^0C, which has also been proven by cymene-ruthenium-nitrogen complexes in Chapter Three.

There were also some byproducts that might form by loss of cymene rings. The very dark coloured oil did not dissolve in acetone or dichloromethane. They might be ruthenium sulfide or polymer, both of which have cymene rings lost. It might be because that S^{2-} is a strong enough base to make dimer decompose. This has been proven by the very low yields of the three clusters. The isolated yield of the $[Ru_3S_2(cymene)_3](PF_6)_2$ cluster was 5.2 %, yield of the $[Ru_5S_4(cymene)_4](PF_6)_2$ cluster was 13.1% and yield of the big cluster or the $[Ru_4S_2(SO)(cymene)_4](PF_6)_2$ cluster was 26.9%. The exact reason was still unknown. The mechanism of formation of the $[Ru_5S_4(cymene)_4](PF_6)_2$ cluster and the $[Ru_3S_2(cymene)_3](PF_6)_2$ cluster will be discussed in detail later in proposed mechanism section.

Valence electrons and the structure Metal sulfur clusters are expected to provide good systems for the study on structural changes of polynuclear complexes triggered by perturbation in their electronic states because sulfur-based ligands behave as effective bridging ligands and prevent the cluster cores from fragmenting into metal species of lower nuclearity on redox reactions.

It is widely accepted that the number of metal-metal bonds in cluster complexes corresponds with their total electron counts [104]. Recently, Hidai et.al made a series hetero-metal penta-nuclear clusters, $[(Cp^*Ir)_2(\mu_3\text{-}S)M(\mu_3\text{-}S)(IrCp^*)_2]^{n+}$ (M = Fe, Co, Ni; n = 1,2) providing the examples of 78-81e$^-$ bow-tie clusters, which showed interesting structure changes depending on their valence electron counts [81].

If a cluster has 78 valence electrons, the cluster core is expected to have most typically six metal-metal single bonds [81]. In all cases, the Ir-Ir distances were diagnostic of a single metal-metal bond, while the interaction between the iridium and the central hetero-metal atom varied significantly with the oxidation state of the cluster core and the nature of the hetero-metal atoms. For 78e$^-$ cluster $[(Cp^*Ir)_2S_2FeS_2(IrCp^*)_2]^{2+}$, all the Ir-M bonds were short (2.60-2.79 Å). For 79e$^-$ clusters $[(Cp^*Ir)_2S_2FeS_2(IrCp^*)_2]^{+}$, $[(Cp^*Ir)_2S_2CoS_2(IrCp^*)_2]^{2+}$ and 80e$^-$ cluster $[(Cp^*Ir)_2S_2CoS_2(IrCp^*)_2]^{+}$, they each had two short Ir-M bonds and two long Ir-M bonds (2.85-2.94 Å). These bond lengths still fell into the bonding range although the bonding changed to be weaker while the bond length changed to be longer. But for 80e$^-$ cluster $[(Cp^*Ir)_2S_2NiS_2(IrCp^*)_2]^{2+}$, there was two short distances and two nonbonding distances (3.124 Å and 3.135 Å). When it gained one electron to 81e$^-$ cluster $[(Cp^*Ir)_2S_2NiS_2(IrCp^*)_2]^{+}$, one of the nonbonding distances changed to weak bonding distance (2.941 Å) while another changed to be longer (3.281 Å). The structure of this cluster was distorted (Figure 49) [81].

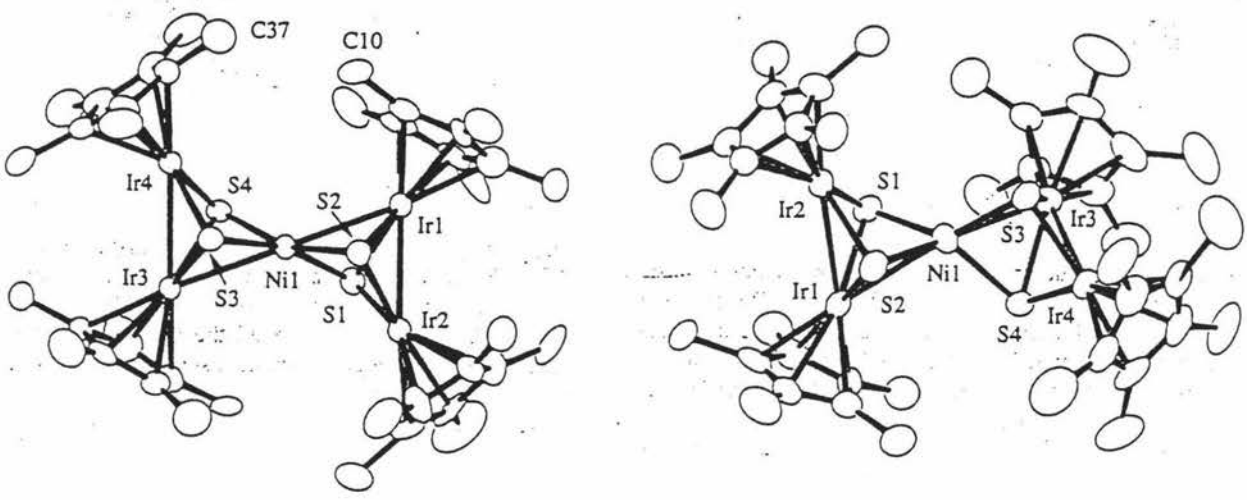

Figure 49 Structures of 80e⁻ and 81e⁻ clusters with nonbonding distances

$[Ru_5S_4(cymene)_4]^{2+}$ cluster with 78 valence electrons agrees this very well. It has six short metal-metal single bonds (2.6953-2.7375 Å), which all fall into the range of strong bonding. This gives the strong evidence of the above discussion. Ab initio calculation also shows that the bond distances change to longer when it gains one extra electron to 79 valence electrons.

Bond lengths and valence electron numbers of these bowtie clusters are listed in Table 12.

Compounds	Valence electron numbers	Bond lengths / Å
$[Ru_5S_4(cymene)_4]^{2+}$	78	2.6953-2.7375
$[(Cp^*Ir)_2S_2FeS_2(IrCp^*)_2]^{2+}$	78	2.60-2.79
$[(Cp^*Ir)_2S_2FeS_2(IrCp^*)_2]^{+}$	79	Two 2.60-2.79 and two 2.85-2.94
$[(Cp^*Ir)_2S_2CoS_2(IrCp^*)_2]^{2+}$		(weak bonding)
$[(Cp^*Ir)_2S_2CoS_2(IrCp^*)_2]^{+}$	80	Two 2.60-2.79 and two 2.85-2.94
$[(Cp^*Ir)_2S_2NiS_2(IrCp^*)_2]^{2+}$	80	Two 2.60-2.79 and two 3.124 and 3.135 (non bonding)

$[(Cp^*Ir)_2S_2NiS_2(IrCp^*)_2]^+$	81	Two 2.60-2.79, 2.941 (weak bonding)and 3.281 (non bonding)

Table 12 Bond lengths vary with valence electron numbers of some bowtie clusters

Dihedral angles The dihedral angle between the two metal framework planes is not determined by the number of valence electrons but by the type of the central metal atoms and side metal atoms. That is, their dihedral angles are similar when the central metal atom is isoelectronic to the side metal atoms. Dihedral angle of 78 valence electron cluster $[Ru_5S_4(cymene)_4]^{2+}$ was 56.1^0 while the dihedral angle of another 78e⁻ cluster $[(Cp^*Ir)_2S_2FeS_2(IrCp^*)_2]^{2+}$ was 73.4^0 that was quite different to the former. But for 79 valence electron cluster $[(Cp^*Ir)_2S_2CoS_2(IrCp^*)_2]^{2+}$, the dihedral angle was 49.9^0 [81] that was close to that of the $[Ru_5S_4(cymene)_4]^{2+}$ cluster (56.1^0) (Figure 17). It might be because Co and Ir were the same group transition metals therefore the $[(Cp^*Ir)_2S_2CoS_2(IrCp^*)_2]^{2+}$ cluster was more similar to the mono-metal cluster $[Ru_5S_4(cymene)_4]^{2+}$ with the same charge. That is, the central metal atom was isoelectronic to the side metal atoms in these two clusters. This might be the main influence to dihedral angle of the two metal framework in one cluster. The dihedral angle of $[(Cp^*Ir)_2S_2FeS_2(IrCp^*)_2]^+$ (57.6^0) [81] was also similar to that of the $[Ru_5S_4(cymene)_4]^{2+}$ cluster. It was also an 79e⁻ cluster as is $[(Cp^*Ir)_2S_2CoS_2(IrCp^*)_2]^{2+}$ but not 78e⁻ cluster. The one extra electron might be added on the central metal Fe atom making it have same electrons and similar character with Co atom in the $[(Cp^*Ir)_2S_2CoS_2(IrCp^*)_2]^{2+}$ cluster (Figure 17) [81].

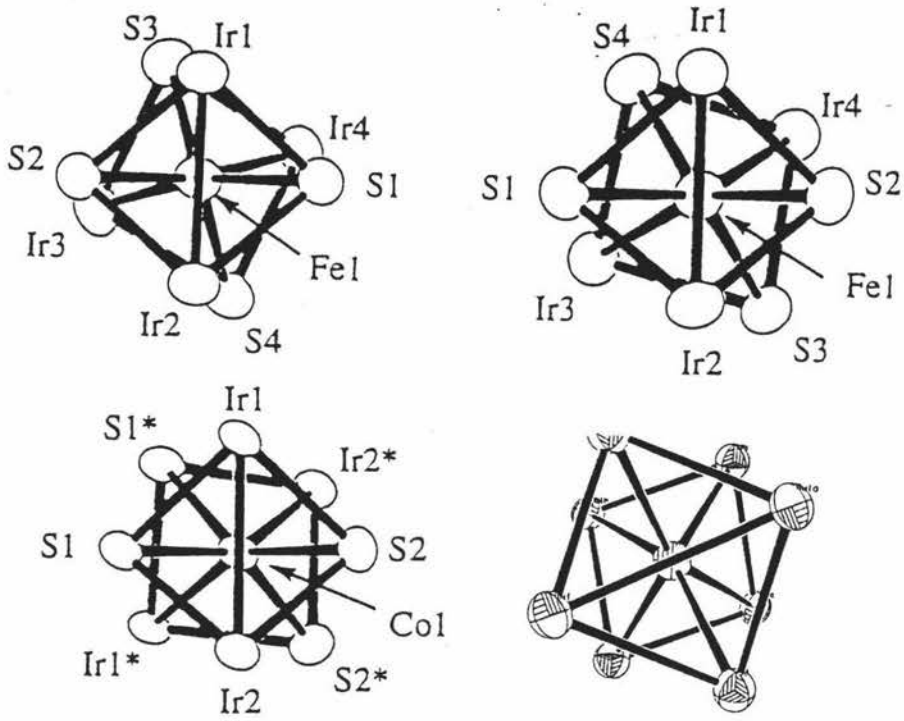

Figure 17 Compare the dihedral angle of $[(Cp^*Ir)_2S_2FeS_2(IrCp^*)_2]^{2+}$, $[(Cp^*Ir)_2S_2FeS_2(IrCp^*)_2]^{+}$, $[(Cp^*Ir)_2S_2CoS_2(IrCp^*)_2]^{2+}$ and $[Ru_5S_4(cymene)_4]^{2+}$

The dihedral angles, the central and side metal atoms of these bowtie clusters are listed in Table 13.

Compounds	Central metal atoms	Side metal atoms	Valence electron numbers	Dihedral angles
$[Ru_5S_4(cymene)_4]^{2+}$	Ru (2+)	Ru	78	56.1^0
$[(Cp^*Ir)_2S_2CoS_2(IrCp^*)_2]^{2+}$	Co (2+)	Ir	79	49.9^0
$[(Cp^*Ir)_2S_2FeS_2(IrCp^*)_2]^{+}$	Fe (1+)	Ir	79	57.6^0
$[(Cp^*Ir)_2S_2FeS_2(IrCp^*)_2]^{2+}$	Fe (2+)	Ir	78	73.4^0

Table 13 Dihedral angles of some bowtie clusters

Hidai and co-workers have attempted to understand the different angles using Extended Huckel Molecular Orbital calculations (EHMO calculations). For the hypothetical $[(Cp^*Ir)_2S_2FeS_2(IrCp^*)_2]^{2+}$ cluster ($78e^-$) with D_2-idealised structure [81], its total energy of this cluster was found to decrease with increasing the dihedral angle (θ) between the two Ir_2Fe planes from 0 to 60^0, but it was independent of θ values for higher ones. The deviation of the dihedral angle from 90^0 (D_{2d} symmetry) was described mainly to the steric congestion between the Cp* on each Ir_2Fe fragment and the sulfur ligands on the other Ir_2Fe moiety. So the dihedral angle was idealised at 73.4^0.

Similar calculations were also done for $79e^-$ clusters $[(Cp^*Ir)_2S_2FeS_2(IrCp^*)_2]^+$ and $[(Cp^*Ir)_2S_2CoS_2(IrCp^*)_2]^{2+}$ with D_{2d} symmetry modeled and C_2 structure ($\theta = 90^0$) modeled, respectively [81]. Both clusters exhibit closely related structures to each other, in which only two of the four Ir-M bonds were significantly lengthened. It appeared that the extra electron was added to an Ir-M anti-bonding orbital to decrease the Ir-M bond order. The calculation results are shown in Figure 52. In the mono cationic cluster $[(Cp^*Ir)_2S_2FeS_2(IrCp^*)_2]^+$, there were two conformations with the θ values of 45^0 and 135^0. Since in the conformer with θ value of 135^0 the Cp* ligands on two Ir atoms were considered to be brought close together so that congestion made this conformation much less stable. So the θ value of approximately 45^0 was expected. The crystallography gave the dihedral angle of 57.6^0 that was very close to the prediction from the calculation. Similar result was also obtained for another $79e^-$ cluster $[(Cp^*Ir)_2S_2CoS_2(IrCp^*)_2]^{2+}$ (49.9^0).

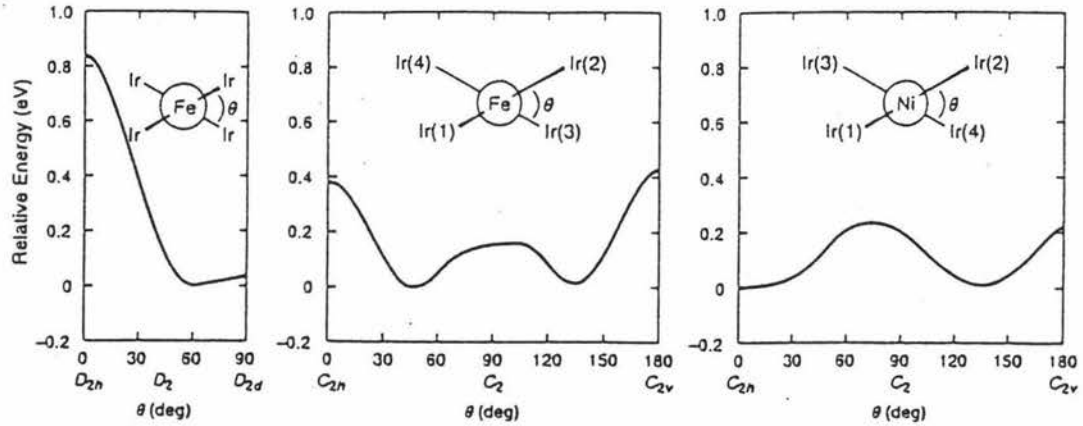

Figure 52 Dihedral angle dependence of the total energies for $[(Cp^*Ir)_2S_2FeS_2(IrCp^*)_2]^{2+}$, $[(Cp^*Ir)_2S_2FeS_2(IrCp^*)_2]^+$ and $[(Cp^*Ir)_2S_2CoS_2(IrCp^*)_2]^{2+}$

Molecular aggregation and molecular structure Transition metal clusters have properties that are intermediate between those of dispersed and bulk metals [103]. These properties depending on intermolecular aggregation of clusters would influence the catalytic ability on the surface during the reaction. So it is very important to know the solid state structure of the cluster as well as its molecular structure. X-ray analysis can give some information on the molecular organization in the crystals as well as the molecular structure.

Originally, information on the molecular organization in solid has appeared mainly as a byproduct of the primary analytical goal. Little is known about the factors responsible for intermolecular aggregation of clusters, crystal formation and crystal stability. In 1990s, great progress has been made in this area. The most interesting molecular arrangement was found by Johnson et.al in 1991. The difference in molecular structures (different coordination modes of benzene rings) leads to the difference in crystal structures (different molecular aggregations) between isomeric bis-arene clusters $Ru_6C(CO)_{11}(\mu_3\text{-}\eta^2\text{:}\eta^2\text{:}\eta^2\text{-}C_6H_6)(\eta^6\text{-}C_6H_6)$ [109] and $Ru_6C(CO)_{11}(\eta^6\text{-}C_6H_6)_2$ [110]. Their snake-like and row-like molecular aggregations are shown in Figure 53 in Chapter one, respectively.

The way of molecular aggregation in crystals (solid states) is determined by its specific molecular structure. From the crystallography of one unit cell for $[Ru_5S_4(cymene)_4](PF_6)_2$ cluster, the molecular aggregation in the crystals can be seen clearly. In the crystal, the cymene rings of two adjacent $[Ru_5S_4(cymene)_4](PF_6)_2$ clusters pack almost parallel. The shortest distances between the two carbon atoms on different cymene rings in different clusters are around 3.351 Å. Although the direct distance between two cymene rings of different clusters is not known, it is sure that it must be shorter than the distance observed above. The distance would fall into the range of π-π interactions, which implies that π-π interactions exist between two clusters via two cymene rings in crystals. The two rings are parallel with two edges of them opposite directly (Figure 18). Four cymene rings on one cluster pack with the other four cymene rings on other four different clusters in pairs in different directions giving a 3-D network

in the crystals. This is the way that molecular structure of clusters determines the intermolecular aggregation of clusters.

Figure 18 Moleclar aggregation of $[Ru_5S_4(cymene)_4]^{2+}$

On the other hand, molecular aggregation in crystals might influence the molecular structure of the cluster reversibly. In one unit, there are two clusters that are slightly different in bond lengths and bond angles because of different aggregation of clusters in crystals (Figure 16). In cluster X, bond length of Ru1-Ru2 and Ru1-Ru1a are 2.7904(6) Å and 2.6953(5) Å, respectively. The bond lengths of central ruthenium atom and one of the side ruthenium atoms are almost 0.1 Å shorter than those between two side ruthenium atoms. But in cluster Y, the bond lengths of Ru3-Ru4 and Ru3-Ru3a are 2.7310(4) Å and 2.7375(6) Å, respectively. The bond lengths between two side ruthenium atoms are only slightly longer than those between the central ruthenium atom and side ruthenium atoms. The bond angles of metal frameworks in the two clusters are also different because of the influence of aggregation of clusters during crystallization. In cluster X, the bond angle of Ru1-Ru2-Ru1a and Ru1b-Ru2-Ru1a are $62.350(15)^0$ and $125.626(15)^0$, respectively. In cluster Y, the bond angle of Ru3-Ru4-Ru3a and Ru3c-Ru4-Ru3a are $60.157(14)^0$ and $127.803(15)^0$, respectively. The bowtie structure of cluster Y is longer than that of cluster X. This might be because of the influence of molecular aggregation during crystallization.

2.2.3. Formation of $[Ru_4S_2(SO)(cymene)_4](PF_6)_2$

A mixture of Na_2S : $[RuCl_2(cymene)]_2$: NH_4PF_6 = 1 : 2 : 3 in methanol was stirred for one and half hours at room temperature. The reasulting dark brown solid was extracted into a solvent mixture of CH_2Cl_2 : $CHCl_3$: acetone : MeOH = 20 : 10 : 5 : 1. TLC was run in the same solvent giving three spots ranging in colour from orange-brown, red-brown to purple-brown. The compound with the lowest R_f was shown to be the big cluster or the novel high nuclearity $[Ru_4(S_2)(SO)(cymene)_4](PF_6)_2$ cluster. The solid has purple brown colour. The reaction for the formation of the $[Ru_4(S_2)(SO)(cymene)_4]^{2+}$ cluster might be:

$$2\ [RuCl_2(cymene)]_2 + 3\ Na_2S + \tfrac{1}{2}\ O_2 \longrightarrow [Ru_4(S_2)(SO)(cymene)_4]Cl_2 + 6\ NaCl$$

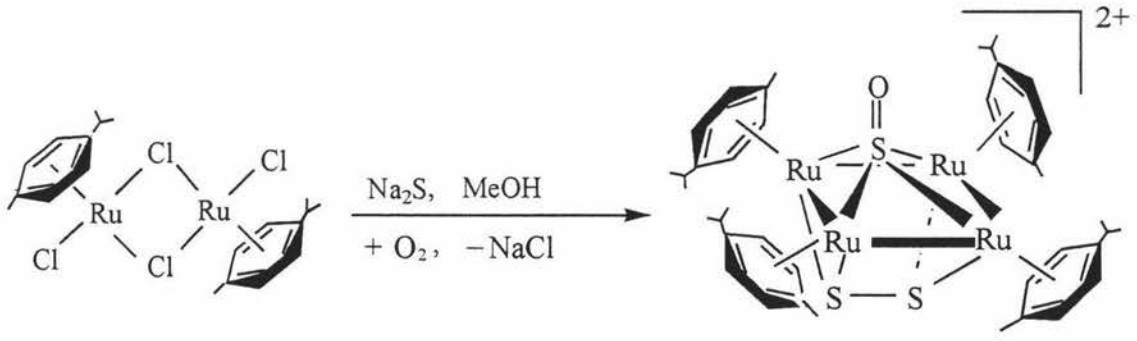

This part of the product was very easy to stick on the column when chromatography technique was used to separate the product. So usually these three compounds were separated by two different solvents into two parts. Firstly all the products were extracted using acetone after the methanol had been removed. After acetone was removed in vacuo, dichloromethane was used to extract $[Ru_3S_2(cymene)_3](PF_6)_2$ and $[Ru_5S_4(cymene)_4](PF_6)_2$ clusters, while the solid that was insoluble in dichloromethane was the third part of products, the big cluster or the $[Ru_4(S_2)(SO)(cymene)_4](PF_6)_2$ cluster.

The big cluster (Ru_{10} ?) This part of products was firstly detected on ^1H NMR spectrum as multiple peaks from about 6 ppm to 7 ppm (Figure 19). It seemed that the cymene rings could not move freely in the compound and the compound had asymmetric structure, which might cause the magnetic inequivalence of all the four hydrogen atoms on the cymene rings. The compound was not very soluble in normal deuterium solvents, which made the peaks too weak to tell the details. But from the chemical shift range, it seemed that the compound might be a two plus cation or even higher plus cation.

The electrospray mass spectrum gave the biggest peak at 2526.8 mass units (Figure 20), which implied that the molecular ion peak might be around 2380 mass units. If the big cluster was a two plus cation, this peak might be a mono-cation formed by the two plus cation combining one PF_6^- anion. (This was the same with $[Ru_5S_4(cymene)_4(PF_6)]^+$ and $[Ru_3S_2(cymene)_3(PF_6)]^+$ mono cations which were described in section 2.2.2 and 2.2.1, respectively). There was a big gap between 2526.8 mass units and 1180.9 mass units that was the molecular ion peak of the $[Ru_5S_4(cymene)_4]^{2+}$ cluster. Therefore, it seemed that the compound might be a big cluster formed by joining two $[Ru_5S_4(cymene)_4]$ fragments in some way, which might contain at least 10 ruthenium atoms in the cluster (Ru_{10} ?). Elemental analysis gave the percentage of H and C, 2.52 % and 18.97 %, respectively, which suggested that the ratio of cymene to ruthenium in the cluster should be lower than 1.0 and 0.8 which are for the $[Ru_3S_2(cymene)_3](PF_6)_2$ cluster and the $[Ru_5S_4(cymene)_4](PF_6)_2$ cluster, respectively. There might be other ruthenium atoms without coordinating cymene rings in the big cluster.

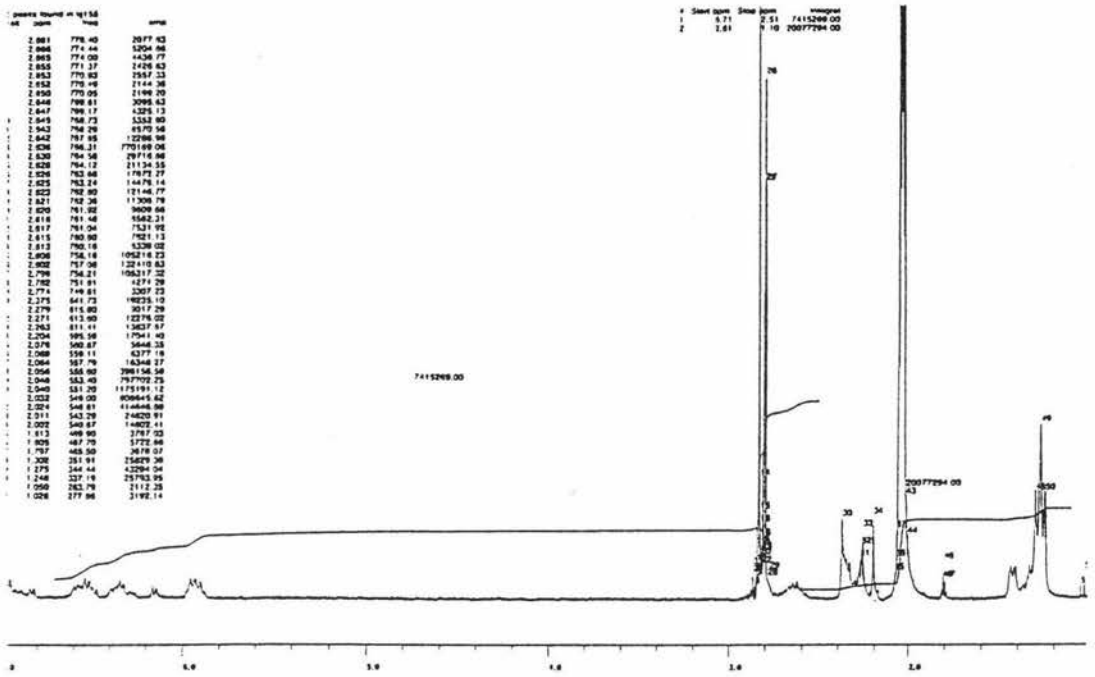

Figure 19 ^{1}H NMR spectrum of the big cluster

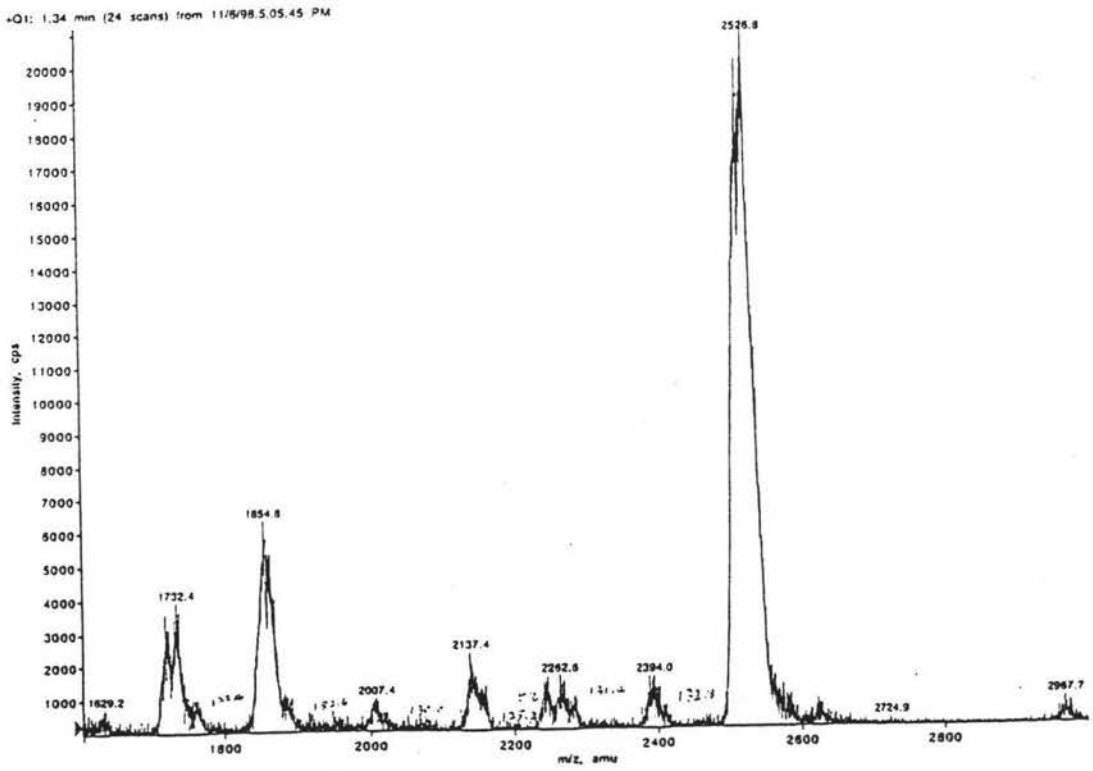

Figure 20 Electrospray mass spectrum of the big cluster

^{1}H NMR spectrum of $[Ru_4(S_2)(SO)(cymene)_4](PF_6)_2$ cluster The recrystallization of purple brown solid usually needed more than ten days to achieve. The black thin square-like crystals were obtained by isobestic technique using acetone / chloroform or acetone / (diethylether + isopropylether) as solvents. The sample of this cluster in D_6-acetone was made by putting the saturated solution with some undissolved crystals together into an autoclave under the nitrogen of 3.8 atm for two hours. The spectrum was very clear giving the signal of hydrogen atoms on cymene rings as two pairs of doublet-of-doublet peaks at 6.14, 6.16; 6.46, 6.49; 6.81, 6.83; 7.06, 7.08 ppm (Figure 21). This is very unusual and will be discussed later.

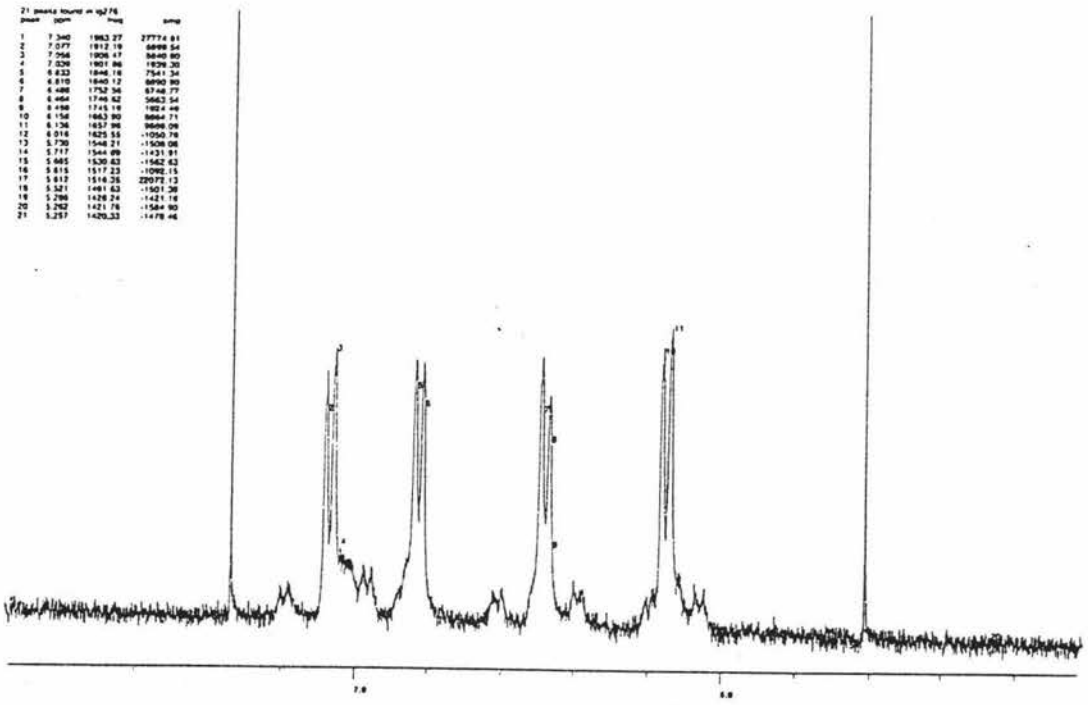

Figure 21 ^{1}H NMR spectrum of $[Ru_4(S_2)(SO)(cymene)_4]^{2+}$

The structure of $[Ru_4S_2(SO)(cymene)_4](PF_6)_2$ X-ray crystallography for the black thin square like crystal gave the structure of the $[Ru_4S_2(SO)(cymene)_4](PF_6)_2$ cluster. The ORTEP view of the structure of this cluster is shown in Figure 22. The metal framework is a square containing four ruthenium atoms with one cymene ring on each of them. On one face of the square, there is a terminal SO ligand with sulfur atom μ_4-coordinating to four ruthenium atoms. On the other face, there is a disulfide ligand with both sulfur atoms μ_2-coordinating to two ruthenium atoms, respectively. The four cymene rings are not perpendicular to the plane of metal framework but incline to SO side. Some selected bond lengths and bond angles are listed in Table 8.

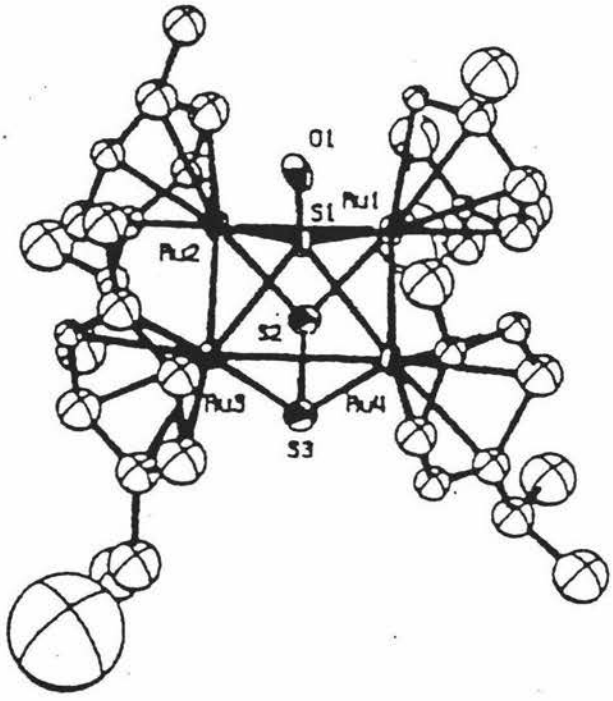

Figure 22 ORTEP structure of $[Ru_4(S_2)(SO)(cymene)_4]^{2+}$

	Bondlengths/Å		Bond angles (^{0})
Ru1-Ru2	2.8004 (0.0046)	Ru3-Ru2-S3	81.81 (0.45)
Ru3-S1	2.2791 (0.0107)	Ru2-Ru1-S1	52.21 (0.27)
Ru1-Ru4	2.8079 (0.0046)	Ru1-Ru2-S2	52.72 (0.49)
Ru4-S1	2.2898 (0.0111)	Ru1-Ru4-S2	142.59 (0.99)
Ru1-S2	2.2850 (0.0185)	Ru1-Ru4-S1	52.19 (0.28)
Ru1-S1	2.2885 (0.0108)	Ru2-Ru3-S1	51.54 (0.27)
S1-O1	1.4868 (0.0289)	Ru3-Ru4-S3	51.62 (0.46)
Ru3-S3	2.2660 (0.0173)	Ru3-Ru4-S1	52.65 (0.28)
Ru2-S1	2.2985 (0.0113)		
Ru2-S2	2.3048 (0.0194)		
Ru2-Ru3	2.8004 (0.0046)		
Ru4-S3	2.2471 (0.0181)		
Ru3-Ru4	2.7831 (0.0047)		

Table 8 X-ray crystallographic data of $[Ru_4S_2(SO)(cymene)_4](PF_6)_2$

The metal framework is a twisted square with each bond length different from others. However, the average of 2.80 Å is longer than those in $[Ru_3S_2(cymene)_3](PF_6)_2$ and $[Ru_5S_4(cymene)_4](PF_6)_2$ clusters (2.78 Å and 2.70 Å, respectively).

However, the electrospray mass spectrum and elemental analysis did not support the X-ray crystal structure. The peak at 1052 mass units that was the molecular ion peak of the $[Ru_4S_2(SO)(cymene)_4]^{2+}$ cluster was not found on the spectrum. The ratio of cymene to ruthenium in the $[Ru_4S_2(SO)(cymene)_4](PF_6)_2$ cluster is 1:1 that is much higher than what it might be in the purple-brown solid. The structure of the purple-brown solid might have changed during recrystallization. The oxygen atom might be added on sulfur atom by breaking one of the disulfide bridge therefore the SO ligand might not be initially formed.

The thin shape of the crystal brought difficulties in collecting X-ray diffraction data. The R number is 0.18, which was very high.

Disordered structure The structure of the $[Ru_4S_2(SO)(cymene)_4](PF_6)_2$ cluster is disordered because the disulfide ligand might coordinate to different metal atoms on the metal framework. There are two possibilities that disulfide ligand coordinating to ruthenium atoms:

Scheme 16 Disordered structure of $[Ru_4S_2(SO)(cymene)_4](PF_6)_2$

The ratio of two positions is approximately 50% : 50%. This might influence the bond lengths of the metal-metal bonds, which might be the reason why the metal-metal bonds in this cluster were different to each other.

Clusters with SO ligands Only a few sulfur monoxide complexes have been known. The first authenticated sulfur monoxide complex $[Fe_3(S)(SO)(CO)_9]$ was made by Marko et.al. in 1980 [99, 82], although several other complexes were claimed to contain this ligand [83,84]. Each known coordination mode of SO has been confirmed by one X-ray structure analysis (Figure 23), which are normally μ_2- or μ_3-coordination. In the $[Fe_3(CO)_9(S)(SO)]$ cluster, S-O bond length is 1.471(2) Å. A strong band at 1107 cm^{-1} (in KBr) can be assigned to the SO stretching vibration.

The $[Ru_4S_2(SO)(cymene)_4](PF_6)_2$ cluster is the first cluster with μ_4-coordinated SO ligand. The bond length of S-O is 1.4868 (0.0288) Å. It has been tried for several times to get the IR spectrum, but it was failed because the crystal was too sticky in the air to be grinned well.

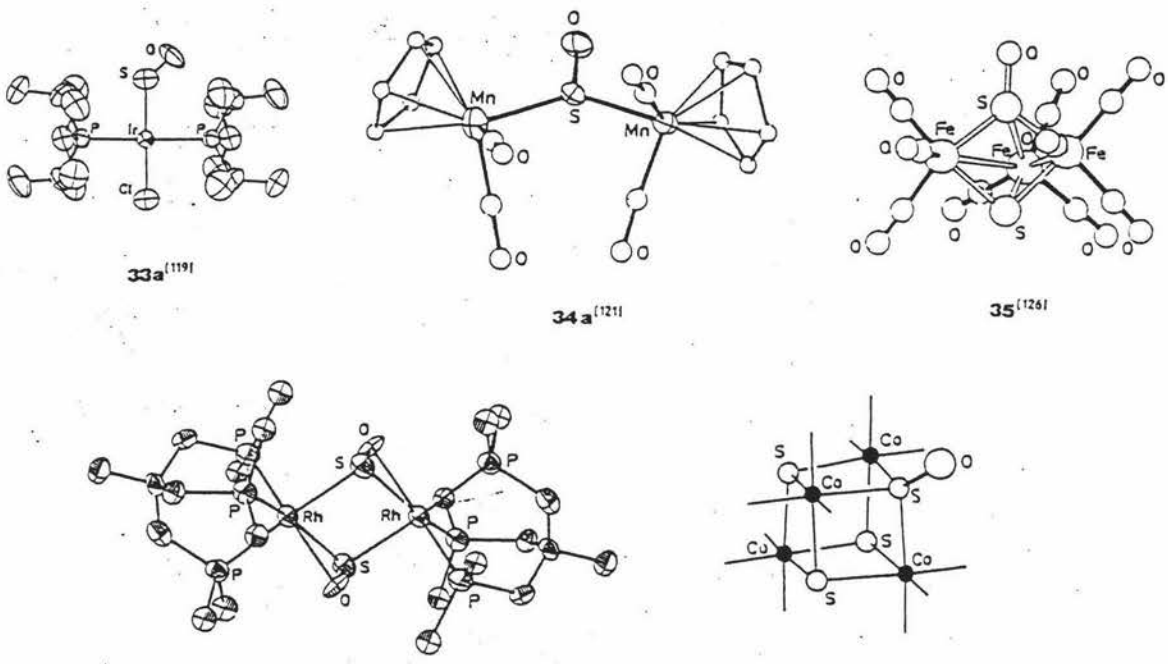

Figure 23 X ray structures of SO containing complexes

Disulfur as ligand compared to SO It is very common for transition metal clusters containing disulfide ligands (S_2^{2-}). The mechanism of formation of S_2^{2-} from S^{2-} has been well investigated as it was mentioned in Chapter one [35].

$$2\,S^{2-} + 2\,e^- \longrightarrow S_2^{2-}$$

The way that the disulfide ligand and the SO ligand coordinate to the metal framework is very different. The HOMOs of $[Ru_4S_2SO(cymene)_4]^{2+}$ with coordinating disulfide and SO ligands are shown in Figure 50. From Figure 50, it can be seen that the disulfide ligand coordinates to metal framework by its π^* orbitals in the way of face-to-face while the SO ligand coordinates to metal framework by the π^* orbitals in the way of edge-to face.

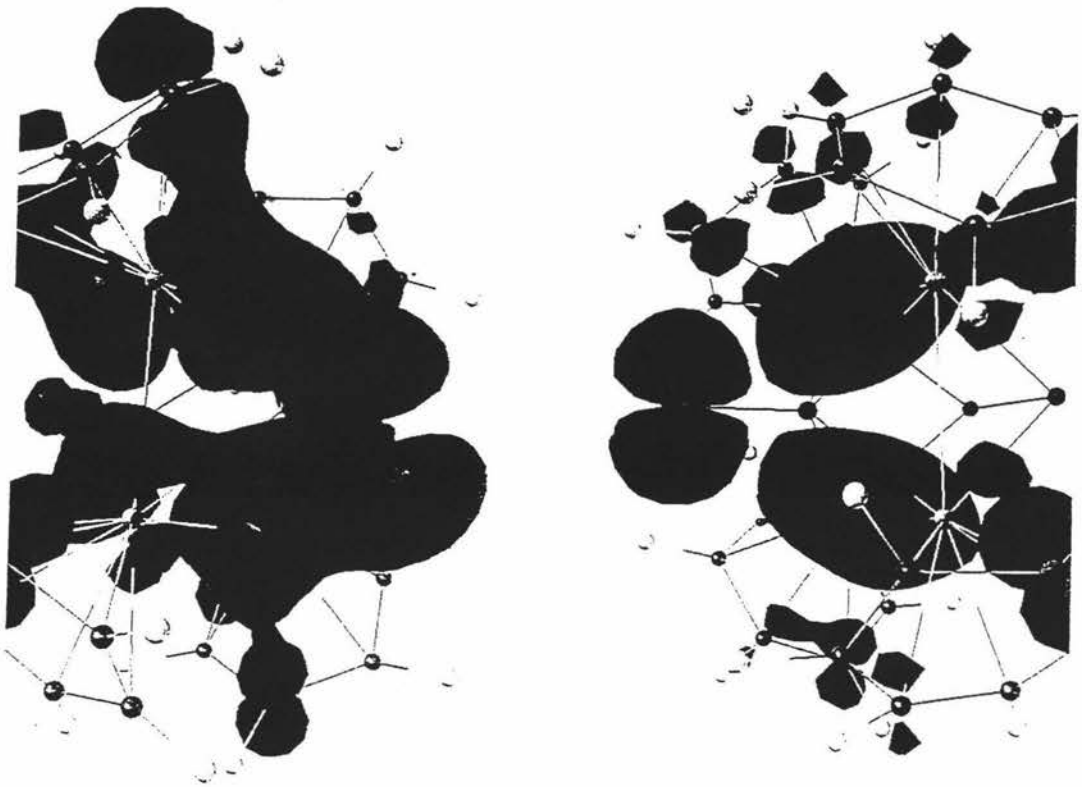

Figure 50 HOMOs of $[Ru_4S_2SO(cymene)_4]^{2+}$ coordinated by disulfide and SO

Formation of SO ligand in the $[Ru_4S_2SO(cymene)_4]^{2+}$ cluster Sulfur monoxide is an important intermediate in sulfur oxide chemistry. Usually it is unstable and generally disproportionates to S_2O and SO_2. Chemists tried to trap it as ligands in transition metal complexes. The first authenticated sulfur monoxide complex, $[Fe_3(S)(SO)(CO)_9]$ [99] has μ_3- coordinating SO ligand and other clusters with μ_2- coordinating SO ligands were also found during last twenty years, but the $[Ru_4S_2SO(cymene)_4]^{2+}$ cluster is the only cluster with μ_4- coordinating SO ligand.

In the reaction that formation of $[Ru_4S_2SO(cymene)_4]^{2+}$, it seemed that there might be a big cluster formed with at least two disulfide ligands and consequently, one of the disulfide ligand might be oxidized by O_2 when the reaction or crystallization was exposed in the air.

The reaction of formation of the big cluster (RU_{10} ?) and the $[Ru_4S_2SO(cymene)_4]^{2+}$ cluster might be:

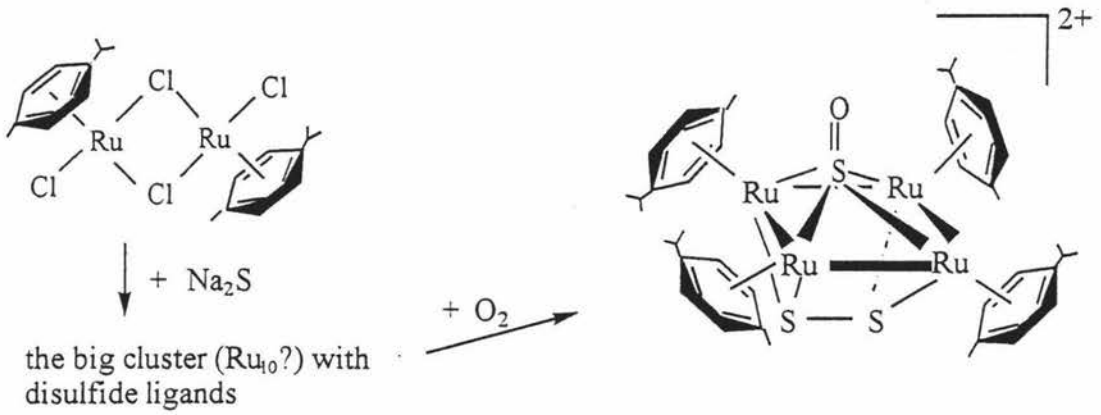

It is easy to understand this by bonding study. The frontier orbitals of SO are largely similar in energy and size to those of CO (Figure 31). The two extra valence electrons occupy the antibonding 3π orbital and are responsible for the $^3\Sigma^-$ ground state of SO. So μ_2- and μ_3- coordination modes are normal for SO ligand to use the two antibonding orbitals and the lone pair electrons as donors.

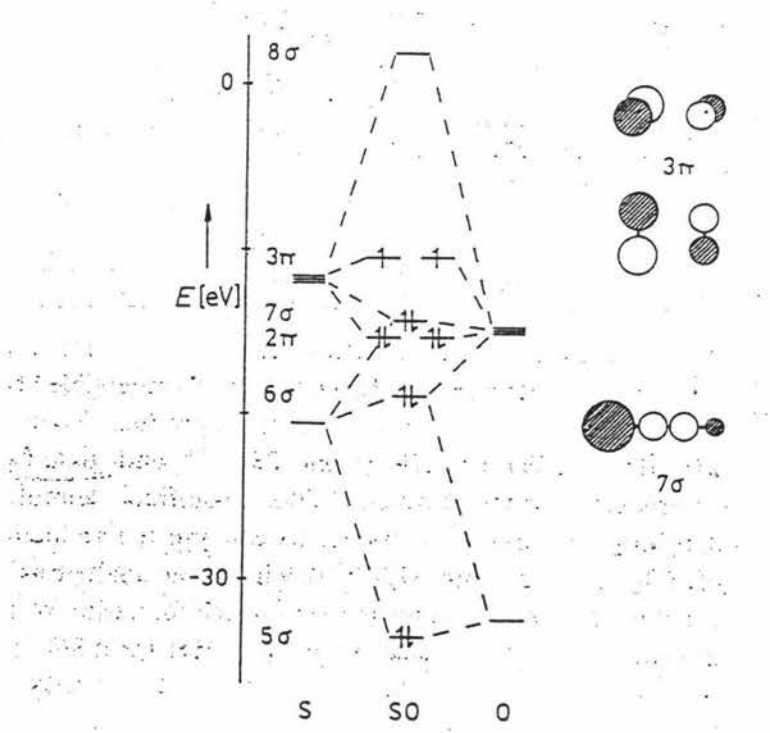

Figure 31 MO diagram and frontier orbitals of SO

Comparation of chemical shifts of the three clusters The chemical shifts of the hydrogen atoms on the cymene rings in these three cymene-ruthenium-sulfur clusters are different while they are all two plus cations. The chemical shift of hydrogen atoms on cymene rings is dependent on how much they are shielded by the corresponding ruthenium atoms and the shielding effect is sensitive to the distance of cymene ring from the ruthenium atom. The longer the distance, the less the shielding effect on the hydrogen atoms of the cymene ring, the lower field the chemical shift will be in. The distances of cymene rings to corresponding ruthenium atoms for the three clusters are: $[Ru_5S_4(cymene)_4](PF_6)_2$ < $[Ru_3S_2(cymene)_3](PF_6)_2$ < $[Ru_4S_2(SO)(cymene)_4](PF_6)_2$. The chemical shifts of hydrogen atoms on cymene rings are in the same order, which means that the chemical shift of the hydrogen atoms on the cymene rings in the $[Ru_4S_2(SO)(cymene)_4](PF_6)_2$ cluster is in the lowest field among the three clusters.

These distances are related to the metal cores of the three clusters, in which steric forces are the determinant. For the two triangular clusters, the three cymene rings are more apart from ruthenium atoms in the $[Ru_3S_2(cymene)_3](PF_6)_2$ cluster than those in the $[Ru_5S_4(cymene)_4](PF_6)_2$ cluster. In the $[Ru_3S_2(cymene)_3](PF_6)_2$ cluster, the three cymene rings are almost perpendicular to the triangular metal framework, in which they tend to apart from each other and consequently from the ruthenium atoms. In the $[Ru_5S_4(cymene)_4](PF_6)_2$ cluster, the four ruthenium atoms with cymene rings are far away because they are separated by the central ruthenium atom occupying a 3-D space. The steric forces between the cymene rings are less than those in the $[Ru_3S_2(cymene)_3](PF_6)_2$ cluster. Therefore the four cymene rings are closer to corresponding ruthenium atoms comparing to the $[Ru_3S_2(cymene)_3](PF_6)_2$ cluster, on which the hydrogen atoms are more shielded by ruthenium atoms. The chemical shift of hydrogen atoms on cymene rings is in higher field for the $[Ru_5S_4(cymene)_4](PF_6)_2$ cluster compared to the $[Ru_3S_2(cymene)_3](PF_6)_2$ cluster.

For the $[Ru_4S_2(SO)(cymene)_4](PF_6)_2$ cluster, the Ru-Ru bond lengths on the square-like metal framework are longer than those on the triangle metal frameworks in $[Ru_3S_2(cymene)_3](PF_6)_2$ and $[Ru_5S_4(cymene)_4](PF_6)_2$ clusters. The distance of cymene to ruthenium atom is the longest. On the other hand, the $[Ru_4S_2(SO)(cymene)_4](PF_6)_2$ cluster contains the SO ligand that strongly withdraw electrons from ruthenium atoms. So the hydrogen atoms on cymene rings in the $[Ru_4S_2(SO)(cymene)_4](PF_6)_2$ cluster are the least

shielded by ruthenium atoms among the three clusters, for which the chemical shift is in the lowest field.

The unusual ^{1}H NMR signals of the cymene-ruthenium-sulfur clusters The three cymene-ruthenium-sulfur clusters all gave unusual signals on ^{1}H NMR spectra for the hydrogen atoms on the cymene rings. They were all different with those mono- or di-nuclear complexes that gave the normal one pair of doublet-of-doublet peaks. $[Ru_5S_4(cymene)_4](PF_6)_2$ and $[Ru_3S_2(cymene)_3](PF_6)_2$ clusters both gave one single peaks while the $[Ru_4(S_2)(SO)(cymene)_4](PF_6)_2$ cluster gave two pairs of doublet-of-doublet peaks and the proposed big cluster (Ru_{10} ?) gave multiple peaks.

Normally for mono- and di-nuclear complexes such as $[RuCl_2(NH_3)(cymene)]$, only two pairs of chemically equivalent hydrogen atoms on the cymene ring (see Figure 54). Since the cymene ring could rotate freely and there is a mirror place in the molecule, the two H_a atoms and the two H_b atoms are not only chemically equivalent respectively but also magnetically equivalent respectively. Then the spin-spin coupling between these two pairs of hydrogen atoms splitting the signal into four doublet-of-doublet peaks as shown in Figure 36 in Chapter three.

But for $[Ru_5S_4(cymene)_4](PF_6)_2$ and $[Ru_3S_2(cymene)_3](PF_6)_2$ clusters, they both give one single peak. This is unusual. It might be because of coincidence giving one big peak in the middle and two little peaks on each side. (This has been described in section 2.2.1) and the NMR machine being used (270 M Hz) could not tell the two little peaks from the noises therefore giving one single peak only.

The $[Ru_4(S_2)(SO)(cymene)_4](PF_6)_2$ cluster is different with those mono- and di-nuclear complexes being described in Chapter three. It is also different with $[Ru_5S_4(cymene)_4](PF_6)_2$ and $[Ru_3S_2(cymene)_3](PF_6)_2$ clusters. Instead of giving one single peak or four doublet-of-doublet peaks, it gives two pairs of doublet-of-doublet peaks (eight peaks altogether). This is very unusual. It might be because of the asymmetric structure of this cluster caused by the disulfide ligand and the SO ligand. Because the cymene rings in this cluster were locked by each other, the hydrogen atoms on the cymene rings changed to be magnetically inequivalent (e.g. H_a and H_a'; H_b and H_b').

Comparing to $[Ru_5S_4(cymene)_4](PF_6)_2$ and $[Ru_3S_2(cymene)_3](PF_6)_2$ clusters, cymene rings in the $[Ru_4(S_2)(SO)(cymene)_4](PF_6)_2$ cluster have not got enough space to

move. For the $[Ru_5S_4(cymene)_4](PF_6)_2$ cluster, four cymene rings occupy a 3-D space because there is a dihedral angle between the two triangular planes (56.1^0). For the $[Ru_4(S_2)(SO)(cymene)_4](PF_6)_2$ cluster and the $[Ru_3S_2(cymene)_3](PF_6)_2$ cluster, they both have plane (2-D) metal framework. But only three cymene rings pack in the space of 360^0 in the $[Ru_3S_2(cymene)_3](PF_6)_2$ cluster while there are four cymene rings in the $[Ru_4(S_2)(SO)(cymene)_4](PF_6)_2$ cluster packing in the same space. So the cymene rings in both $[Ru_5S_4(cymene)_4](PF_6)_2$ and $[Ru_3S_2(cymene)_3](PF_6)_2$ clusters can rotate much more freely comparing to the $[Ru_4(S_2)(SO)(cymene)_4](PF_6)_2$ cluster. Figure 56 shows the distance between cymene rings in the $[Ru_5S_4(cymene)_4](PF_6)_2$ cluster and the locked cymene rings in the $[Ru_4S_2(SO)(cymene)_4](PF_6)_2$ cluster.

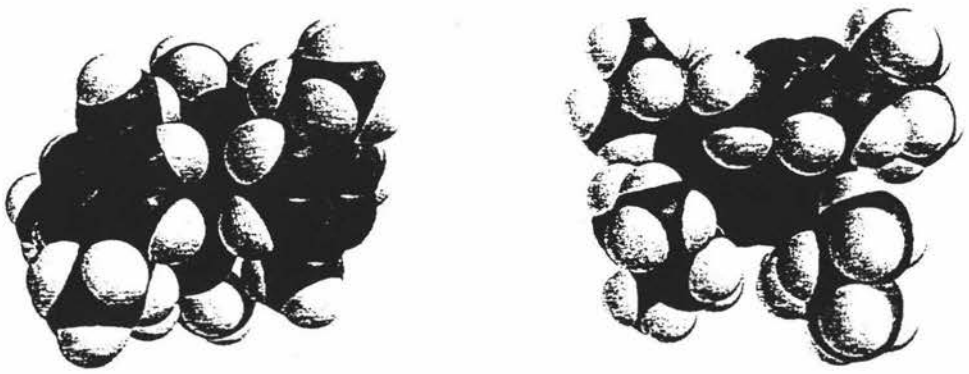

Figure 56 Space filling models of $[Ru_4(S_2)(SO)(cymene)_4](PF_6)_2$ and $[Ru_5S_4(cymene)_4](PF_6)_2$

The locked cymene rings give two different coordination directions to the asymmetric metal-sulfur core, methyl groups on disulfide side or on SO side (Figure 55). The asymmetric structure of this cluster is caused by disulfide and SO ligands on different sides of the metal framework. So the asymmetric structure and the different coordination directions of the locked cymene rings make a joint effort of affording different

environment to H_a and H_d, H_b and H_c, respectively. Therefore the pair of H_c atoms is different to the pair of H_b atoms and so do H_a atoms and H_d atoms. Then two H_a atoms couple to two H_b atoms giving different chemical shift with that do between two H_c atoms and two H_d atoms. Therefore there are two pairs of doublet-of-doublet peaks appearing on the spectrum indicating different coupling between H_a and H_b, H_c and H_d, respectively.

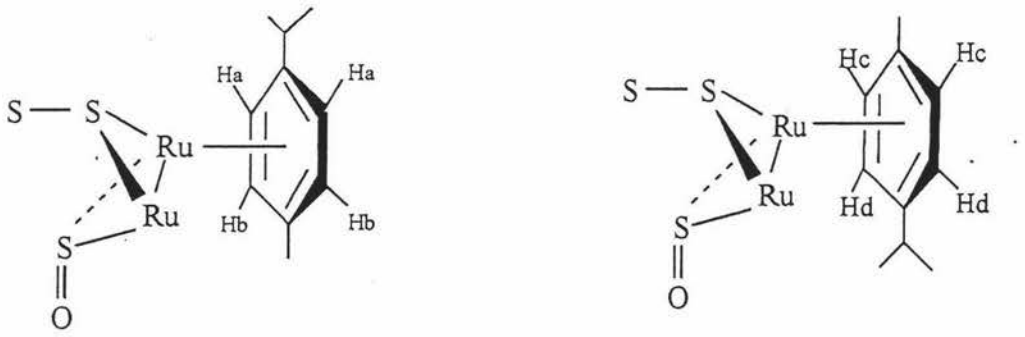

Figure 55 Different coordination directions of cymene rings in the $[Ru_4(S_2)(SO)(cymene)_4](PF_6)_2$ cluster

Another influence to hydrogen atoms on the cymene ring might come from the disulfide ligand itself. Figure 57 shows the different environments of the hydrogen atoms on the cymene ring caused by the two sulfur atoms of disulfide ligand. The symmetric plane between the two H_a atoms and two H_b atoms disappear. H_a is different from H_a' while H_b is similar to H_b'.

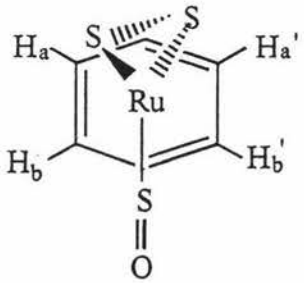

If the cymene rings were all in the same coordinating direction, i.e., with methyl groups all up or all down, then H_a and H_b, H_a' and H_b' would couple to each other giving two pairs of doublet-of-doublet peaks as did in the $[Ru_4(S_2)(SO)(cymene)_4](PF_6)_2$ cluster.

If the cymene rings were in different coordinating directions, i.e. some up and some down or in other directions, multiple peaks would be observed as did the big cluster (Ru_{10} ?) (Figuire 57).

For the proposed big cluster (Ru_{10} ?), there are two possibilities of giving multiple peaks. One might be that there are different kinds of cymene rings in this cluster. This might be because they coordinate to different ruthenium atoms with different other ligands coordinating on them. Another might be because different cymene rings were locked in different directions. In the later case, the cymene rings in the big cluster might pack more tightly than the $[Ru_4(S_2)(SO)(cymene)_4](PF_6)_2$ cluster therefore the cymene rings in the big cluster could not rotate freely even in the solution and be locked in different directions. Then the hydrogen atoms of the same position but on different cymene rings would be different giving multiple peaks. H_a and H_a' are different with H_d and H_d', respectively. H_b and H_b' are different with H_c and H_c', respectively. So when they couple to each other, i.e., H_a and H_b, H_a' and H_b', H_c and H_d, H_c' and H_d', couple to each other, multiple peaks would be observed.

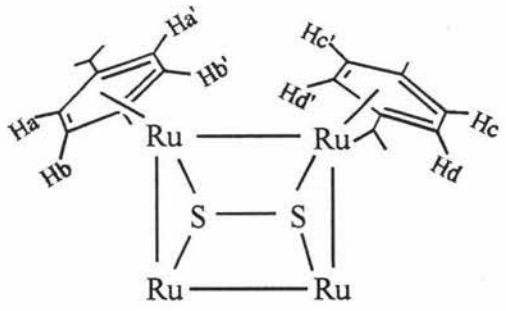

Figure 57 Cymene rings coordinate to Ru atoms in different directions

2.3. Electrochemistry of arene-ruthenium-sulfur clusters

In order to compare the electrochemical characters of the three clusters, especially the two new higher nuclearity cymene-ruthenium-sulfur clusters to the known $[Ru_3S_2(cymene)_3](PF_6)_2$ cluster, cyclic voltammetry techniques were used.

For the reaction, Oxidant + ne^- $\leftrightharpoons$ Reductant, normally it is hard to prove its reversibility. It needs six steps' diagnostic tests for cyclic voltammograms depending on Randles-Sevcik equation ($I_p = -2.69*10^5 n^{3/2} c_O^{\infty} D^{1/2} \nu^{1/2}$ at 25°C, Where I_p is the peak current density [100]). In the case of the reversible system, the electron transfer rates at all potentials are significantly greater than the rate of mass transport. When the rate of electron transfer is insufficient to maintain this surface equilibrium, the system will tend to be irreversible. It is quite common for a process that is reversible at low sweep rates to become irreversible at higher ones after having passed through a region known as quasi-reversible at intermediate values. But even quasi-reversiblity needs four steps' diagnostic tests.

Figure 42 shows what the current response looks like when the potential sweep is reversible. It is noted that the charge associated the anodic process is low compared to the forward reduction process. This is because there is a concentration difference driving reductant away from the electrode. Most of the reductant therefore diffuses into the bulk solution and can not be reoxidised on the time scale of a cyclic voltammetric experiment.

Figure 43 shows how the potential sweep change from reversible to irreversible when the sweep rates increase.

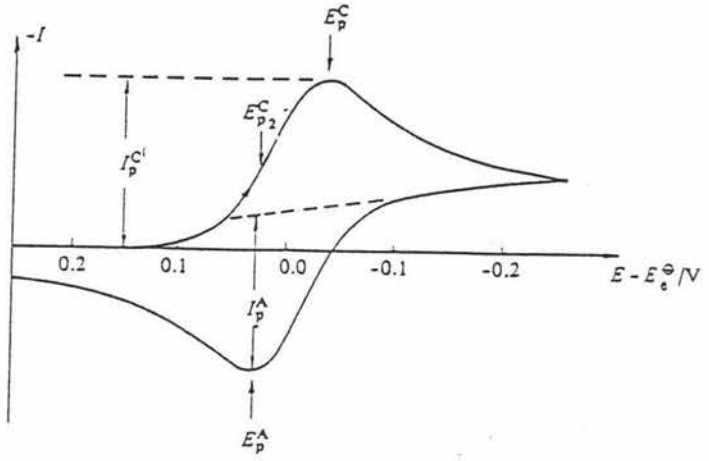

– Cyclic voltammogram for a reversible process, O + e^- ⇌ R. Initially only O present in solution.

Figure 42 Cyclic voltammetry for a reversible reaction

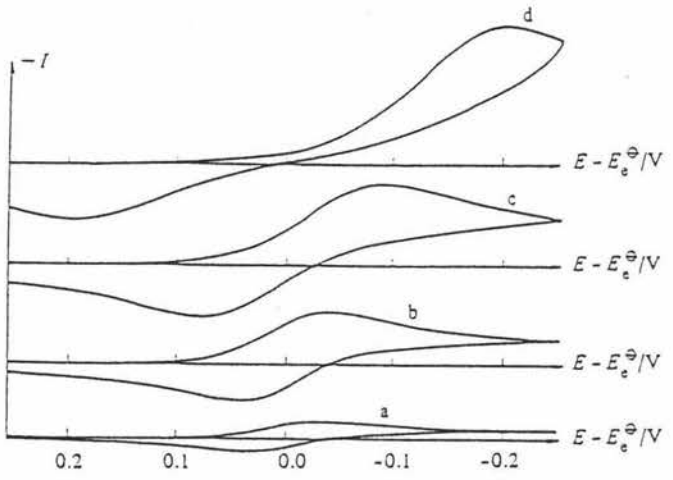

– Simulated cyclic voltammograms for reaction O + e^- ⇌ R when D = 10^{-5} cm s^{-1} and $k^\ominus = 10^{-2}$ cm s^{-1}. Only O initially present in solution. Potential sweep rates (a) 0.13 V s^{-1}, (b) 1.3 V s^{-1}, (c) 4 V s^{-1}, (d) 13 V s^{-1}.

Figure 43 From reversible to irreversible when sweep rates increase

The cyclic voltammetry of the $[Ru_3S_2(cymene)_3](PF_6)_2$ cluster has been measured by Rauchfuss et.al (Figure 24 [5]). It was run in 1.0 mM solution of CH_2Cl_2. The scan rate was 0.100 V/s and the reference electrode was Ag / AgCl. $[Ru_3S_2(cymene)_3](PF_6)_2$ cluster underwent two closely spaced one-electron reductions at –0.567 V and –0.704 V vs Ag / AgCl. It was established that one metal-metal bond opened when the cluster gained two electrons and that reduction was reversible [5].

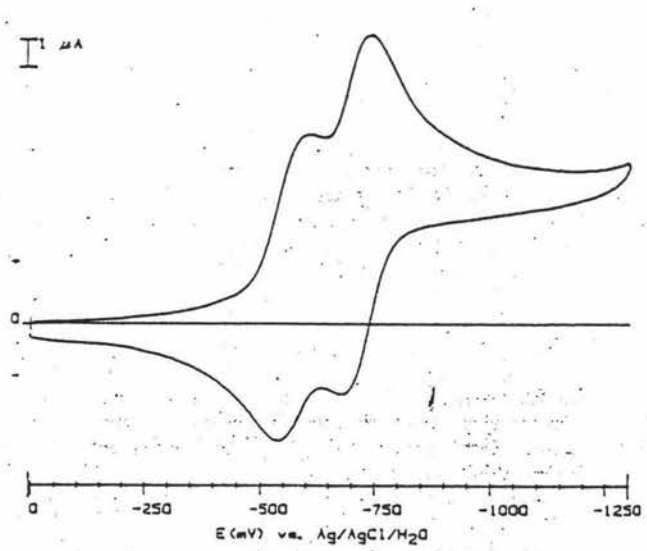

Cyclic voltammogram of $[1](PF_6)_2$, 1.0 mM in CH_2Cl_2. The Ru_3S_2 core structures are shown for the electrochemically interrelated $[1]^{2+}$ and $[1]^0$. The scan rate is 0.100 V/s and the reference electrode is Ag/AgCl.

Figure 24 Electrochemistry of $[Ru_3S_2(cymene)_3]^{2+}$ [5]

Cyclic voltammetry for $[Ru_3S_2(cymene)_3](PF_6)_2$, $[Ru_5S_4(cymene)_4](PF_6)_2$ and $[Ru_4S_2(SO)(cymene)_4](PF_6)_2$ clusters were measured in saturated MeCN solutions (with the crystals of the three clusters, respectively) using $^tBu_4NPF_6$ as supporting electrolyte, a 10 micron carbon microelectrode as working electrode, Ag / AgCl electrode as reference electrode and Pt electrode as counter electrode. The sweep rates were in a range from 0.05 V/s to 1.0 V/s. The microelectrode used was on the purpose of minimizing the charging currents and the effects of uncompensated resistance.

The method was checked by cyclic voltammetry for $[Ru_3S_2(cymene)_2](PF_6)_2$ cluster matching the literature very well. The first electron reduction was at –0.570 V and the second electron reduction was at –0.700 V vs Ag / AgCl. These potentials meant that the cationic cluster $[Ru_3S_2(cymene)_3]^{2+}$ was relatively easy to be reduced.

The cyclic voltammetry for the $[Ru_5S_4(cymene)_4](PF_6)_2$ cluster and $[Ru_4S_2(SO)(cymene)_4](PF_6)_2$ cluster were measured under the same condition with that did the $[Ru_3S_2(cymene)_3](PF_6)_2$ cluster (Figure 25 and Figure 26). The $[Ru_5S_4(cymene)_4](PF_6)_2$ cluster underwent two closely spaced one-electron reductions at –0.480 V and –0.760 V vs Ag / AgCl. The reduction of the $[Ru_5S_4(cymene)_4](PF_6)_2$ cluster

might be reversible (or quasi-reversible but the sweep rate was in the reversible range) while the cyclic voltammetry of the $[Ru_4S_2(SO)(cymene)_4](PF_6)_2$ cluster might be irreversible (or quasi-reversible but the sweep rate was in the irreversible range). Anyway, all the three clusters could be reduced easily.

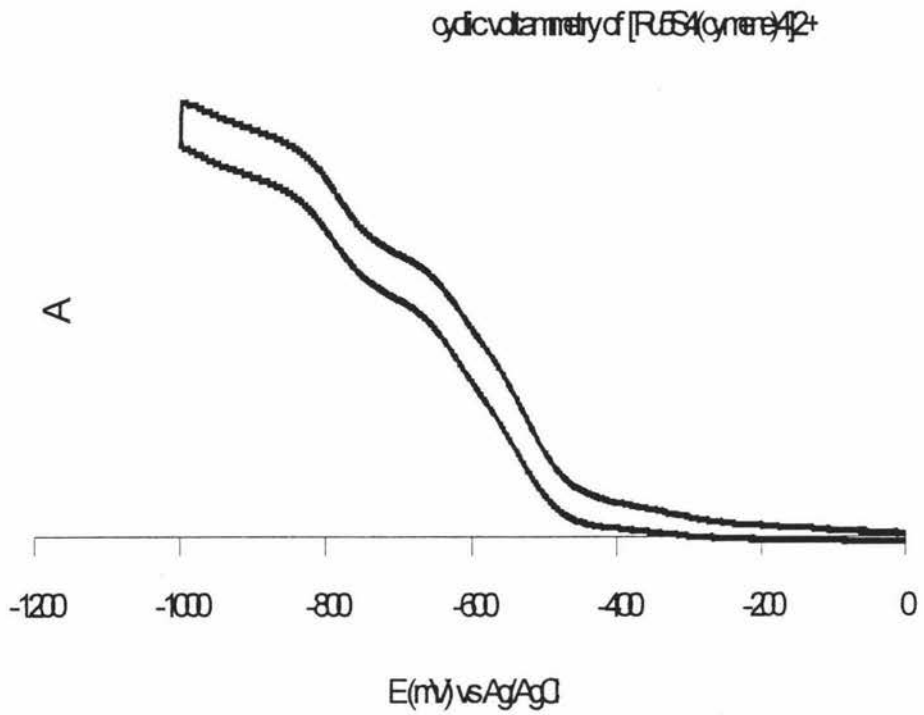

Figure 25 Electrochemistry of $[Ru_5S_4(cymene)_4]^{2+}$

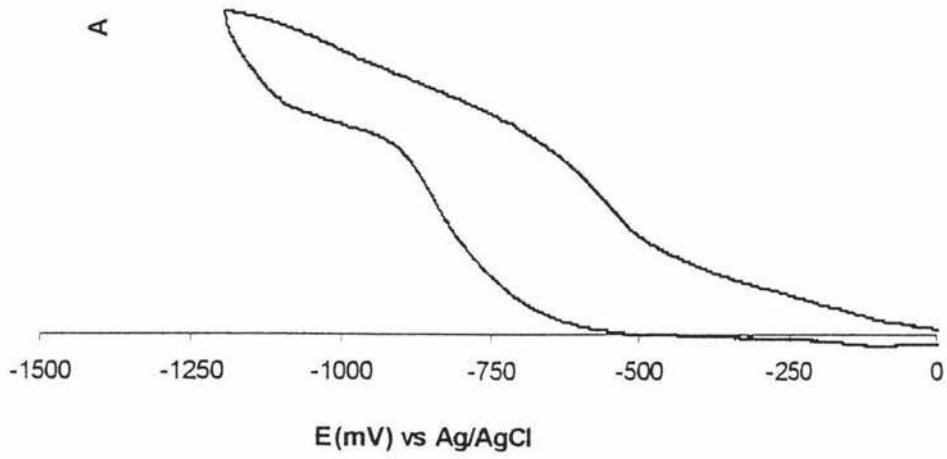

Figure 26 Electrochemistry of $[Ru_4(S_2)(SO)(cymene)_4]^{2+}$

2.4. Conditions that influence the distribution of the products

Originally the reaction of making the three cymene-ruthenium-sulfur clusters ran for one and half hours stirring in methanol solution at room temperature ($[(cymene)Cl_2Ru]_2$: Na_2S : NH_4PF_6 = 1 : 2 : 3). Many reactions have been done under varies conditions to investigate how the product distribution was influenced. There are several aspects that influence the distribution of the products:

Temperature At lower temperature, such as stirring at −10°C (by putting the container into salted ice water) for one and half hours, the reaction had no difference with that did at room temperature. When the reaction underwent at 50-60°C (by heating in the oil bath), the ratio of the $[Ru_5S_4(cymene)_4](PF_6)_2$ cluster and the big cluster (or the $[Ru_4S_2(SO)(cymene)_4](PF_6)_2$ cluster) both increased. A little bit of the $[Ru_3S_2(cymene)_3](PF_6)_2$ cluster was found when recrystallized.

pH The reaction was very sensitive to pH. Under acidic condition (very dilute solution of CF_3COOH in methanol was added), the formation of the $[Ru_3S_2(cymene)_3](PF_6)_2$ cluster was favorable [5] (the highest yield of this cluster obtained in acidic condition was 35.4%). Some crystals of the $[Ru_5S_4(cymene)_4](PF_6)_2$ cluster were also found to be co-crystallized as byproduct but almost no the big cluster (or the $[Ru_4S_2(SO)(cymene)_4](PF_6)_2$ cluster) formed.

When three drops of base, $NaN(SiMe_3)_2$ was added into the reaction mixture at 50°C, the products of the reaction were mainly the $[Ru_5S_4(cymene)_4](PF_6)_2$ cluster and a little bit of the $[Ru_3S_2(cymene)_3](PF_6)_2$ cluster without the big cluster (or the $[Ru_4S_2(SO)(cymene)_4](PF_6)_2$ cluster) formed. The products of the reaction with another base, triethylamine added were mainly $[Ru_5S_4(cymene)_4](PF_6)_2$ cluster and a little bit yellow compounds that seemed like mono-nuclear complex from ^1H NMR spectrum (Figure 27). There was no big cluster (or $[Ru_4S_2(SO)(cymene)_4](PF_6)_2$ cluster) formed, either.

The distribution of the products influenced by pH is summarized in Table 4. From Table 4, it seemed that the big cluster (or the $[Ru_4S_2(SO)(cymene)_4](PF_6)_2$ cluster) did not form under either acidic or basic conditions. Only under neutral condition (no acid or base added, only using MeOH as solvent), the big cluster (or the $[Ru_4S_2(SO)(cymene)_4](PF_6)_2$ cluster) could be obtained.

Compounds	Acidic (CF_3COOH)	Neutral (normal methanol)	Basic (triethyl amine)	Basic ($NaN(SiMe_3)_2$)
$[Ru_3S_2(cymene)_3](PF_6)_2$	Mainly	A little	A little	None
$[Ru_5S_4(cymene)_4](PF_6)_2$	A little	Some	Mainly	Mainly
The big cluster or $[Ru_4S_2(SO)(cymene)_4](PF_6)_2$	None	Some	None	None
Other products	None	None	None	Some

Table 4 Product distribution influenced by pH

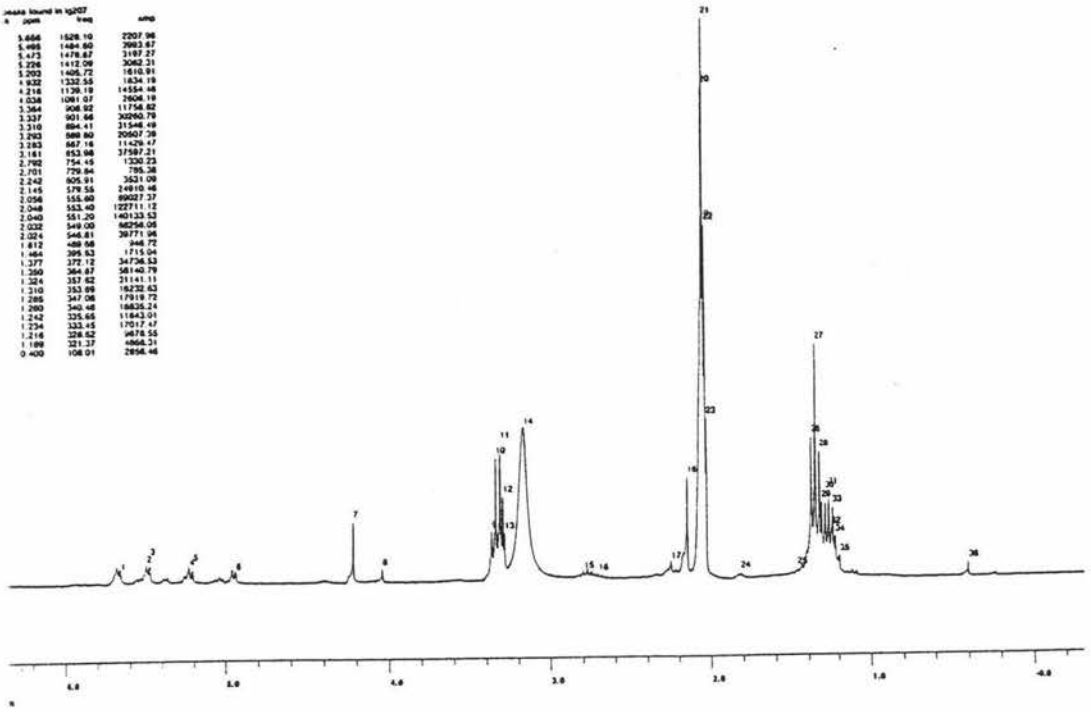

Figure 27 ^{1}H NMR spectrum of reaction mixture in basic condition

Amount of NH_4PF_6 High nuclearity cluster $[Ru_5S_4(cymene)_4](PF_6)_2$ and the unknown big cluster (Ru_{10} ?) (or the $[Ru_4S_2(SO)(cymene)_4](PF_6)_2$ cluster) were both favorable to form when the amount of NH_4PF_6 increases within the ratio of 3:1 for NH_4PF_6 to $[RuCl_2(cymene)]_2$. Above 3:1, there was no effect on the distribution of the products when the amount of NH_4PF_6 increased.

Amount of Na_2S When the amount of Na_2S increases, the reaction tended to form the $[Ru_5S_4(cymene)_4](PF_6)_2$ cluster and the big cluster (or the $[Ru_4S_2(SO)(cymene)_4](PF_6)_2$ cluster). This also matched the ratios of sulfur atoms to ruthenium atoms in the three clusters. The ratios of sulfur atoms to ruthenium atoms in $[Ru_5S_4(cymene)_4](PF_6)_2$ and $[Ru_4S_2(SO)(cymene)_4](PF_6)_2$ clusters are bigger than that in the $[Ru_3S_2(cymene)_3](PF_6)_2$ cluster, which are 4/5, 3/4 and 2/3 in $[Ru_5S_4(cymene)_4](PF_6)_2$, $[Ru_4S_2(SO)(cymene)_4](PF_6)_2$ and $[Ru_3S_2(cymene)_3](PF_6)_2$ clusters, respectively

2.5. Proposed mechanism of formation of the clusters

SH^- and S^{2-} The sensitivity of the reaction to pH in aqueous Na_2S and the reasult of the reaction using NaSH in methanol were reported to suggest that the cationic cluster formed via the SH^- [5]. The reaction in methanolic NaSH gave higher yield than the aqueous Na_2S by using SH^- directly instead of S^{2-}. The reaction of aqueous Na_2S was very sensitive to pH, with neutral to acidic conditions favoring the formation of the $[Ru_3S_2(cymene)_3]^{2+}$ cluster because in acidic condition more SH^- might be produced.

Calculation of equilibrium constant for the equilibrium, $S^{2-} + H_2O \leftrightharpoons HO^- + SH^-$, also supports this suggestion. The equilibrium constant, $k = [HO^-][SH^-] / [S^{2-}][H_2O] = K_{a\ H2O} / K_{a\ SH} = 0.0018$, then $[SH^-] = 0.04\ [S^{2-}]^{1/2}[H_2O]^{1/2}$ ($pK_{a\ SH-/S2-} = 12.92$ and $pK_{a\ H2O/OH-} = 15.7$). When excess of S^{2-} is used in the reaction, concentration of SH^- would increase. In acidic condition, the equilibrium will move to the direction of giving SH^- ($H^+ + HO^- \rightarrow H_2O$).

The reaction described in this chapter was different from the one of Rauchfuss and co-workers. SH^- might play the main role in both of the reactions in aqueous Na_2S and methanolic NaSH [5]. But in the reaction described in this chapter, S^{2-} might play an important role. The calculation for the equilibrium, $S^{2-} + MeOH \leftrightharpoons MeO^- + SH^-$, shows that the $[SH^-]$ in methanol is about 14 times lower than that in H_2O ($k = [MeO^-][SH^-] / [S^{2-}][MeOH] = K_{a\ MeOH} / K_{a\ SH} = 0.000008$, $[SH^-]_{H2O} / [SH^-]_{MeOH} = 14$). because excess Na_2S was used in the reaction, S^{2-} existed mostly in the solution.

The reducing potential of S^{2-} and SH^- shows another difference. The reducing potential of S^{2-} is slightly stronger than that of SH^- (the reducing potentials of theirs are –0.508 v for $S + 2e^- \rightarrow S^{2-}$ and –0.478 v for $S + H_2O + 2e^- \rightarrow SH^- + OH^-$, respectively). This might be the main reason that the reaction is not specific and all the three products of this reaction had very low yields.

$[Ru_2(\mu_2\text{-}SH)_2(cymene)_2]$ and $[Ru_2(\mu_2\text{-}S)_2(cymene)_2]$ fragments From the work of Rauchfuss et.al., it was proposed that the sulfide bridge between two ruthenium atoms formed via SH^- [5]. That was, S^{2-} got a H^+ from the solvent (H_2O) giving SH^- firstly and

then SH^- substituted chloride atom as bridge giving $[ClRu(\mu_2\text{-}SH)(cymene)]_2$ fragment that would have further α-elimination to give $[Ru_2(\mu_2\text{-}S)_2(cymene)_2]$ fragment.

$$S^{2-} + H_2O \rightleftharpoons SH^- + OH^-$$

$$[RuCl_2(cymene)]_2 + 2\ SH^- \rightarrow [Ru(\mu_3\text{-}SH)(cymene)Cl]_2 + 2\ Cl^-$$

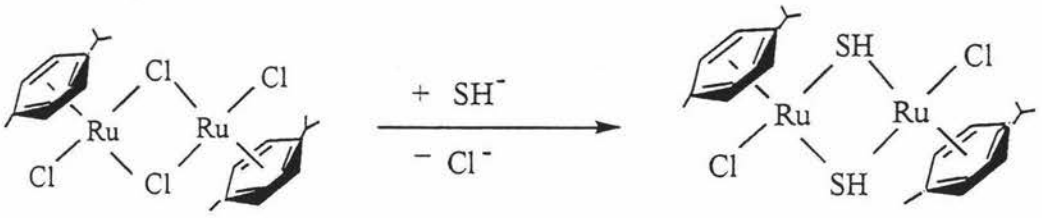

α-elimination of hydrogen halides or alkanes has been recognized as a valuable route to prepare species with metal-ligand multiple bonds [116]. But for dimer-like starting material, α-elimination would give an unsaturated di-nuclear center with two coordination sites that might lead to forming clusters with either metal-metal bonds or metals joined by other ligands such as sulfur atoms:

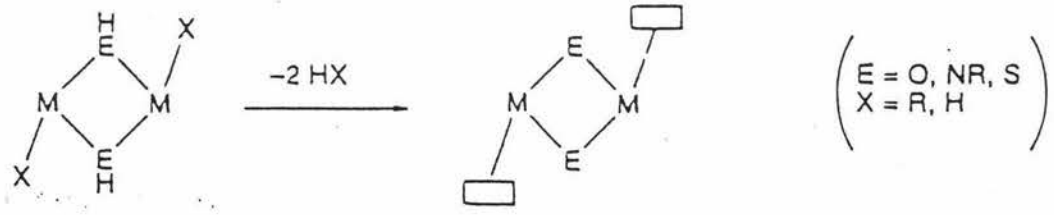

For $[ClRu(\mu_2\text{-}SH)(cymene)]_2$, HCl might be eliminated giving two coordination sites as well as sulfido ligands.

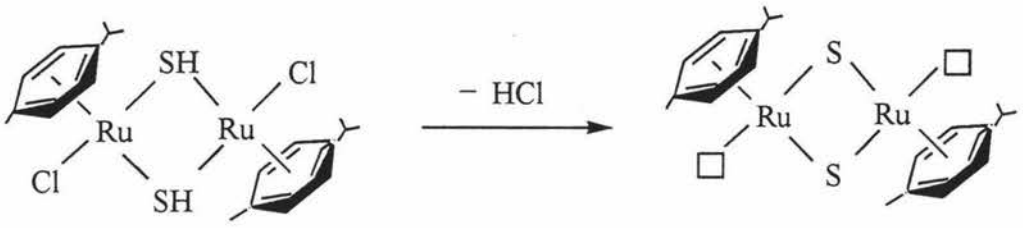

Recently, Hidai et al. demonstrated that the hydrosulfido-bridged di-ruthenium, dirhodium and diiridium complexes with Cp* as ligands, $[Cp^*M(\mu_2\text{-}SH)Cl]_2$ (M = Ru, Rh, Ir) served as precursors to not only the dithiolene-bridged di-nuclear complexes but also the tri- and tetra-ruthenium sulfido clusters $[Ru_3(\mu_3\text{-}S)_2(\mu_2\text{-}H)Cp^*_3Cl(PPh_3)_2]$ and $[M(\mu_3\text{-}S)Cp^*]_4$ (M = Ru, Rh, Ir) [86] (Scheme 17).

For $[Cp^*RuCl(\mu_2\text{-}SH)]_2$, it has two valence electrons less than that of corresponding rhodium and iridium complexes. There is one Ru-Ru bond in the hydrosulfido precursor and two Ru-Ru bonds in the produced cubane clusters (Scheme 17). There is no metal-metal bond in the later complexes, $[Cp^*MCl(\mu_2\text{-}SH)]_2$ (M = Ru, Ir) and their corresponding cubane clusters (Scheme 17). $[(cymene)RuCl(\mu_2\text{-}SH)]_2$ with cymene ligands has the same valence electrons with that of rhodium and iridium complexes with Cp* ligands, $[Cp^*MCl(\mu_2\text{-}SH)]_2$ (M = Ru, Ir). So it is proposed that there was $[(cymene)RuCl(\mu_2\text{-}SH)]_2$ formed during the reaction without Ru-Ru bond.

It was suggested that the formation of the coordinatively unsaturated sulfido-bridged intermediates, $[Cp^*M(\mu_2\text{-}S)]_2$ (M = Ru, Rh, Ir) was upon treatment of $[Cp^*MCl(\mu_2\text{-}SH)]_2$ (M = Ru, Rh, Ir) with base, by which α-dehydrohalogenation of later complexes gave higher nuclearity clusters via the intermediate fragments [86]. Although the di-ruthenium intermediate was too active to be observed, it had already been proven by trapping it using different compounds such as alkynes, $[RuH_2(PPh_3)_4]$, $NaBH_4$ and CO [86].

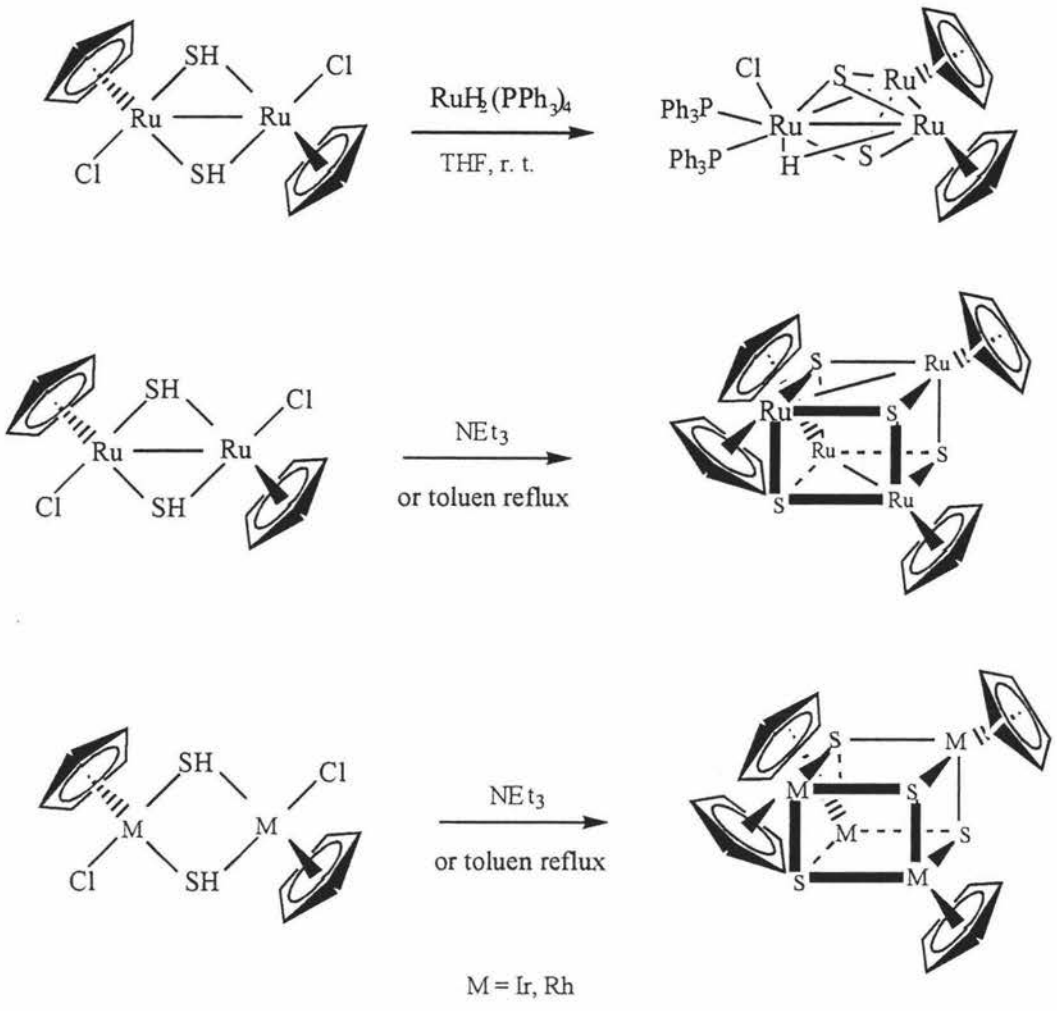

Scheme 17 $[Cp^*RuCl(\mu_2\text{-}SH)]_2$ as precursors and difference between Rh,Ir compounds and Ru compound

Formation of such an intermediate is common with the corresponding di-iridium and di-rhodium complexes that have been detected by ^1H NMR [98]. So it is reasonable that their iso-valence-electronic fragment $[(cymene)Ru(\mu_2\text{-}S)]_2$ might form as an intermediate during the reaction described in this Chapter.

The reactions of forming $Ru_3S_2(cymene)_3]^{2+}$ and $[Ru_5S_4(cymene)_4]^{2+}$ might be:

$[(cymene)RuCl(\mu_2\text{-}SH)]_2 \xrightarrow{-HCl} [(cymene)Ru(\mu_2\text{-}S)]_2 \longrightarrow Ru_3S_2(cymene)_3]^{2+}$ or $[Ru_5S_4(cymene)_4]^{2+}$

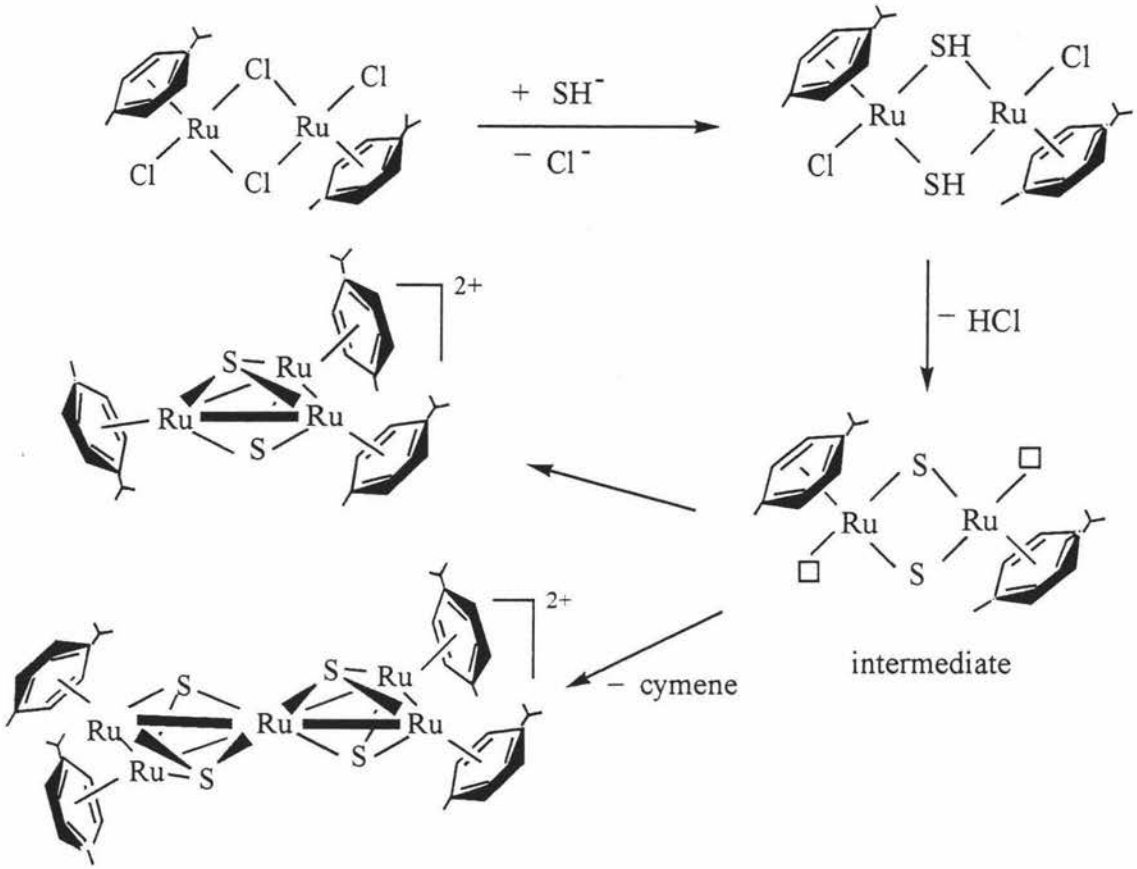

Formation of metal-metal bond from the bridged metal atoms For $[Ru_3S_2(cymene)_3](PF_6)_2$ and $[Ru_5S_4(cymene)_4](PF_6)_2$ clusters, the formation of Ru-Ru bonds might come from the intramolecular interaction in the clusters. An intramolecular example of metal-metal bond / nonbond equilibrium was proposed by Kolle et.al. [85] to account for the temperature dependence of the ^1H NMR spectrum of $[(C_5R_5)_2Ru_2X_4]$ complexes (X = Cl, Br) in 1991. There are two kinds of crystals of dimer which differ with respect to their Ru-Ru distance (Figure 29).

On the other hand, the equilibrium of metal-metal bond / nonbond also exists in the clusters when they gain or loose electrons,. Except the case of the $[Ru_3S_2(cymene)_3](PF_6)_2$ cluster in section 3.3.1 [5], Rauchfuss et.al. have studied the

equilibrium of cubane type ruthenium clusters $[(RC_5H_4)_4Ru_4E_4]^{0/2+}$ (E = S, Se, Te) (Figure 30) [80]. When the cluster loses two electrons, another Ru-Ru bond formed while the Ru-Ru bond opens when the later gains two electrons, which is similar to $[Ru_3S_2(cymene)_3](PF_6)_2$ cluster. (Scheme 1, see section 1.1)

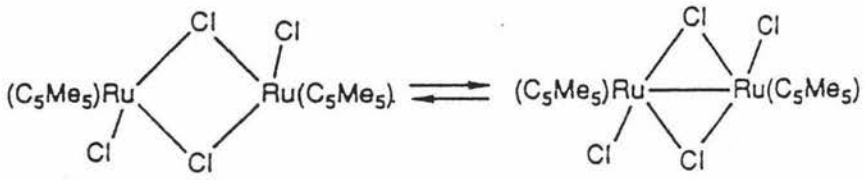

Figure 29 Metal-metal bond / nonbond equilibrium of Ru dimer

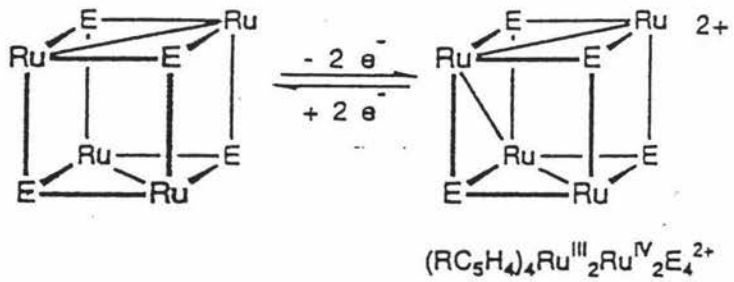

Figure 30 Metal-metal bond / nonbond equilibrium of Ru cubane cluster

Cubane type cluster and coordination The $[Ru_4S_2(SO)(cymene)_4]^{2+}$ cluster is similar to the cubane cluster $[Ru_4S_4Cp^*_4]^{2+}$ in number of atoms while it is a cluster with a

distorted square-like metal framework instead of cubane structure. The main reason might be because the different coordination to metal atom of RCp (R = H, Me_5, ^iPr) and cymene. Consequently they have different contributions to total electron count, five electrons for each RCp while six electrons for each cymene. At the same time, RCp has one negative charge on the Cp ring while cymene is neutral.

A lot of work has been done for ruthenium sulfur RCp (R = H, Me_5, ^iPr) clusters. Cubane type clusters are very normal for RCp clusters no matter halides, nitrogen or sulfur being as ligands. But only dimer and tri- or penta-nuclear clusters have been made for cymene clusters (only two cubane type clusters with benzene as ligands have been found, $[Ru_4H_4(benzene)_4]^{2+}$ [30] and $[Ru_4(OH)_4(benzene)_4]^{4+}$ [4]. It might be because the coordination to the metal atom is different between those two ligands. RCp is usually five coordination to metal atom while cymene is usually six coordination to metal atom, which might strongly influence the coordination ways of ruthenium atoms to other atoms such as sulfur atoms. In the cubane cluster, $[Ru_4S_4Cp^*_4]^{2+}$, one ruthenium atom coordinates to three sulfur atoms while it only coordinates to two sulfur atoms in the square like cluster $[Ru_4S_2SO(cymene)_4]^{2+}$.

Conclusion and future work High nuclearity arene-ruthenium sulfur clusters $Ru_3S_2(cymene)_3]^{2+}$, $[Ru_5S_4(cymene)_4]^{2+}$ and $[Ru_4S_2SO(cymene)_4]^{2+}$ might be made by hydrochloride α-elimination of $[(cymene)RuCl(\mu_2\text{-}SH)]_2$ via an intermediate of $[(cymene)Ru(\mu_2\text{-}S)]_2$ fragment. The proposed mechanism scheme is shown in Scheme 18:

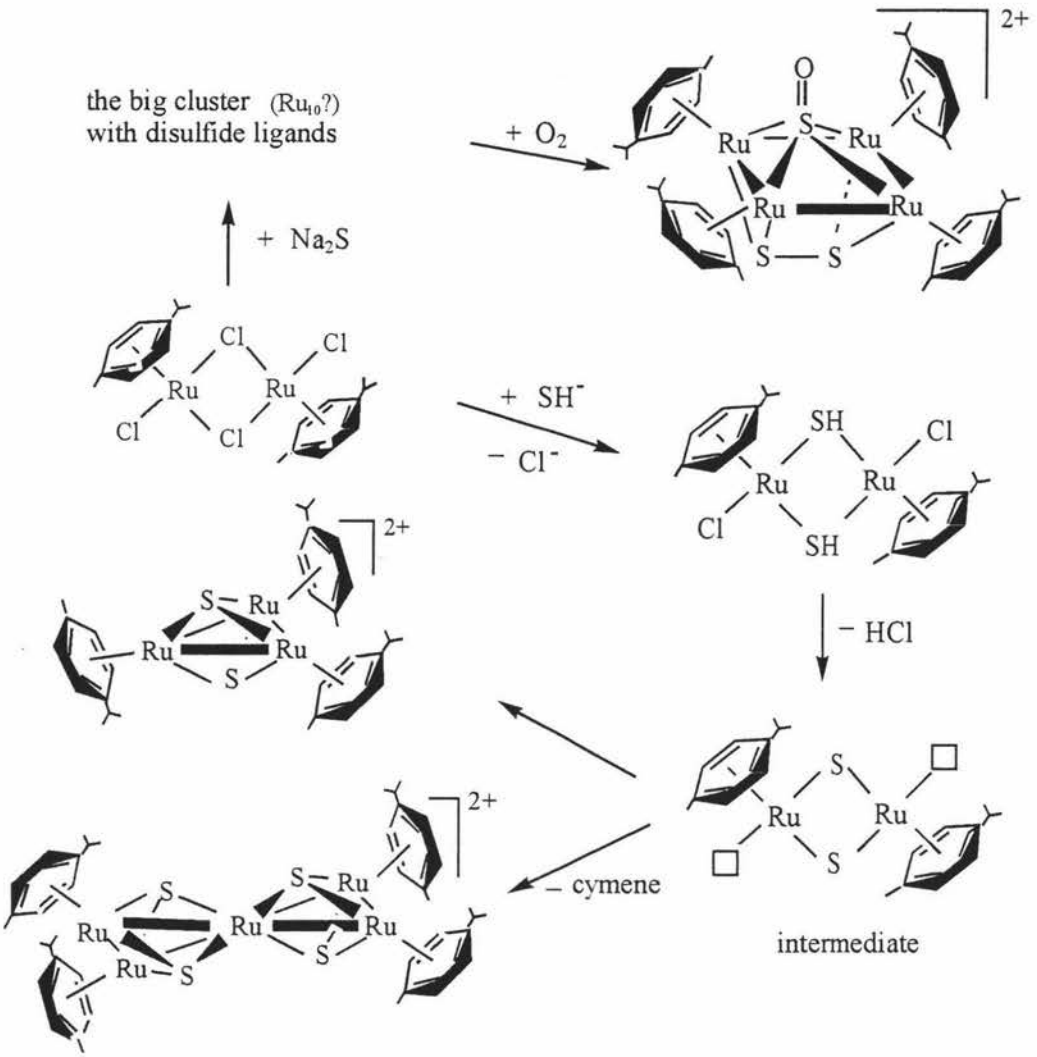

Scheme 18 Proposed mechanism of arene-ruthenium-sulfur clusters

The main task in the future is reducing the cationic clusters to neutral ones and doing further research work on them. The neutral clusters will be investigated with dihydrogen, dinitrogen, CO and other organic substrates in various conditions, especially under different pressure and with different reductants. The structure and reactivity of the big cluster needs to be investigated.

2.6. Reactions of ruthenium sulfur clusters

After the three cymene-ruthenium-sulfur clusters were made, it became very interesting to investigate the reactivity of them.

With H^+ It would be interesting to know which atoms that H^+ would attack firstly when the clusters react with acid. When CF_3COOH (diluted by D_6-acetone) was added in the sample of $[Ru_5S_4(cymene)_4](PF_6)_2$ in D_6-acetone, ^1H NMR was followed. There was a hydride signal at about -15.2, which meant that the H^+ attack the metal atoms firstly when the cluster reacted with acid. But the signal disappeared too quickly to get the spectrum with that signal. Similar experiments were done for $[Ru_3S_2(cymene)_3](PF_6)_2$ and $[Ru_4S_2(SO)(cymene)_4](PF_6)_2$ clusters. There was a little signal at around 14.0 for the $[Ru_3S_2(cymene)_3](PF_6)_2$ cluster but it was hard to tell it was a hydride peak or noisy. No signal observed for the $[Ru_4S_2(SO)(cymene)_4](PF_6)_2$ cluster with acid.

In order to last the hydride intermediate longer to get a clear spectrum, these experiments would run at lower temperature in the future research work.

With H_2 The reactivity of transition metal sulfur clusters toward H_2 is very important in the processes of hydrogenation and hydrodesulfurization. Therefore it is very interesting to investigate reactivity of cymene-ruthenium-sulfur clusters toward H_2.

Followed by ^1H NMR, it was found that the three clusters had some reactions with H_2 under 100 Psi (about 7 atm) in autoclave during 1-3 hours (Figure 28). The crystals of the $[Ru_5S_4(cymene)_4](PF_6)_2$ cluster was dissolved in D_6-acetone in a little vial. A lid with some little holes was put on the top of it. Then the vial was put into an autoclave. H_2 gas of 100 Psi pressure was filled in and then released for three times to get rid of the air. Keep the pressure under H_2 and followed with ^1H NMR. It was found that within three hours, the NMR spectra changed. But after three hours, the spectrum changed back to its original one. This implies that there might be some reactions occurred but the reactions were reversible. It was still not very clear what had happened. But it had given an excitement to do the further work on it in the future by using more facilitating instruments to do and follow the reactions.

With N_2 Transition metal sulfur clusters play important roles in N_2 reduction in both bio- and chemical systems, especially in nitrogen fixation processes. Similar experiments were run under N_2 instead of H_2 with different reductants in D_6-acetone

solution. There was almost no reactions that the clusters with N_2 under pressure of 3 atm with a mild reductant, Mg (Mg powder was washed in ultra-sound bath in acetone before being used in the experiment). When using a very strong reductant, $LiAlH_4$, the clusters decomposed.

In the further research the solvent will be changed to more polar ones such as H_2O and alcohol. The pressure of N_2 in these experiments was far too low. (Usually it was used as 30-100 atm in chemical systems of nitrogen reduction). So this experiment will be repeated using mild reductants and increasing the pressure of N_2 in the future.

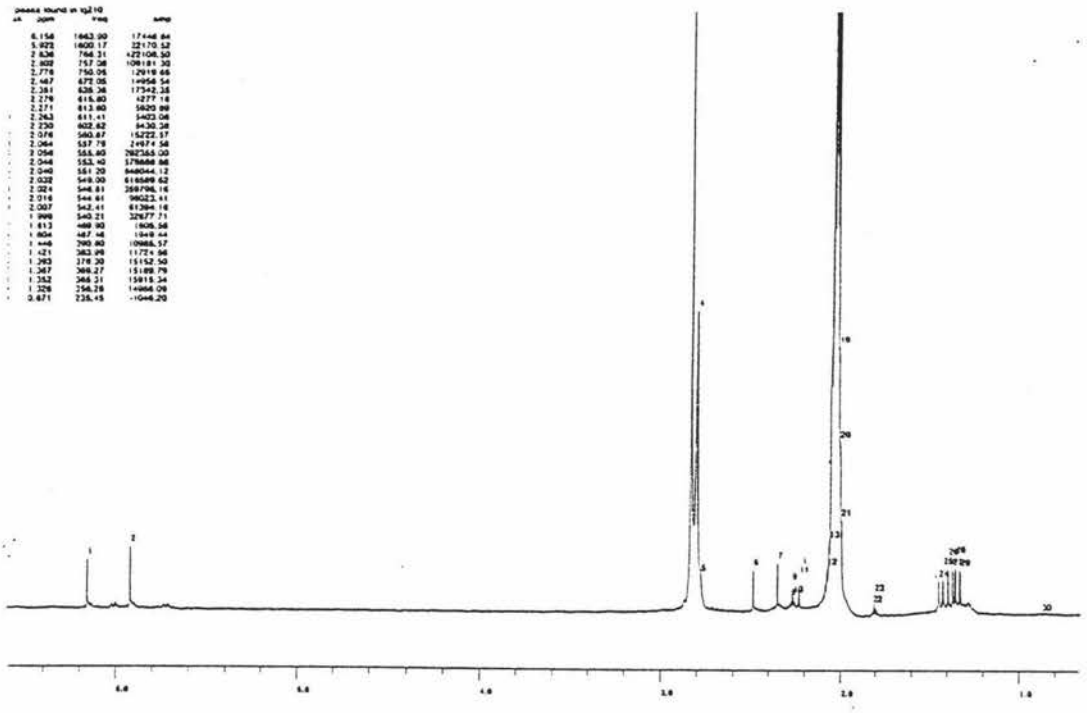

Figure 28 ^1H NMR spectrum of $[Ru_5S_4(cymene)_4]^{2+}$ with hydrogen

^{1}H NMR AND MASS SPECTROMETRY DATA FOR CLUSTERS OF CHAPTER TWO

Compounds	Chemical shift in $CDCl_3$ / ppm	Chemical shift in D_6-acetone / ppm	Chemical shift in CD_2Cl_2 / ppm	Molecular ion peak / mass unit
$Ru_3S_2(cymene)_3](PF_6)_2$	5.87	6.16	d-of-d 5.80-5.78	766.9
$[Ru_5S_4(cymene)_4](PF_6)_2$	5.66	5.92	5.61	1170
$[Ru_4S_2SO(cymene)_4](PF_6)_2$		6.14, 6.16; 6.46, 6.49; 6.81, 6.83; 7.06, 7.08		
Unknown big cluster (Ru_{10} ?)		multiple peaks 5.86-7.23		2526.8

CHAPTER 3. ARENE RUTHENIUM NITROGEN COMPLEXES

3.1. Introduction

Ruthenium sulfur clusters are comparatively easy to make and a number of new high nuclearity arene-ruthenium clusters have been described [114].

However, there are not many other arene-ruthenium clusters known, just the hydride cluster $[(arene)_4Ru_4H_4]^{2+}$ (arene = benzene, p-cymene) [30] and the hydroxide cluster $[(benzene)_4Ru_4(OH)_4]^{4+}$ [4] (the structures are given in Chapter One, Figure 4 a and Figure 2 a). Like the sulfur clusters, $[(arene)_4Ru_4H_4]^{2+}$ is very robust and exhibits the interesting properties of hydrogen absorption under the pressure of 60 atm H_2 and 55°C giving $[(arene)_4Ru_4H_6]^{2+}$ (Scheme 21) [119].

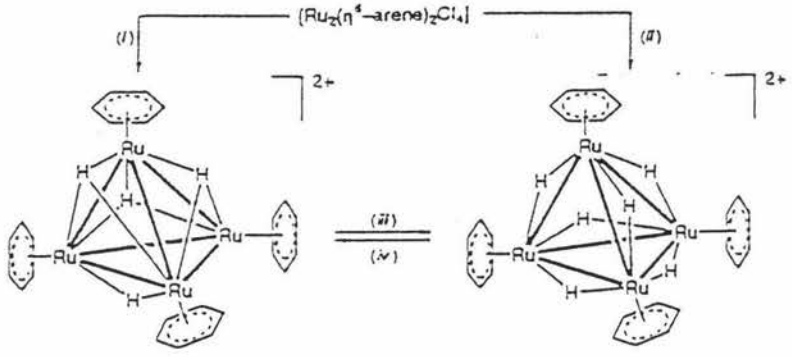

(*iii*) 60 atm H_2, 55 °C; (*iv*) $+0.5\ O_2$, $-H_2O$

Scheme 21 Dihydrogen absorption by $[Ru_4(benzene)_4H_4]^{2+}$

On the contrary, $[(benzene)_4Ru_4(OH)_4]^{4+}$ [4] is very labile in solution. It decomposes with hydroxide ion to corresponding bi-nuclear complexes. So an obvious target set of clusters are those based on nitrogen. These might be expected to have a stability intermediate between the oxygen and sulfur examples. As has been described in Chapter One and Chapter Two, sulfur clusters are very robust keeping the metal core together while losing or gaining electrons. The oxygen clusters are very labile that they are very easily to fall apart during the reaction. Nitrogen is smaller and more electronegative than

sulfur, but not as small and electronegative as oxygen. So nitrogen containing clusters might be an interesting area of research.

In addition, transition metal complexes with nitrogen containing ligands are of interest as intermediates in nitrogen fixation and for their involvement in nitrogen atom transfer reactions to both inorganic and organic substrates. From the oxidation-reduction cycle of the Fe-protein of nitrogenase (Figure 45 [87]), it can be seen that there are at least five nitrogen containing clusters involved in the process of nitrogen fixation.

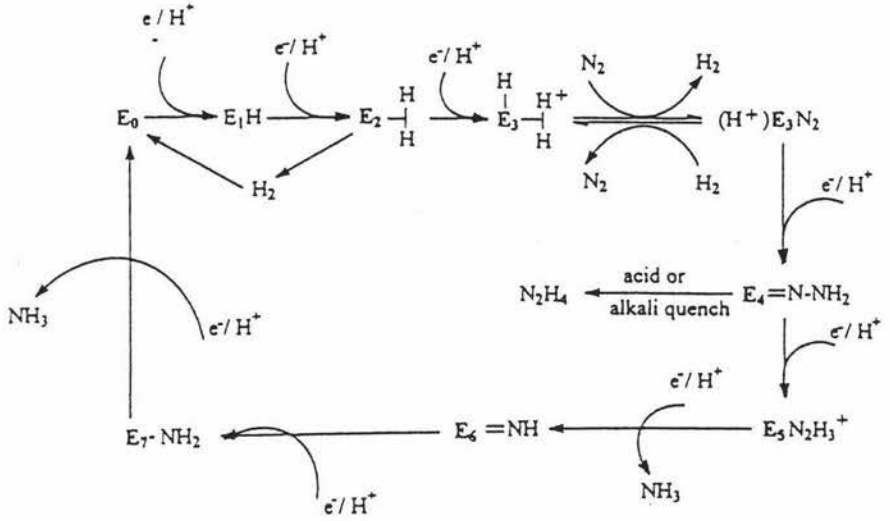

(E_0, resting state of MoFe-protein, N_2 binds to species E_3 displacing H_2)[87]

Figure 45 The catalytic cycle for the reduction of N_2 by Mo-nitrogenase of K. pneumoniae

The interest in nitrido complexes derives from the investigation of the reactivity of small molecules bound to metal complexes with sulfur-rich coordination [89]. A number of ruthenium carbonyl nitrido clusters have been made in the last a few decades, such as $(N^nBu_4)[M(N)(S_2C_6H_4)_2]$ (M = Ru, Os) [116], $[\mu\text{-}N\{Ru(PCy_3)('S_4)\}_2](BPh_4)$ [117] and $[Ru(CO)_{13}(\mu\text{-}H)(\mu_5\text{-}N)(\mu_3\text{-}\eta^2\text{-}PhC_2Ph)_2]$ [118] (Figure 58).

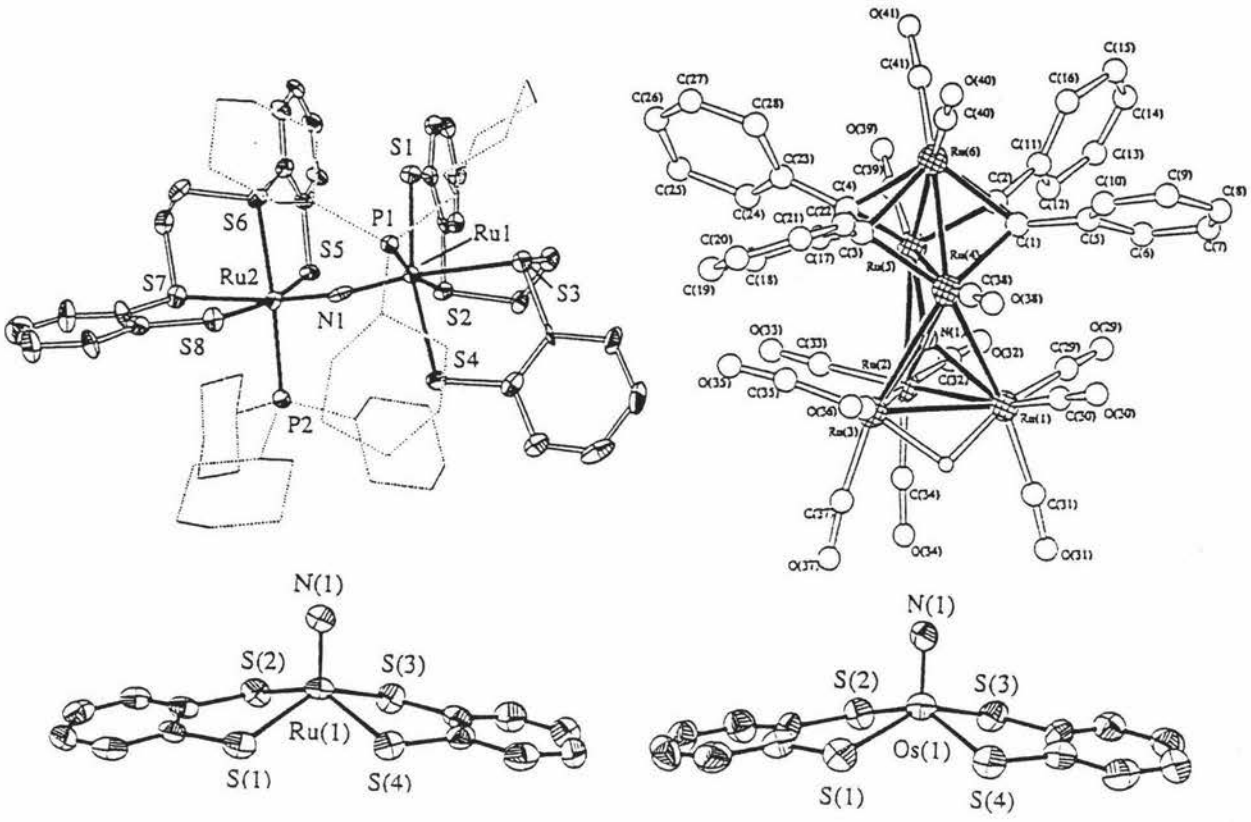

Figure 58 Examples of ruthenium nitrido carbonyl clusters

Clusters containing nitrogen atoms that are three-coordinated to the triangular faces of transition metal arrays are common for the elements of group 4 and 5 transition metals. The cubane cluster of Ti with nitrogen and Cp* as ligands has been made by Mena et al. in 1995 [90] (Figure 59 a) and the analogue of V has been made by Bottomley et al. in 1996 [91] (Figure 59 b). But ruthenium nitride cubane clusters are not yet known.

Ammonia complexes In the last few years, reactions of alkyl organometallic compounds with ammonia have been used as an elegant and efficient entry to the synthesis of polynuclear early transition metal nitrides [92]. In this way, tri-, penta-, and hexa- nuclear complexes have been reported [93].

On the other hand, nitrogen containing ligands such as ammine, hydrazine and ammonia are all involved in the processes of nitrogen fixation.

A synthetic strategy involving α-elimination of hydrogen halides from complexes containing coordinated ammonia might be succeed giving high nuclearity clusters with nitrogen containing ligands. This strategy has been applied to generate some promising results as will be described below.

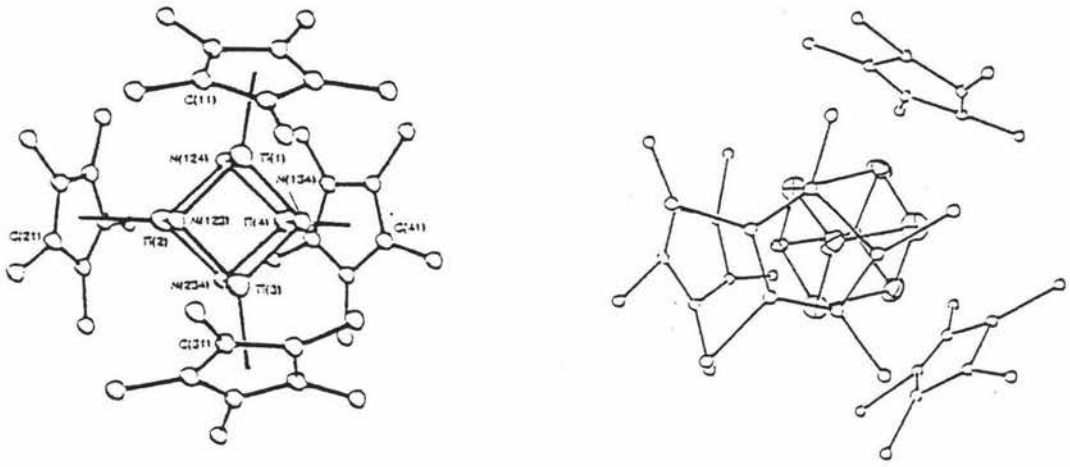

a b

Figure 59 Structures of $[Ti(\mu_3\text{-}N)(Cp^*)]_4$ and $[V(\mu_3\text{-}N)(Cp^*)]_4$

3.2. Synthetic strategy

To use ammonia as the source of nitrogen-containing ligands, one approach is to introduce ammonia to the coordinated sphere of ruthenium first. The complexes could then be combined to form clusters containing nitrogen atoms.

An early stage of this project was started by treating the dimer, $[RuCl_2(\eta^6\text{–cymene})]_2$ with ammonia gas in dichloromethane resulting the bis-ammonia salt $[RuCl(NH_3)_2(\eta^6\text{–cymene})]PF_6$ [113] . The outline of this reaction is shown in Scheme 15:

$RuCl_3 \cdot n H_2O$

↓ introduce η^6–cymene, 90^0C, 1,2-cyclohexadiene

$[RuCl_2(\eta^6\text{–cymene})]_2$

introduce ammonia

NH_3 / CH_2Cl_2 / NH_4PF_6

$[RuCl(NH_3)_2(\eta^6\text{–cymene})]PF_6$

Scheme 15 Reaction scheme of bis-ammonia complex

The suggested reaction next was then to treat the ammonia complex with base, eliminating HCl to give clusters with ammine ligands. But a series of intractable oils that could not be characterised were obtained. However a novel ruthenium dimer was isolated:

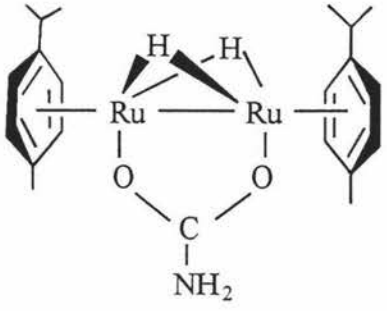

This dimer was isolated in very low yield and details of the reaction in which it was formed were unclear. So the synthesis involved in this chapter started with the dimer $[RuCl_2(\eta^6\text{–cymene})]_2$ and the bis-ammonia complex $[RuCl(NH_3)_2(\eta^6\text{–cymene})]PF_6$.

3.3. Formation of ruthenium nitrogen containing complexes

Starting from the $[RuCl_2(\eta^6\text{–cymene})]_2$ dimer, two new mono-nuclear complexes, one known mono-nuclear complex and one new di-nuclear complex were synthesized. These complexes could be obtained from each other under different conditions.

3.3.1. Formation of the bis-ammonia complex $[RuCl(NH_3)_2(\eta^6\text{–cymene})]PF_6$

From the dimer $[RuCl_2(\eta^6\text{–cymene})]_2$ When the dimer was treated with dichloromethane which is saturated with ammonia, yellow crystals were obtained. The structure of this complex had been determined [113]. It has a half sandwich structure:

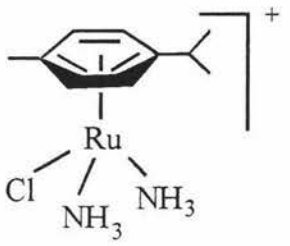

IR spectrum showed that there were four N-H stretch absorption at 3381.5 cm^{-1}, 3337.3 cm^{-1}, 3250.3 cm^{-1} and 3194.6 cm^{-1} (Figure 32). ^1H NMR spectrum for the yellow crystals showed the chemical shifts for the hydrogen atoms on the cymene ring were at 5.703, 5.680 ppm and 5.526, 5.503 ppm (Figure 33).

Shielding effect and chemical shift Comparing to a similar known complex $[RuCl(NNEt_2en)(\eta^6\text{-cymene})]PF_6$ [88], the chemical shift of bis-ammonia complex is at lower field while they are both one plus cations (for $[RuCl(NNEt_2en)(\eta^6\text{-cymene})]PF_6$ chemical shifts are at 5.67, 5.65 ppm; 5.46, 5.44 ppm. see Table 1). This is mainly caused by shielding effect of hydrogen atoms on the cymene ring by delocalized π electrons of the ring. The shielding effect of the cymene ring is strongly influenced by coordinating ruthenium atom.

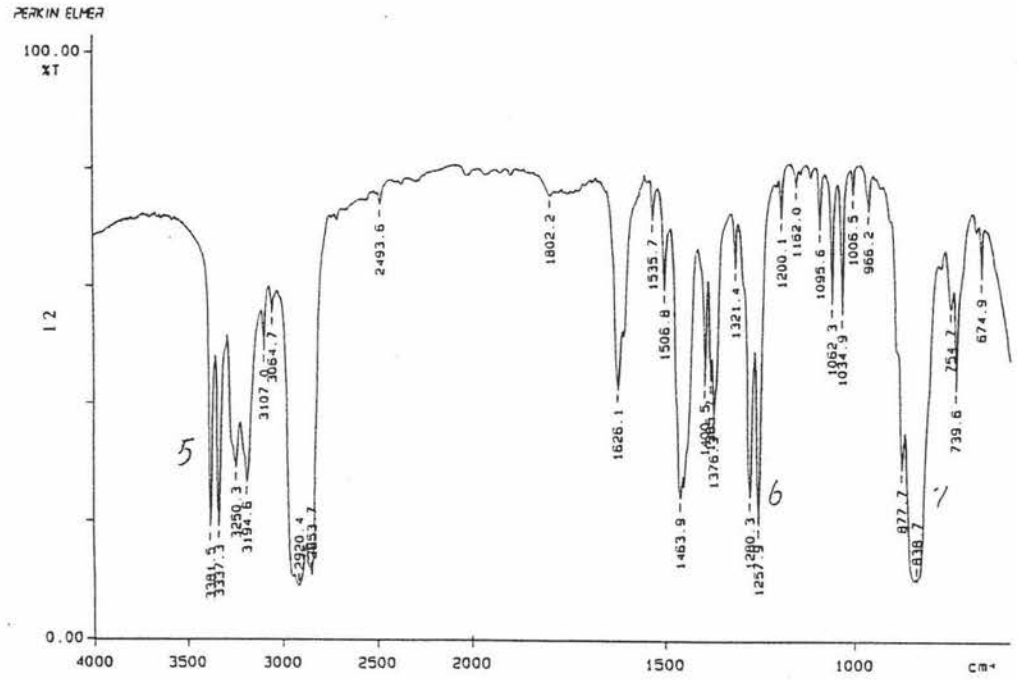

Figure 32 IR spectrum of $[RuCl(NH_3)_2(\eta^6\text{–cymene})]PF_6$

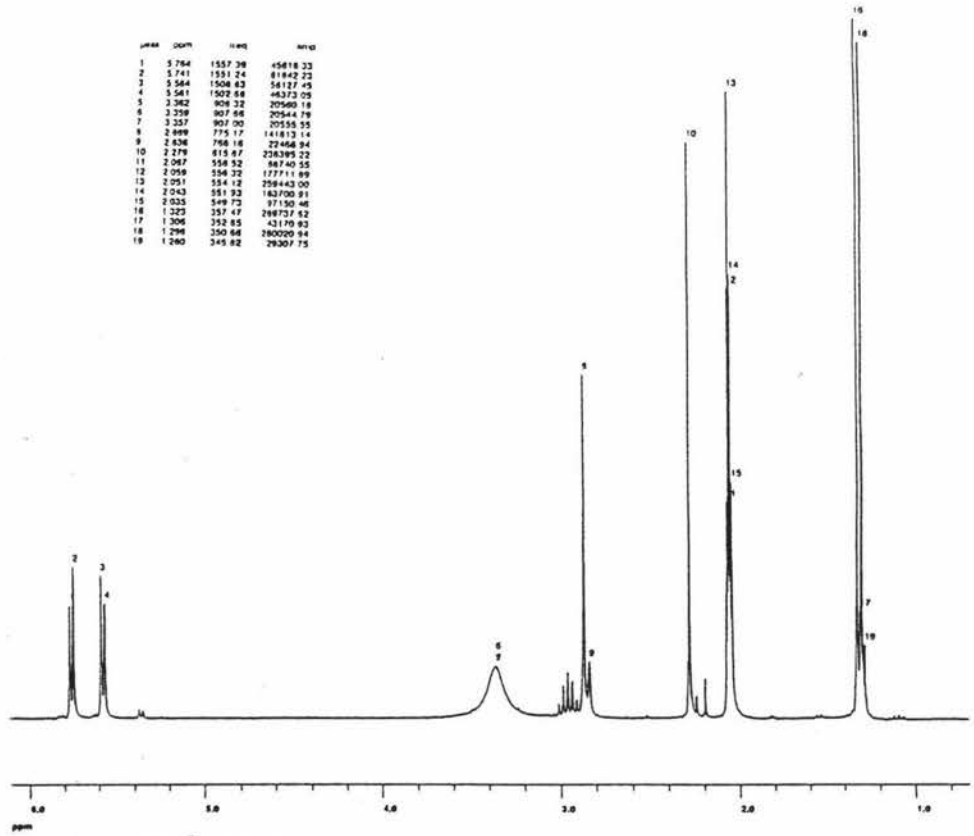

Figure 33 ^1H NMR spectrum of $[RuCl(NH_3)_2(\eta^6\text{–cymene})]PF_6$

Usually the chemical shifts of the hydrogen atoms on aromatic ring are at lower field (about 7.27 ppm) than that calculated for a corresponding ring system with alternating single and double bonds (about 5.7 ppm). They are even lower than those hydrogen atoms on aliphatic groups such as methyl and ethyl groups (1.3-1.5 ppm). This is because the shielding effect from the delocalized π electrons of the aromatic ring. The delocalized π electrons on the aromatic ring have an induced electron circulation under the added magnetic field, B_0, which gives an interior magnetic field (Scheme 20). From the scheme, it can be seen that in the middle of the ring, the induced magnetic field is opposite to the added magnetic field B_0 and decreases it while on the edge of the ring where the hydrogen atoms sit, the induced magnetic field has the same direction with B_0 and increases it. So the chemical shift of the hydrogen atoms on cymene ring moves to the low field.

When the aromatic ring coordinates to a metal atom, it is usually a π- and σ-donor to metal atom and a σ-acceptor from the metal atom (see Scheme 20). Both donor and acceptor will lessen the shielding effect that delocalized π electrons give to the hydrogen atoms. Subsequently, the chemical shift of hydrogen atoms on coordinating aromatic ring will move to the higher field than that of free aromatic ring. Different aromatic ring with different coordination to metal atoms will give different chemical shift on ^{1}H NMR spectrum. The other groups coordinating to the metal atoms also influence the shielding effect through donating electrons to the metal atom or withdrawing electrons from it. The more potential of other coordinating groups donating electrons to the metal atom, the more acception of the aromatic ring from the metal atom, the less shielded the hydrogen atoms on the aromatic ring by the delocalized π electrons, the higher the chemical shift will be.

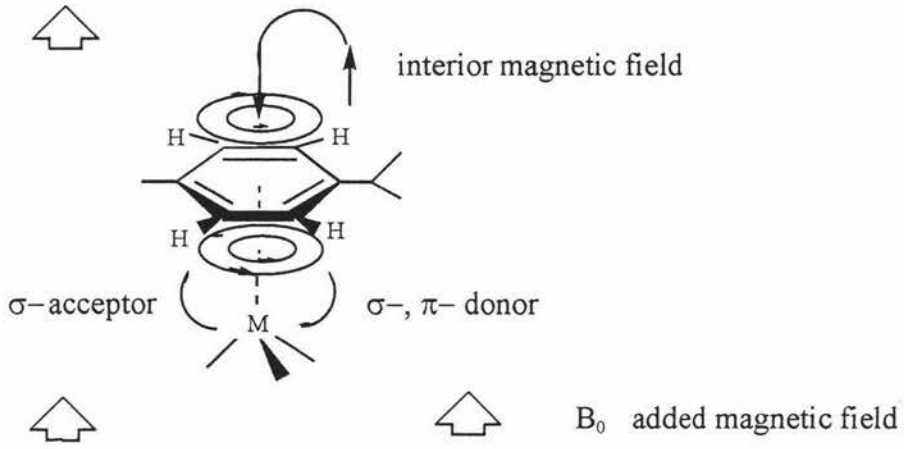

Scheme 20 Interior magnetic field and donor / acceptor of cymene ring

For these two cationic complexes, there are two opposite aspects that influence the shielding effect of the delocalized π electrons to the hydrogen atoms on the cymene ring. These two aspects give opposite influence resulting that the chemical shift of the bis-ammonia complex is slightly lower than that of $[RuCl(NNEt_2en)(\eta^6\text{-cymene})]PF_6$ complex. On one side, they both have two nitrogen atoms coordinating to the ruthenium atom. But the groups connecting to the nitrogen atoms are different, six hydrogen atoms for bis-ammonia complex and one Et_2en group for $[RuCl(NNEt_2en)(\eta^6\text{-cymene})]PF_6$ complex. Et_2en group has more potential of pushing electrons to ruthenium atom than the six hydrogen atoms on ammonia ligands do. So there is less electron density on the ruthenium atom for bis-ammonia complex than $[RuCl(NNEt_2en)(\eta^6\text{-cymene})]PF_6$ complex, which the ruthenium atom in the bis-ammonia complex influences the shielding effect less than that in $[RuCl(NNEt_2en)(\eta^6\text{-cymene})]PF_6$ complex. Therefore the chemical shift of bis-ammonia complex should be in the higher field than that of $[RuCl(NNEt_2en)(\eta^6\text{-cymene})]PF_6$ complex. On the other side, the Et_2en group cause an effort of pushing the cymene ring further. The longer distance of Ru-cymene will lessen the influence of ruthenium atom to the shielding effect that the delocalized π electrons do to the hydrogen atoms on cymene ring. The distance of the cymene ring to ruthenium

atom for bis-ammonia complex is slightly shorter than that for $RuCl(NNEt_2en)(\eta^6$-cymene)]PF_6 complex, they are 1.646 (14) Å and 1.683 (3) Å, respectively (Table 1). So these two opposite influences join together making the chemical shift of hydrogen atoms on the cymene ring in bis-ammonia complex is slightly lower than that of $RuCl(NNEt_2en)(\eta^6$-cymene)]PF_6 complex.

complex	distances of Ru-cymene / Å	Ru-N bond lengths / Å	Chemical shifts / ppm
$[RuCl(NH_3)_2(\eta^6$–cymene)]PF_6	1.646 (14)	2.138, 2.176 (15)	5.76, 5.74; 5.58, 5.56
$RuCl(NNEt_2en)(\eta^6$-cymene)]PF_6	1.687 (3)	2.118, 2.241 (5)	5.67, 5.65; 5.46, 5.44

Table 1 Compare the chemical shifts of two cationic nitrogen containing complexes

The reaction is shown below. The yield of this reaction is 82.6%.

$$[RuCl_2(\eta^6\text{–cymene})]_2 + 4\ NH_3 \longrightarrow 2\ [RuCl(NH_3)_2(\eta^6\text{–cymene})]^+ + 2\ Cl^-$$

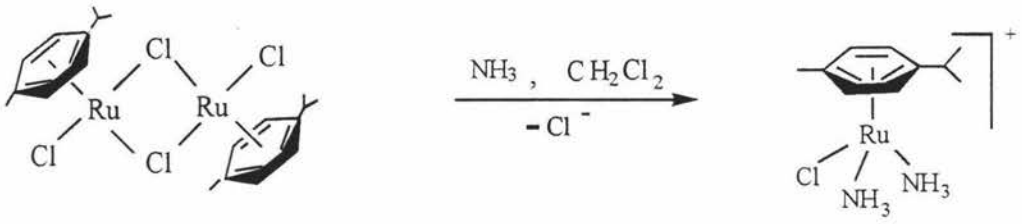

Forming in liquid ammonia Originally liquid ammonia was used as solvent hoping to form the tris-ammonia complex, $[Ru(NH_3)_3(cymene)](PF_6)_2$. But when the dimer, $[RuCl_2(cymene)]_2$ was added to liquid ammonia (ammonia excess) with stirring for two hours, only the bis-ammonia complex, $[RuCl(NH_3)_2(cymene)]PF_6$ was obtained. The yield was better than that of the reaction in dichloromethane (increasing from 82.6 % to 93.4 %). The precipitate of bis-ammonia complex might prevent the formation of tris-ammonia complex.

From the mono-ammonia complex [$RuCl_2(NH_3)(\eta^6$–cymene)] When the reactivity of the mono-ammonia complex was explored, it was a surprise finding that the bis-ammonia complex could also be obtained from the mono-ammonia complex. After being heated with two equivalents of DBU in dichloromethane at 60-70^{0}C for about an hour, the yellow solution was treated with NH_4PF_6. Some red-brown crystals were obtained. The red-brown crystals were shown to be the bis-ammonia complex by comparing its ^{1}H NMR spectrum, IR spectrum and the unit cell data of X-ray crystallography with the data from an authentic sample. The yield was very low since the mono-ammonia complex is not very soluble in dichloromethane.

The reaction is:

$$[RuCl_2(NH_3)(\eta^6\text{–cymene})] + NH_3 \xrightarrow{2DBU} [RuCl(NH_3)_2(\eta^6\text{–cymene})]^+ + Cl^-$$

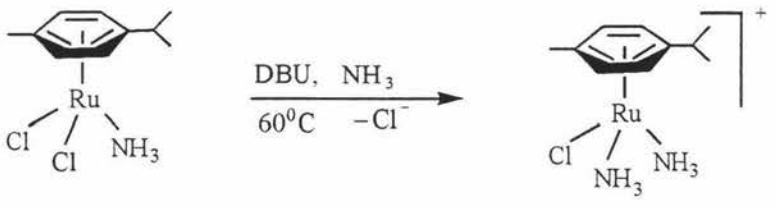

3.3.2. Formation of the mono-ammonia complex [$RuCl_2(NH_3)(\eta^6$ –cymene)]

From the dimer [$RuCl_2(\eta^6$–cymene)]$_2$ When the solution with precipitate of the bis-ammonia complex from the reaction in 3.3.1 (from the dimer [$RuCl_2(\eta^6$–cymene)]$_2$) was heated to 90°C under reflux for an hour instead of being treated with NH_4PF_6, red-brown crystals were obtained. There were four N-H stretch absorption at 3346 cm^{-1}, 3298 cm^{-1}, 3236 cm^{-1} and 3154 cm^{-1} (all m and sharp) on IR spectrum (Figure 35). But the shapes and positions of the peaks were different from that of the bis-ammonia complex. The ^{1}H NMR spectrum gave rise to four doublet-of-doublet peaks for the four hydrogen atoms on the cymene ring at 5.522, 5.449 ppm and 5.291, 5.272 ppm (Figure 36).

X ray crystallography gave the structure of the complex (Figure 37).

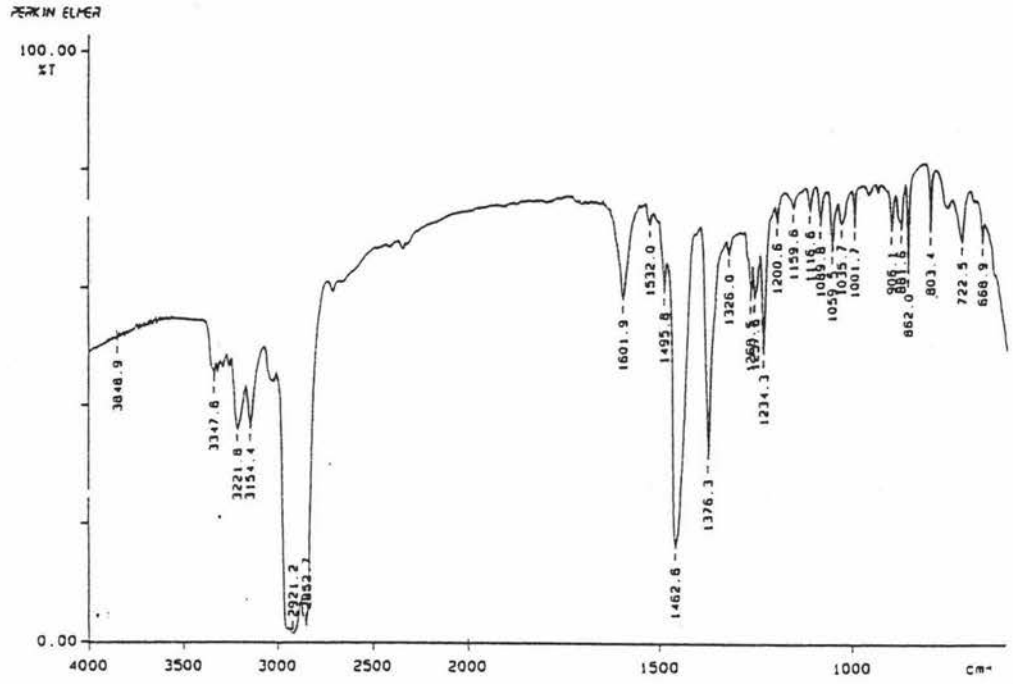

Figure 35 IR spectrum of $[RuCl_2(NH_3)(\eta^6\text{–cymene})]$

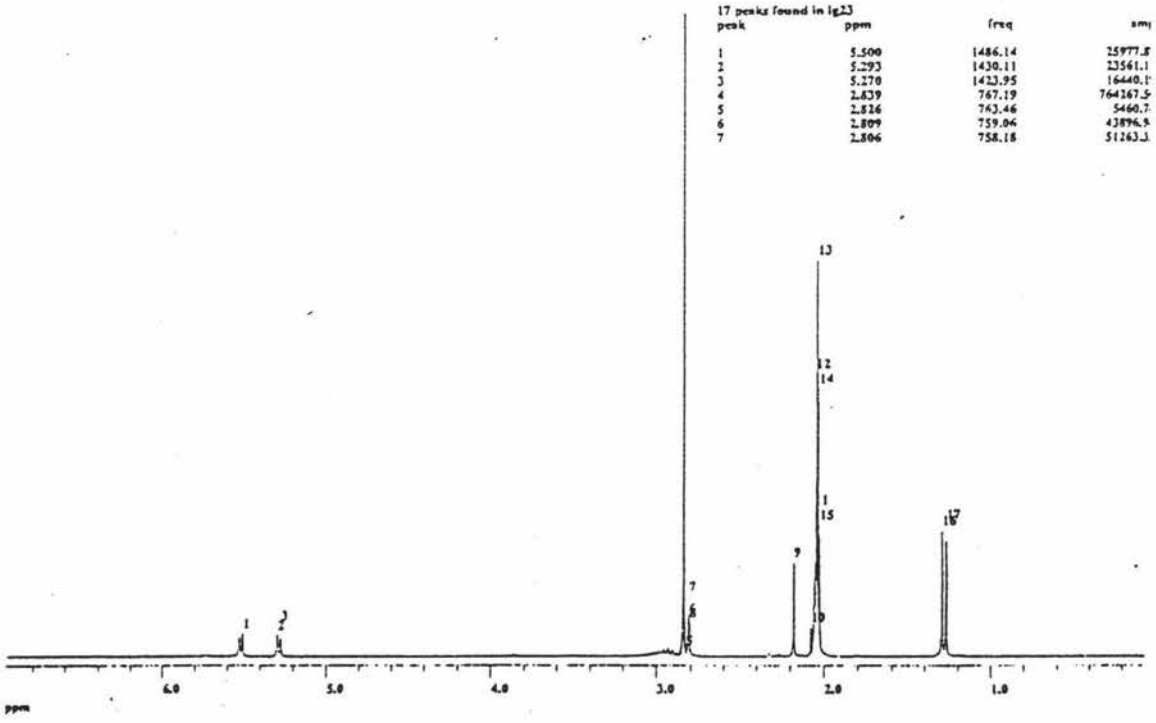

Figure 36 NMR spectrum of $[RuCl_2(NH_3)(\eta^6\text{–cymene})]$

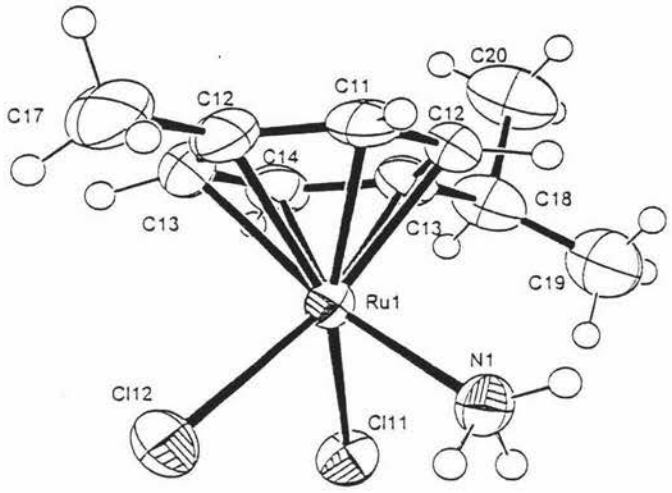

Figure 37 X ray crystal structure of $[RuCl_2(NH_3)(\eta^6\text{–cymene})]$

The crystal is triclinic, of space group $P_{\bar{1}}$. This implies that the crystal has inversion symmetry. There are three separate molecules in one asymmetric unit. The overall half sandwich structure of the complex is pseudo-octahedral with N-Ru-Cl bond angles are 84.6° (2) and 85.1° (2) respectively, which is similar to that of the bis-ammonia complex. The distances of the two chloride atoms to the ruthenium atom are slightly different in the three molecules, there are all one shorter bonds and one longer bonds. The cymene ring is essentially planar and the distance of the cymene ring to ruthenium atom is similar to that of the bis-ammonia complex, 1.650 (4) Å and 1.646 (14) Å, respectively. Some selected crystallographic data are listed in Table 2.

The overall reaction is shown below. The yield of this reaction is 90.9%.

$$[RuCl_2(\eta^6\text{–cymene})]_2 + 2\,NH_3 \xrightarrow{90^0C} 2\,[RuCl_2(NH_3)(\eta^6\text{–cymene})]$$

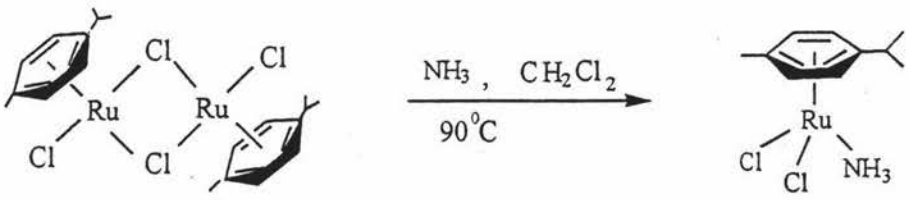

Bond length / Å	Molecule 1	Molecule 2	Molecule 3
Ru-N	2.129 (7)	2.132 (6)	2.115 (6)
Ru-Cl1	2.431 (2)	2.444 (2)	2.435 (2)
Ru-Cl2	2.405 (2)	2.422 (2)	2.418 (2)
Bond angle / ^{0}			
N-Ru-Cl1	84.6 (2)	83.3 (2)	81.8 (2)
N-Ru-Cl2	85.1 (2)	83.2 (2)	83.2 (2)
Cl1-Ru-Cl2	86.49 (7)	88.23 (8)	87.42 (8)

Table 2 Crystallographic data of the mono-ammonia complex

From the bis-ammonia complex When the mixture of bis-ammonia complex $[RuCl(NH_3)_2(\eta^6\text{–cymene})](PF_6)$ and two equivalents of DBU was heated to 90°C in dichloromethane under nitrogen for 4 hours, some red-brown crystals were obtained. IR and ^1H NMR spectra were the same with that of the mono-ammonia complex obtained from the reaction of dimer. This reaction might be a metathesis reaction of ammonia ligands by chloride ligands.

This reaction seemed similar to that of forming from the $[RuCl_2(\eta^6\text{–cymene})]_2$ dimer, but in fact they were different. The reaction from the dimer was heated in the original solution with free chloride ligands in the solution while this reaction was carried on using the pure crystals of the bis-ammonia complex.

The reaction is:

$$[RuCl(NH_3)_2(cymene)](PF_6) + Cl^- \xrightarrow{DBU,\ 90^0C} [RuCl_2(NH_3)(cymene)] + NH_3 + PF_6^-$$

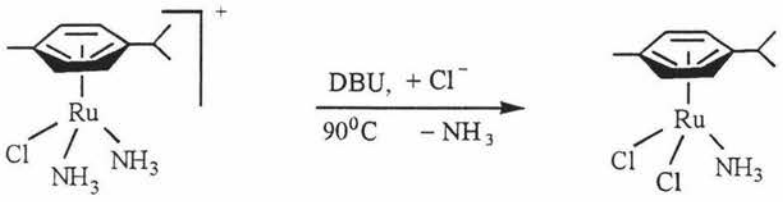

Compare the chemical shifts of these two ammonia complexes The chemical shifts of this neutral complex move to the higher field comparing to the bis-ammonia cation, which implies that the hydrogen atoms on the cymene ring in the mono-ammonia complex is less shielded by the delocalized π electrons (Table 3). As it was described in section 3.3.1, the neutral complex has one more electron to lessen the shielding effect from the delocalized π electrons of the cymene ring than the cationic complex. (More acception of cymene ring from the ruthenium atom in the mono-ammonia complex than that of the bis-ammonia complex). So the hydrogen atoms on the cymene ring are less shielded by the delocalized π electrons therefore the chemical shift of the mono-ammonia complex is in higher field than that of the bis-ammonia complex (average are 5.40 ppm and 5.67 ppm, respectively). This will also be discussed in section 3.3.3 with the tris-ammonia complex together.

complex	Distances of Ru-cymene / Å	Ru-N bond lengths / Å	Chemical shifts / ppm
$[RuCl_2(NH_3)(\eta^6\text{–cymene})]$	1.650 (4)	2.115, 2.132 (7)	5.52, 5.49; 5.29, 5.27
$[RuCl(NH_3)_2(\eta^6\text{–cymene})]PF_6$	1.646 (14)	2.138, 2.176 (15)	5.76, 5.74; 5.58, 5.56

Table 3 Chemical shifts, bond lengths of Ru-N and distances of Ru-cymene for the two ammonia complexes

The equilibria between the crystals and the solution From section 3.3.1 and 3.3.2, it can be seen that the mono-ammonia complex and the bis-ammonia complex can

be made from each other in certain conditions. This might be because there are equilibra between the crystals and solutions:

From the mono-ammonia complex to the bis-ammonia complex:

$[RuCl_2(NH_3)(\eta^6\text{–cymene})] \leftrightharpoons [RuCl(NH_3)(\eta^6\text{–cymene})]^+ + Cl^-$

$[RuCl_2(NH_3)(\eta^6\text{–cymene})] \leftrightharpoons [RuCl_2(\eta^6\text{–cymene})] + NH_3$

$[RuCl(NH_3)(\eta^6\text{–cymene})]^+ + NH_3 \leftrightharpoons [RuCl(NH_3)_2(\eta^6\text{–cymene})]^+$

From the bis-ammonia complex to the mono-ammonia complex:

$[RuCl(NH_3)_2(\eta^6\text{–cymene})]^+ \leftrightharpoons [RuCl(NH_3)(\eta^6\text{–cymene})]^+ + NH_3$

$[RuCl(NH_3)_2(\eta^6\text{–cymene})]^+ \leftrightharpoons [Ru(NH_3)_2(\eta^6\text{–cymene})]^{2+} + Cl^-$

$[RuCl(NH_3)(\eta^6\text{–cymene})]^+ + Cl^- \leftrightharpoons [RuCl_2(NH_3)(\eta^6\text{–cymene})]$

3.3.3. Formation of the tris-ammonia complex $[Ru(NH_3)_3(\eta^6\text{–cymene})](PF_6)_2$

From the dimer $[RuCl_2(\eta^6\text{–cymene})]_2$ Having obtained the mono-ammonia complex and the bis-ammonia complex, the synthesis of the tris-ammonia complex $[Ru(NH_3)_3(\eta^6\text{–cymene})]^{2+}$ was attempted to give another possible substrate for cluster formation and one which contained no chloride ligands.

One approach was using $AgNO_3$ to remove the chloride ligand from bis-ammonia complex. When the $[RuCl_2(\eta^6\text{–cymene})]_2$ dimer was treated with excess ammonia and $AgNO_3$ in dichloromethane, Cl^- could be removed from solution and consequently from the bis-ammonia complex through the equilibrium:

$$Ag^+ + M\text{-}Cl \quad \leftrightharpoons \quad M^+ + Cl^- + Ag^+ \quad \leftrightharpoons \quad M^+ + AgCl$$

However, after worked up, the IR and ^1H NMR spectrum of the yellow product were the similar to that of the bis-ammonia complex. So the product of this reaction might still be the bis-ammonia complex. It might also be the analogue with one or two water as ligands because there might be a competition between ammonia and water that exist in the solution.

Another approach was using liquid ammonia as described in section 3.3.1, ending up with bis-ammonia complex, too.

From the dimer $[RuCl_2(\eta^6\text{–cymene})]_2$ with ammonia in methanol The two reactions above suggested that the more polar solvents could be chosen in a thermal reaction rather than Ag^+ to prevent precipitation of the bis-ammonia complex and obtain tris-ammonia complex by adding another ammonia ligand to bis-ammonia complex. The benzene analogue of this complex in aqueous ammonia solution was tried but very low yield was obtained [96]. The dimer was added to distilled methanol which was saturated with ammonia and gently heated to 50°C, yellow crystals were obtained by evaporating the solution. The IR spectrum (Figure 38) showed two N-H stretch peaks at 3388 $cm^{-1}$and 3335 cm^{-1} (m, sharp). ^1H NMR spectrum (Figure 39) showed the chemical shifts the hydrogen atoms on the cymene ring were 6.008-5.985 ppm and 5.732-5.709 ppm which indicated the complex might be a two plus cation. The integral of the peaks of hydrogen atoms on ammonia ligands to those of hydrogen atoms on the cymene ring was approximately 9 : 4. So the complex is tris-ammonia complex $[Ru(NH_3)_3(\eta^6\text{–cymene})]^{2+}$. Treatment to the cation with NH_4PF_6 gives $[Ru(NH_3)_3(\eta^6\text{–cymene})](PF_6)_2$.

The success of this reaction is probably due to the fact that methanol is a much poorer ligand than water in arene-ruthenium chemistry. The reaction is shown below. The yield of the reaction is around 66.1%.

$$[RuCl_2(\eta^6\text{–cymene})]_2 + 6\,NH_3 \xrightarrow{MeOH,\ 50^oC} 2\,[Ru(NH_3)_3(\eta^6\text{–cymene})]^{2+} + 4\,Cl^-$$

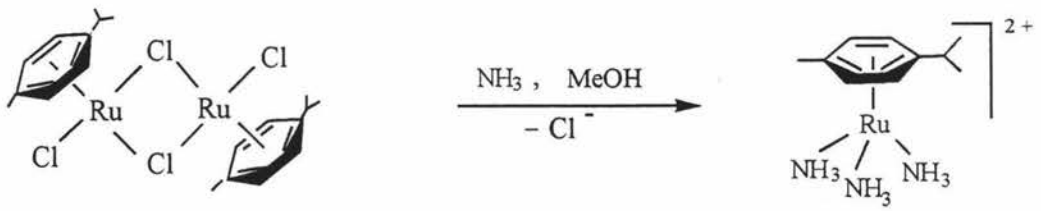

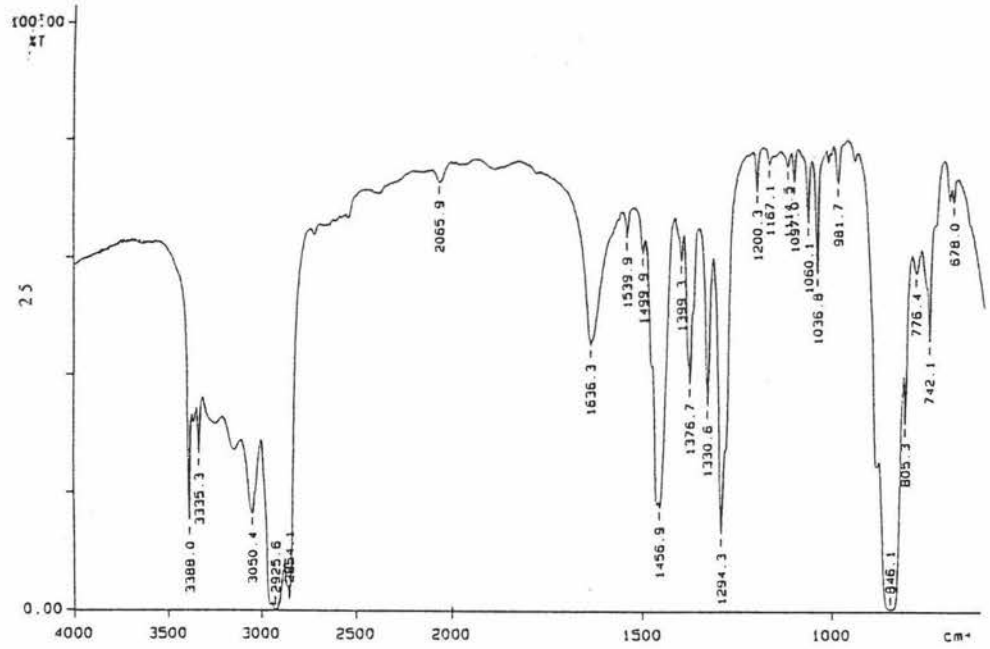

Figure 38 IR spectrum of $[Ru(NH_3)_3(\eta^6\text{–cymene})](PF_6)_2$

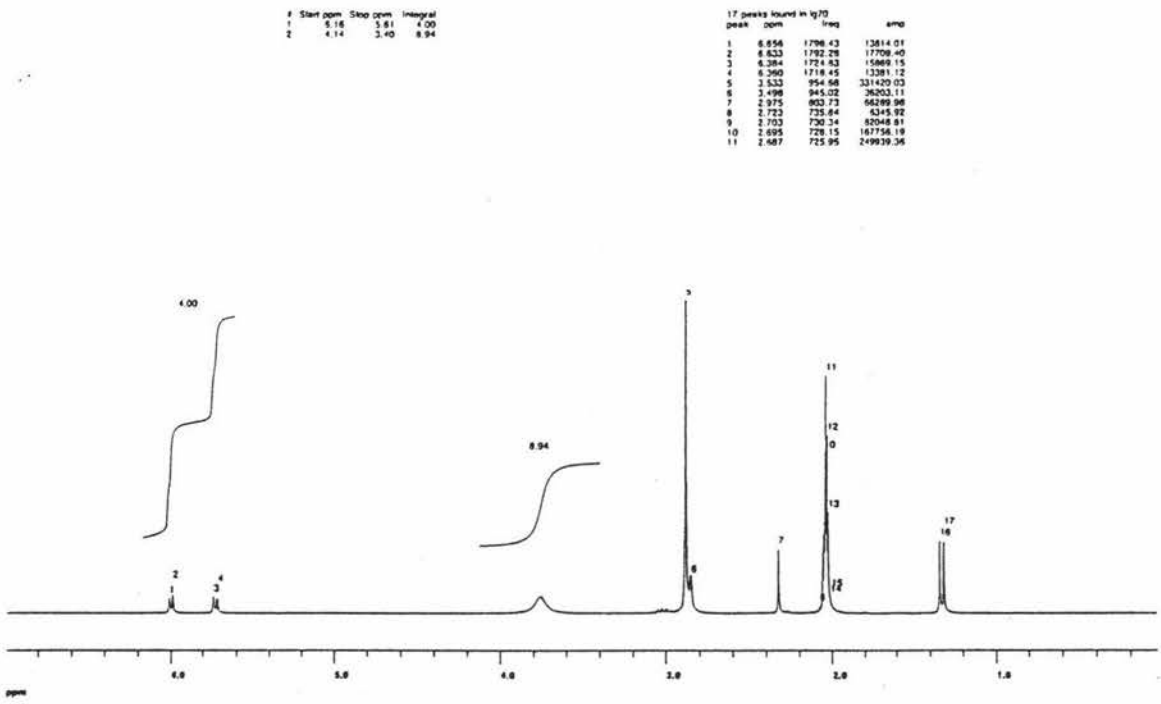

Figure 39 NMR spectrum of $[Ru(NH_3)_3(\eta^6\text{–cymene})](PF_6)_2$

Compare the chemical shifts of the three mono-nuclear ammonia complexes

The chemical shifts of the three mono-nuclear ammonia complexes are listed in Table 5. From the table, it is clear that the chemical shifts of hydrogen atoms on the cymene ring are strongly influenced by the charge of the complexes (the charge on ruthenium atoms). As it has been described in section 3.3.1, from mono-ammonia complex to bis-ammonia complex to tris-ammonia complex, the charge of the complex change from neutral to one plus charge to two plus, the donation of the cymene ring to ruthenium atom in these complexes increases while the acceptation from the ruthenium atom decreases, the shielding effect of delocalized π electrons to hydrogen atoms on the cymene ring are getting more therefore the chemical shift tends to be at higher field. The chemical shift for mono-ammonia complex is 5.52, 5.49; 5.29, 5.27 ppm while for the bis-ammonia complex and the tris-ammonia complex are 5.76, 5.74; 5.58, 5.56 ppm and 6.01, 5.99; 5.73, 5.71 ppm, respectively.

complex	Chemical shifts / ppm
$[RuCl_2(NH_3)(\eta^6\text{–cymene})]$	5.52, 5.49 5.29, 5.27
$[RuCl(NH_3)_2(\eta^6\text{–cymene})]PF_6$	5.76, 5.74 5.58, 5.56
$[Ru(NH_3)_3(\eta^6\text{–cymene})](PF_6)_2$	6.01,5.99 5.73, 5.71

Table 5 Chemical shifts of three mono-nuclear ammonia complexes

3.3.4. Formation of the amide dimer $[RuCl(NH_2)(\eta^6\text{–cymene})]_2$

From the bis-ammonia complex $[RuCl(NH_3)_2(\eta^6\text{–cymene})]PF_6$ DBU is a strong base which could deprotonate ammonia ligands leading to cluster formation. Crystals of the $[RuCl(NH_3)_2(\eta^6\text{–cymene})]PF_6$ complex and two equivalents of DBU were both added into distilled and degassed dichloromethane. The mixture was heated to 60°C for five hours. The red brown solution was evaporated to dryness and a little amount of acetone was added to dissolve the red-brown oil. Then the solution was put into fridge over night and some needle-like bright orange crystals were obtained.

IR and NMR spectra showed the difference of this exciting orange compound to those mono-nuclear complexes. The IR spectrum for the bright orange crystals (Figure 40) showed two N-H stretch absorption at 3339 cm^{-1} and 3259 cm^{-1} (m, sharp), which were different with any of those mono-nuclear complexes described above. ^1H NMR spectrum (Figure 41) showed the chemical shifts of the hydrogen atoms on the cymene ring at 5.047, 5.024 ppm and 4.904, 4.883 ppm which was at higher field compared to those mono-nuclear complexes. Since IR and ^1H NMR spectra both showed the differences with those mono-nuclear complexes obtained before, an X ray crystal structure determination was needed.

Bond lengths / Å		Bond angles / ^{0}	
Ru1-N1	2.091 (4)	N1-Ru1-N1#1	76.0 (2)
Ru1-N1#1	2.088 (4)	N1-Ru1-Cl1	84.48 (10)
Ru1-Cl1	2.4250 (12)	N1#1-Ru1-Cl1	85.20 (10)
Ru1-C1	2.163 (4)	Ru1#1-N1-Ru1	104.0 (2)

Table 10 X-ray crystallographic data of $[RuCl(NH_2)(cymene)]_2$

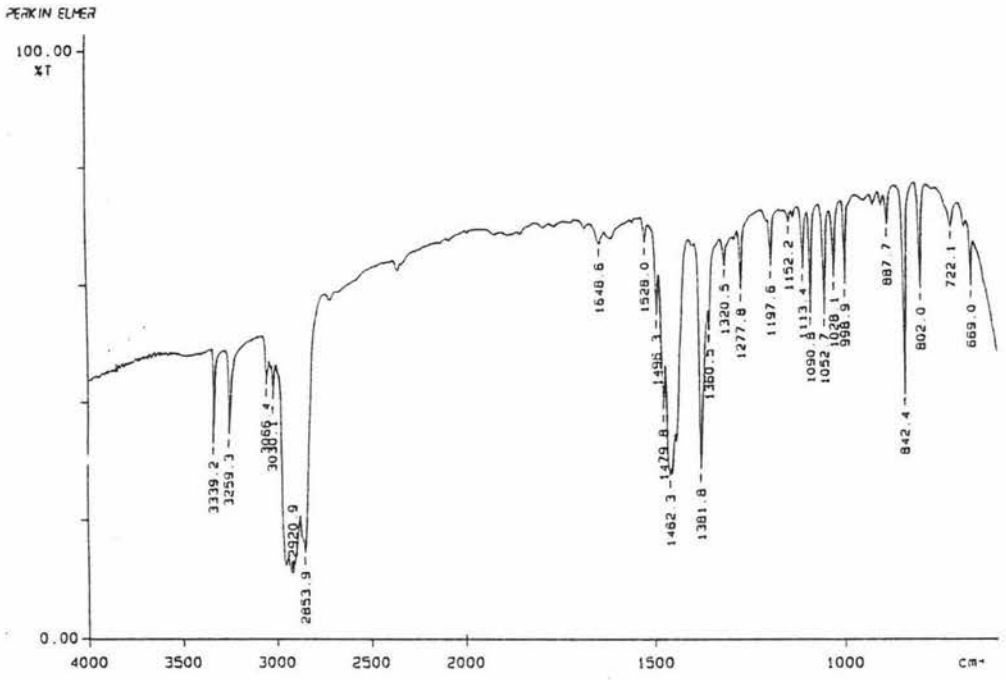

Figure 40 IR spectrum of $[RuCl(NH_2)(\eta^6\text{–cymene})]_2$

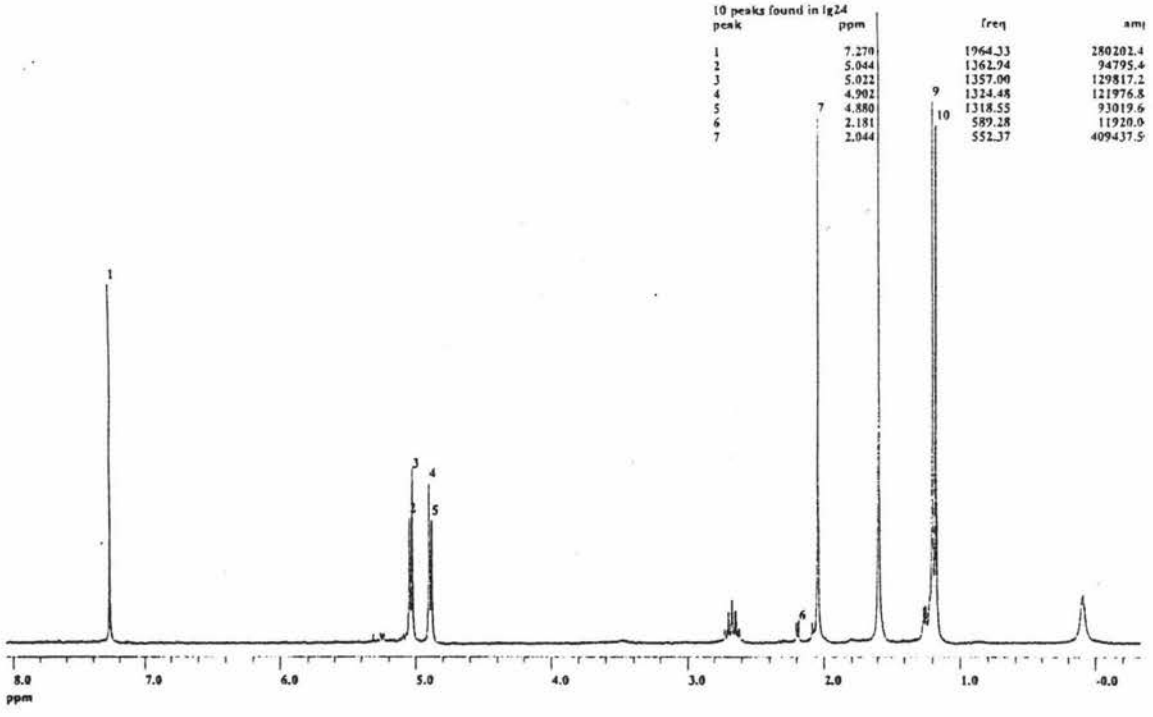

Figure 41 NMR spectrum of $[RuCl(NH_2)(\eta^6\text{–cymene})]_2$

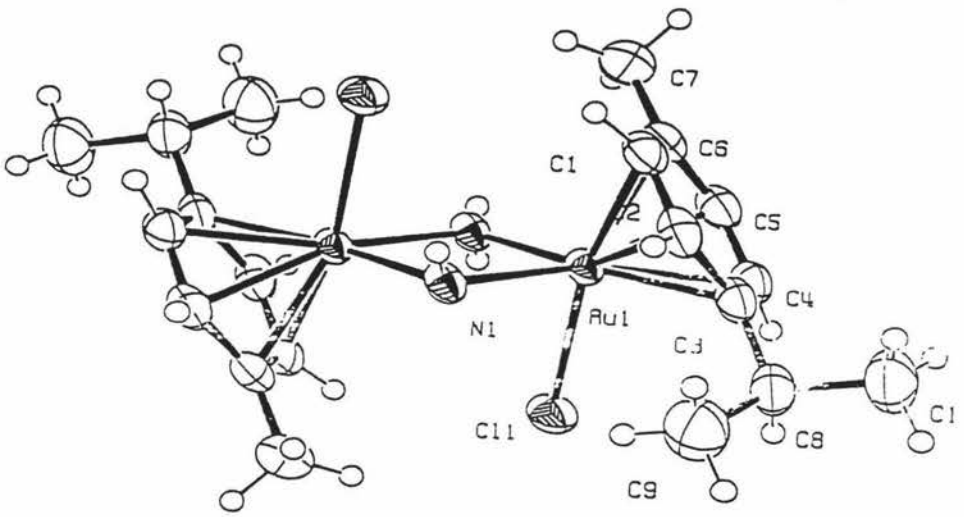

Figure 34 X ray crystallographic structure of $[RuCl(NH_2)(cymene)]_2$

X ray crystallography for the needle-like bright orange crystal gave the structure of this complex (showing in Figure 34). Some selected crystallographic data are shown in Table 10. From the data, it is known that the crystal is triclinic, of space group $P_{\bar{1}}$. The complex has the crystallographically imposed symmetry of a point of inversion, midway between the metal atoms. The consequence of this, is that only half of the structure needs to be solved, as the other half is merely a reflection of the first. Thus the table contains only half of the bond lengths and angles of the complex (as shown in Table 10). The complex is a novel dimer, with two amide ligands bridging the two ruthenium atoms. The structure of the complex has two pseudo-octahedral metal centers with a N-Ru-N bond angle of 76.0° and Cl-Ru-N bond angle of 84.48°. The Ru-C bond lengths of the complex range is from 2.088 Å to 2.091 Å, which is shorter than that of another similar dimer $[RuCl(N_3)(\eta^6\text{–cymene})]_2$ (2.165 Å to 2.176 Å) [94]. The reaction of forming the amide dimer is:

$$2\,[RuCl(NH_3)_2(cymene)]PF_6 + 2\,DBU \xrightarrow{60^\circ C} [RuCl(NH_2)(cymene)]_2 + 2\,(HDBU)PF_6 + 2\,NH_3$$

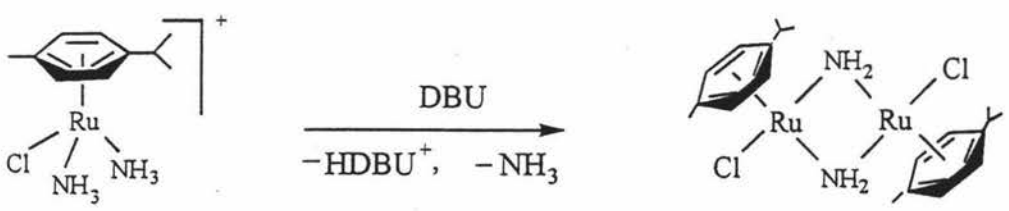

Chemical shifts of three dimeric complexes The cymene ring is essentially planar and the distance from the ring to the metal in three complexes are compared in Table 9 [97]:

complexes	Chemical shifts / ppm	Distances of cymene-ruthenium / Å	Bond lengths of Ru-N / Å	Bond lengths of Ru-Cl / Å
$[RuCl(NH_2)(\eta^6\text{–cymene})]_2$	5.04, 5.02; 4.90, 4.88	1.661 (2)	2.091 (4)	2.4250 (12)
$[RuCl_2(\eta^6\text{–cymene})]_2$	5.44, 5.42; 5.30, 5.28	1.651 (4)		
$[RuCl(N_3)(\eta^6\text{–cymene})]_2$	5.33, 5.31; 5.22, 5.20	1.657 (3)	2.118 (5) 2.241 (4)	2.397 (2)

Table 9 Chemical shifts, bond lengths of Ru-N and the distances of Ru-cymene for three dimeric complexes

From Table 9, it is known that the chemical shifts of these three dimeric complexes are different depending on different bridging groups. The chemical shift of $[RuCl(NH_2)(\eta^6\text{–cymene})]_2$ is in higher field compared to the other two complexes. That is, the hydrogen atoms on the cymene rings are less shielded by the delocalized π electrons on the cymene rings of this complex. The chemical shift of $[RuCl_2(\eta^6\text{–cymene})]_2$ is at the lowest field among the three dimers. But Ru-cymene distances of these dimeric complexes have no significant difference. Then it might be because of the different bridging groups that influence the electron density on ruthenium atoms therefore influence the shielding effect of hydrogen atoms by delocalized π electrons on the cymene ring (see discussion in section 3.3.1).

The chlorine atoms are less electronegative and more bulky than the nitrogen atoms therefore theyt have less influence to ruthenium atoms as bridging atoms. So for $[RuCl_2(\eta^6\text{–cymene})]_2$ dimer, the shielding effect of hydrogen atoms on cymene ring from the delocalized π electrons is more than those of the two nitrogen containing dimers. So the chemical shift is lower than the other two dimers.

For the two nitrogen containing dimers, bond length of N-Ru in $[RuCl(NH_2)(\eta^6\text{–cymene})]_2$ is shorter than that in $[RuCl(N_3)(\eta^6\text{–cymene})]_2$. Also nitrogen

atoms have more potential of withdrawing electrons from the bridging nitrogen atom than and consequently its coordinating ruthenium atom than hydrogen atoms do. Therefore the hydrogen atoms on the cymene ring of the $[RuCl(NH_2)(\eta^6\text{–cymene})]_2$ complex are less shielded by the delocalized π electrons on the cymene rings compared to the $[RuCl(N_3)(\eta^6\text{–cymene})]_2$ complex and the chemical shift is in higher field than the later one (average 4.96 ppm and 5.26 ppm, respectively).

3.3.5. Discussion of the reaction conditions

After the first experiment, a range of experiments with various reacting conditions were carried out to maximise the yield of the amide dimer.

Temperature Different temperatures not only give different yields, but also give different products. When the experiments were carried out at 50-70°C in dichloromethane with DBU, the amid dimer $[RuCl(NH_2)(\eta^6\text{–cymene})]_2$ was obtained (best yield of 30.1% was obtained at around 60°C). But when the experiments were heated at 85-130°C in dichloromethane, the mono-ammonia complex $[RuCl_2(NH_3)(\eta^6\text{–cymene})]$ was obtained. When the reaction was run at 80-82°C for five hours, a few bright red-orange crystals were obtained. The crystals changed their colour very quickly in the air to grey-brown colour without brightness at all. IR spectrum of the crystals was similar to that of the amide dimer. However the FAB mass spectrum gave a major ion at 577 that was 2 units more than that of the amide dimer. It might be another dimer with two ammonia ligands instead of amide ligands. The exact structure was still unknown because the crystal could not diffract at all.

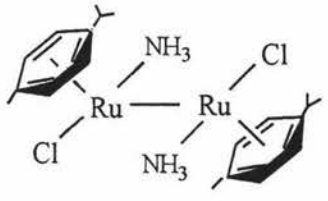

Amount of base Another factor in the reaction is the amount of DBU. Two equivalents of DBU were required. Excess did not effect the production of the new amide

dimer, however excess DBU had a strong effect on the crystallizing process and the yield of the product. When two equivalents of DBU were added, crystals of the amide dimer $[RuCl(NH_2)(\eta^6\text{–cymene})]_2$ in 30% yield were obtained, which was the highest yield obtained. When more than three equivalents of DBU were used, the amide dimer could not be crystallized from the acetone solution because of the influence of excess DBU. When more than four equivalents of DBU were used, the colorless crystals of DBU salt came out first and no new dimer crystals obtained at all.

Solvent The nature of the solvent is also important for the reaction. It was found that the best yield of all this kind of reaction was obtained by using dichloromethane as solvent. It was better than that using dichloroethane at 60°C. Some very pure yellow crystals of the amide dimer was obtained in toluene at 90°C (yield was around 10%), although the starting material was not very soluble in it. The product was not obtained in tetrachloroethane, THF and DMSO. Experiments in which the amount of solvent was varied did not appear to have a major influence on the yield.

Inert atmosphere The atmosphere of the reaction is also very important. Water and oxygen in the solvent was shown to react with complex competitively and could prevent formation of the new amide dimer (see section 3.3.3 and 3.3.4). Also, ruthenium amide dimer was not very stable in the air and could decompose in the process of crystallization from solution. When the reactions were run at 60°C without protecting gas, no new dimer obtained.

Conclusions From the range of reactions carried out, it was known that the condition of the reaction was very strict and the yield of amide dimer was quite low. Other products might form at the same time but they might not be as stable as the amide dimer in the solution so they were not obtained. Also some products obtained might not be stable in the air. The best yield of the new dimer was only around 30%. Some times, a little change of condition of the reaction might get to the result of no crystals obtained at all (as described above for reaction conditions).

The reaction forming the amide dimer was best carried out in an inert (N_2) atmosphere at around 60°C in a nonpolar solvent such as dichloromethane or toluene with two equivalents of DBU. However the yield is disappointingly low, making the exploration of the chemistry of the new dimer difficult.

3.4. Reactions of cymene-ruthenium-nitrogen complexes

After the four cymene-ruthenium-nitrogen complexes were synthesized, many reactions were carried on to synthesize clusters using these complexes as starting materials. Although there was no crystal structures of cymene-ruthenium-nitrogen clusters obtained yet, some reactions were found to be very interesting especially the reactions using the novel amide dimer as starting material. It was also found that these complexes could be interconverted under different conditions.

3.4.1. Reactions of bis-ammonia complex

The bis-ammonia complex should be a good starting material to form cymene-ruthenium-nitrogen clusters. If the bis-ammonia complex reacted with a base, the hydrogen atoms of the ammonia and the chloride ligands might be eliminated by the base giving two coordinating spaces that might join together to form clusters. The proposed reaction is shown below.

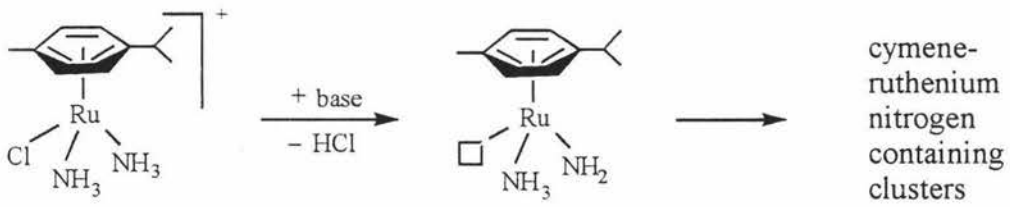

With DBU DBU is a relatively strong base that can deprotonate the hydrogen atoms of ammonia leading to the combination of the mono-nuclear complexes to dimeric complexes or clusters.

As described in the formation section, when the mixture of bis-ammonia complex was heated to 60^0C in dichloromethane under nitrogen for four hours, the new amide dimer formed. But when the reaction refluxed at 90^0C in dichloroethane, the mono-ammonia complex formed.

With triethylamine The yield of new dimer was relatively low and there was always some black product in the reaction. The possibility that the base, DBU, might be

too strong was explored. So triethylamine which is a much weaker base than DBU was tested. When the mixture of the reactants was heated to 80^0C for 10 hours, a red-brown solution was obtained. ^{1}H NMR spectrum for the solution showed that the chemical shifts of the hydrogen atoms on the cymene ring were from 5.700 ppm to 5.071 ppm. There were several other peaks which indicated that the products were a mixture containing some of the amide dimer but only a small amount.

With $AgNO_3$ and Zn If the chloride ligands were removed by Ag^+ in the presence of zinc as a reducing agent, the $[Ru(NH_3)_2(\eta^6\text{–cymene})]$ fragment with a vacant coordination site might be obtained, which might be a good intermediate leading to the formation of the cymene-ruthenium nitrogen containing clusters.

Both $Ag^+$and Tl^+ can give precipitates with Cl^- in the solution since there is an equilibrium in the solution as it was described in the formation section of the tris-ammonia complex. $AgNO_3$ is a convenient Ag^+ source to use in this reaction. Zinc powder was used as a mild reductant.

When the bis-ammonia complex $[RuCl(NH_3)_2(\eta^6\text{–cymene})]PF_6$ and $AgNO_3$ were mixed in ethanol, a white precipitate and yellow-brown solution were obtained. After filtration and treatment of the solution with zinc powder, a few yellow crystals were obtained. These crystals did not dissolve in dichloromethane or acetone. IR spectrum showed two N-H stretch absorptions at 3292 $cm^{-1}$and 3179 cm^{-1} (m, broad). ^{1}H NMR spectrum showed the chemical shift of a-b pair doublets of hydrogen atoms on the cymene ring was at 5.738, 5.715 ppm and 5.535, 5.513 ppm. The chemical shift showed that it might be a mono-nuclear cationic complex that was not the expected product.

3.4.2. Reactions of mono-ammonia complex $[RuCl_2(NH_3)(\eta^6\text{–cymene})]$

The mono-ammonia complex should also be a good starting material for the formation of the new dimer $[RuCl(NH_2)(\eta^6\text{–cymene})]_2$ or cymene-ruthenium-nitrogen clusters. However the mono-ammonia complex was not very soluble in dichloromethane so the reflux in dichloromethane did not give the expected product but some the bis-ammonia complex as it was described in section 3.3.1.

With $AgNO_3$ An attempt was made to remove the chloride ligands from the complex by $AgNO_3$ (through the equilibrium between the crystals and the solution) to improve the reaction. Because the mono-ammonia complex was not very soluble in nonpolar solvents such as dichloromethane and toluene, the reaction was run in ethanol. The starting material was treated with DBU with stirring for about 30 minutes at room temperature. The ^1H NMR spectrum of the reaction mixture showed that there were some amide dimer $[RuCl(NH_2)(\eta^6\text{–cymene})]_2$ in the solution which gave chemical shifts of the hydrogen atoms on the cymene ring at 5.003, 4.982 ppm and 4.955, 4.936 ppm.

With sodium anthracene Sodium anthracene is a very powerful reducing agent. So the reaction was tried without heating. The mixture of the mono-ammonia complex and sodium anthracene in dichloromethane was stirred at room temperature for one hour. ^1H NMR for the dark reaction mixture showed that no peaks at the region of 4 ppm to 6.5 ppm indicating that there was no coordinated cymene rings in the products. It might be because the sodium anthracene was too strong that the starting material was decomposed.

3.4.3. Reactions of the tris-ammonia complex $[Ru(NH_3)_3(\eta^6\text{–cymene})](PF_6)_2$

In the light of the above reactions, the tris-ammonia complex should be an interesting starting material because there is no chloride ligands in this complex. When the tris-ammonia complex was treated with two equivalents of DBU and heated to 60^0C for three hours, two complexes presented in the reaction mixture. ^1H NMR spectrum (Figure 46) showed the chemical shift of hydrogen atoms on the cymene ring at 5.065, 5.044 ppm, 4.890, 4.869 ppm and 5.242, 5.219 ppm, 5.011, 4.991 ppm. The first pair was very similar to that of the amide dimer $[RuCl(NH_2)(\eta^6\text{–cymene})]_2$ and could also be $[Ru(NH_3)(NH_2)(\eta^6\text{–cymene})]_2(PF_6)_2$. It was difficult to crystallize these products so the structures of the products were still not known.

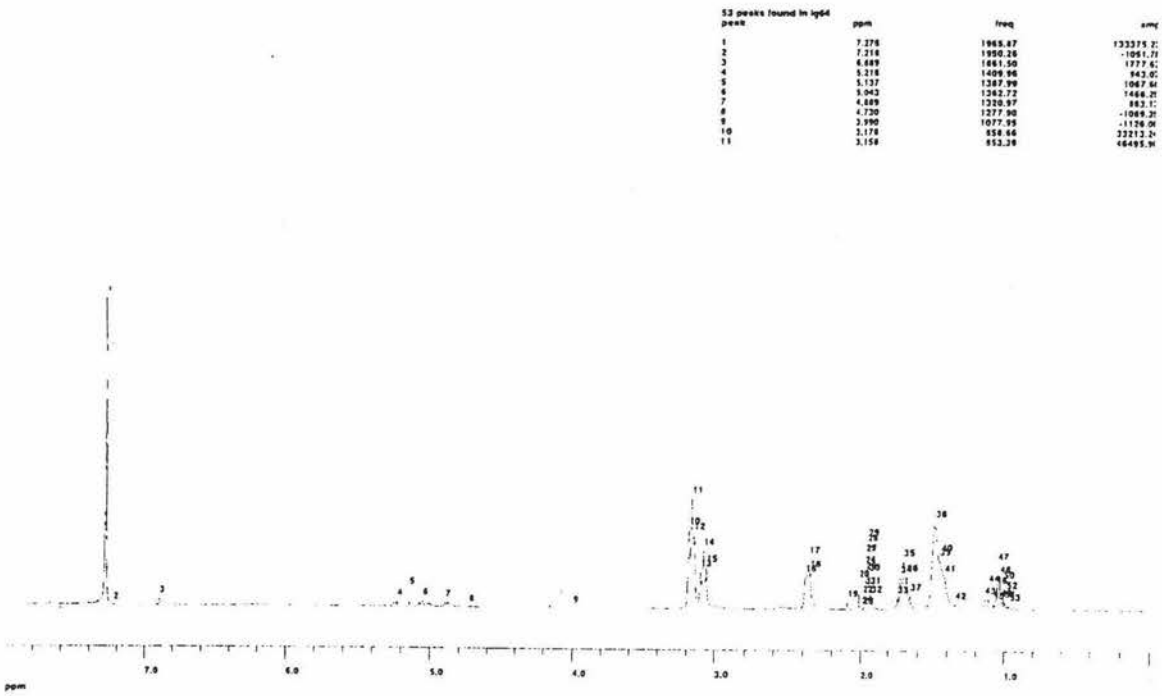

Figure 46 NMR spectrum of mixture of the reaction of $[Ru(NH_3)_3(\eta^6\text{–cymene})](PF_6)_2$ with two equivalents of DBU

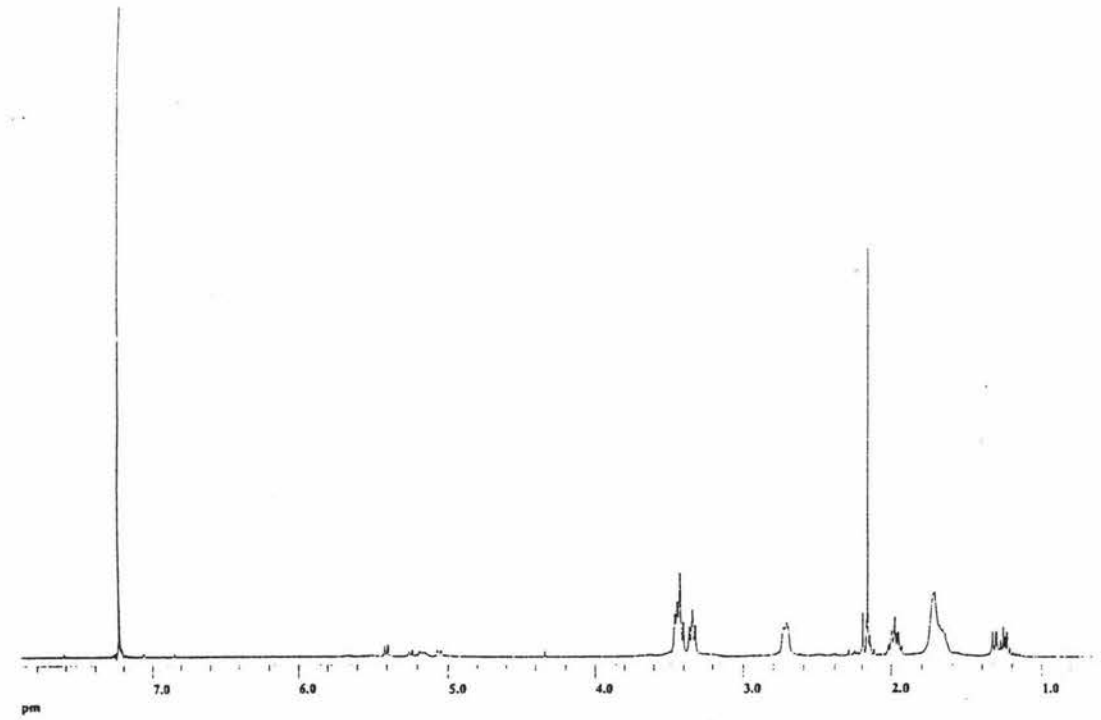

Figure 47 NMR spectrum of mixture of the reaction of $[Ru(NH_3)_3(\eta^6\text{–cymene})](PF_6)_2$ with four equivalents of DBU

However when the amount of DBU was increased to four equivalents, there were also two complexes in the reaction mixture. But the chemical shifts changed to 5.280, 5.257 ppm, 5.090, 5.069 ppm and 5.441, 5.418 ppm, 5.206, 5.176 ppm (Figure 47). The first was similar to one of the products in the first reaction, but there was no sign of the amide dimer. No crystals have been obtained yet. This reaction needs further research.

3.4.4. Reactions of the new dimer $[RuCl(NH_2)(\eta^6\text{–cymene})]_2$

All the reactions tried for mono-nuclear complexes seemed no clusters formed,. so it might need several steps to get the goal.

The amide dimer might be a very good starting material or intermediate that might form cymene-ruthenium-nitrogen clusters. One traditional strategy is reacting with those complexes with labile ligands that can easily fall off, such as acetone and acetonitrile, giving coordination vacancy and subsequently metal-metal bonds [115].

With $[Ru(acetone)_3(\eta^6\text{–cymene})]^{2+}$ Acetone is a very poor ligand which might form metal-metal bonds. When the amide dimer $[RuCl(NH_2)(\eta^6\text{–cymene})]_2$ was treated with $[Ru(acetone)_3(\eta^6\text{–cymene})]^{2+}$ and heated to 90^0C for two hours, the ^{1}H NMR spectrum showed no signals of doublet-of-doublet at 4.5-6.5 ppm which indicated coordinating cymene ring. The reason that the reaction did not work might be because that the temperature was too high. From a range of reactions, it was known that the condition of the reaction was very strict. Other products were not as stable as the amide dimer. This reaction need further research with being gently heated.

With $[Ru(acetonitrile)_3(\eta^6\text{–cymene})](NO_3)_2$ Acetonitrile is a ligand which is almost as poor as acetone. So this time the new dimer was treated with $[Ru(acetonitrile)_3(\eta^6\text{–cymene})](NO_3)_2$ and gently heated to 55^0C for about 8 hours. Two products with pink and orange colours were detected as spots on TLC. They were separated in silica chromatographic column using dichloromethane, acetone and methanol of 1 : 1 : 0.05 as solvent. The pink colored complex had not been detected in the reactions before. Unfortunately, ^{1}H NMR sample for pink colored complex was too dilute to give a

clear spectrum (because of too small amount of it). The pink colored complex changed its color to red-orange in two days in the drawer without any crystals obtained. ^{1}H NMR for orange colored complex showed a mixture which had several peaks from 5.543 ppm to 4.873 ppm. This reaction needs further research.

Thermolysis of the new amide dimer Thermolysis is also a traditional method of making clusters. So the toluene solution of the amide dimer was reflux for 20 hours at 135°C, TLC of the reaction mixture showed a pink coloured spot. ^{1}H NMR showed four doublet-of-doublet peaks for hydrogen atoms on the cymene ring at 5.492, 5.470 ppm and 5.356, 5.333 ppm. It was a new compound but did not seem like a cluster.

Reaction with DBU A reasonable strategy for synthesis of clusters is α-elimination. This method has been widely used on the synthesis of metal-metal multiple bonds for a long time [120] (see Chapter Two, mechanism section) Recently, some scientists started to try to use it to form clusters using di-nuclear complexes as starting materials since α-elimination could provide coordination vacancies [83]. In Chapter two, it has been described the successful formation of metal-sulfur clusters using dimeric complex $[M_2Cl_2(SH)_2(Cp^*)_2]$ (M = Ru, Ir, Rh) as starting materials [83].

The amide dimer $[RuCl(NH_2)(cymene)]_2$ is isoelectronic and has similar structure to the iridium and rhodium hydosulfide dimers, $[M_2Cl_2(SH)_2(Cp^*)_2]$ (M = Ir, Rh). It might also undergo α-elimination of HCl causing the formation of cymene-ruthenium-nitrogen clusters.

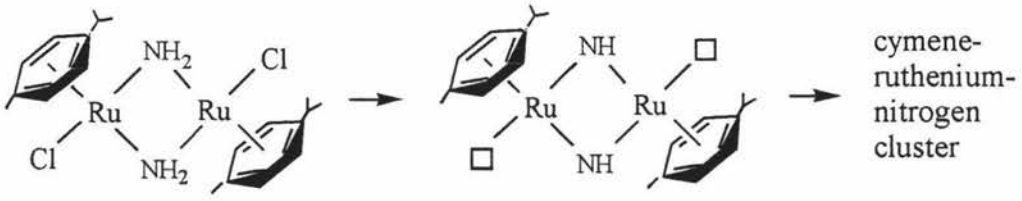

Four drops of DBU (~0.02 ml) was added in dichloromethane solution of the amide dimer stirring for 4 hours. ^{1}H NMR showed a single peak at 5.257 ppm (Figure 48) and the dark brown oil only dissolved in non-polar solvents such as chloroform and dichloromethane, which implied that the product might be neutral. From the chemical

shift and the single peak, it reminded the cymene-ruthenium-sulfur clusters. Both electrospray and FAB mass spectrometry were tried. But no mass spectrum was obtained because of the solubility problem of the products. The poor solubility of the product also caused the problem on crystallization. Although the structure of the compound has not been known yet, it has given a light to continue this work.

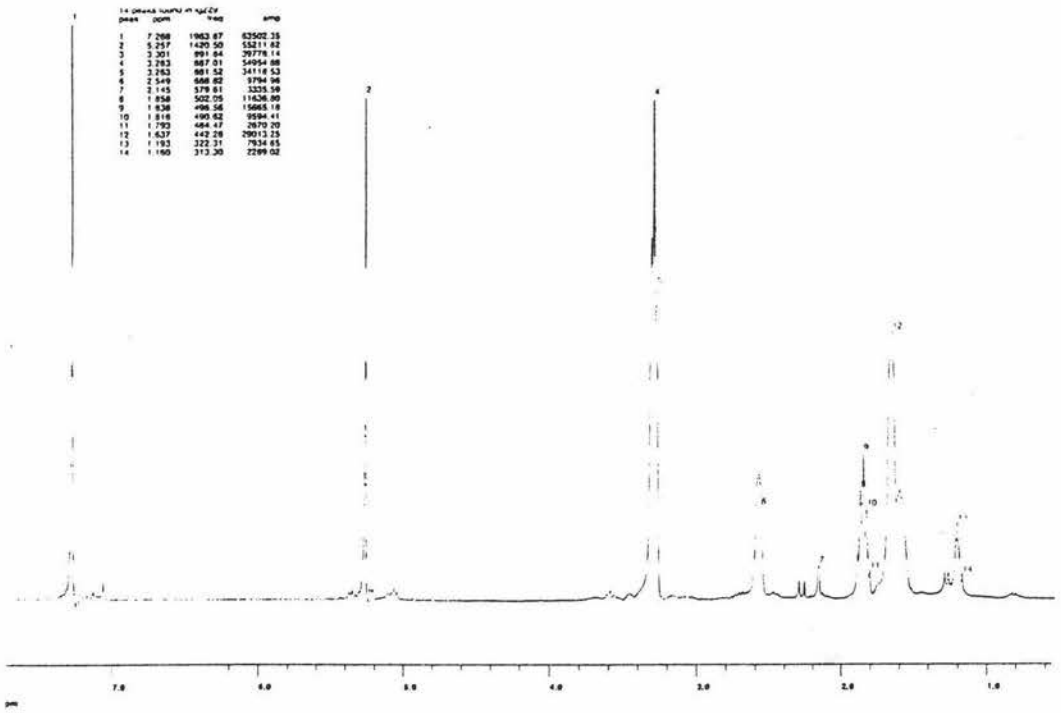

Figure 48 NMR for the product of $[RuCl(NH_2)(\eta^6\text{–cymene})]_2$ with DBU

With acid CF_3COOH

After all the reactions of synthesis, it was interesting to know how the amide dimer would react with acid, that was, to which atom the proton would attack. Reactions that involve transfer of H^+ to nitrogen from the metal could well be important in the future chemistry of these complexes. When acid was added into ^1H NMR tube in which was the amide dimer solution of $CDCl_3$. The solution changed its color from yellow to red-orange very quickly. ^1H NMR spectrum of the solution was run at once. A chemical shift of Ru-H was shown at -13.2 ppm. But after a few seconds, the signal could not be detected at all. When more acid was added, there was still no signal. It was known from this reaction that when H^+ attacked the amide dimer, it firstly attacked the metal core. This reaction needs to be repeated at low temperature.

3.5. Conclusions and further research

The initial goal of the project has been achieved and a range of nitrogen-containing arene-ruthenium complexes are available for cluster synthesis. One reaction leading to dimer formation has been discovered and the new product fully characterized and shown to be very reactive. Three new complexes have been obtained, the mono-ammonia complex $[RuCl_2(NH_3)(\eta^6\text{–cymene})]$, the new dimer $[RuCl(NH_2)(\eta^6\text{–cymene})]_2$ and the tris-ammonia complex $[Ru(NH_3)_3(\eta^6\text{–cymene})](PF_6)_2$

The reactions of these complexes have been studied, particularly reactions that might lead to clusterification. It has been found that they can be changed into each other with DBU under different conditions. The reaction scheme is shown in Scheme 13:

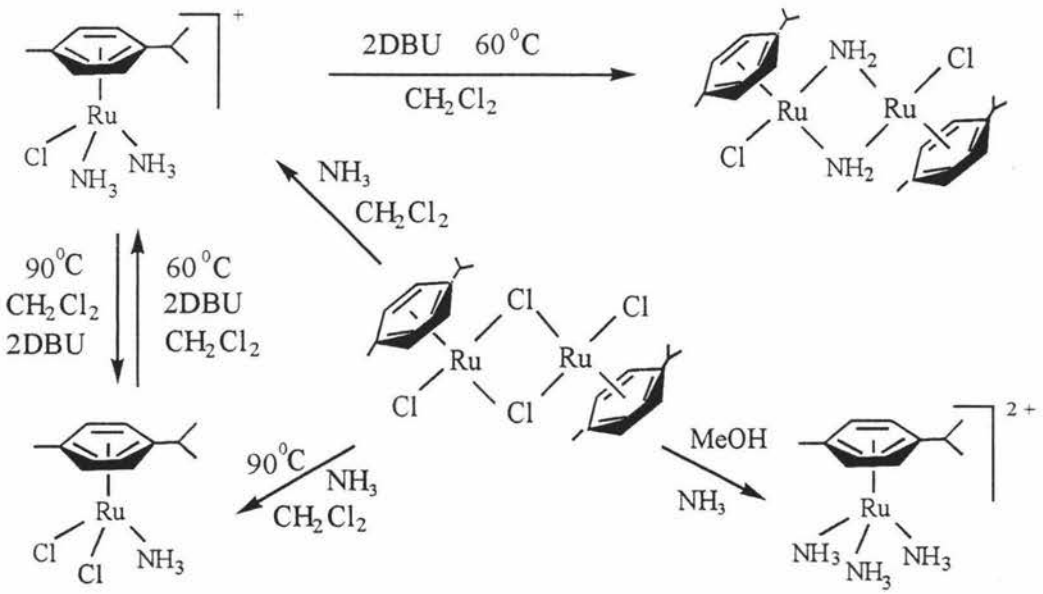

Scheme 13 Reaction scheme of cymene-ruthenium-nitrogen complexes

Several reactions need to be tested in the future work, such as the reactions involving the addition of a ruthenium-cymene fragment to the new dimer $[RuCl(NH_2)(\eta^6\text{–cymene})]_2$. The trial reaction has shown some provinces and needs

repeating. The reaction of the tris-ammonia complex with probably product of $[Ru(NH_2)(NH_3)_2(\eta^6\text{–cymene})]PF_6$ has only been explored in a very preliminary way. The reaction of the amide dimer with DBU is very interesting and needs further research, especially the X-ray crystallographic structure of the product that is very likely to be a arene-ruthenium nitrogen-containing cluster.

It also needs to know some mechanisms of these reactions in catalytic properties and to text the possibilities of producing clusters using ammonia as ligands for next step.

Further in the future different sources of the nitrogen atom for clusters will be explored. $[HN(SiMe_3)_2]$ is a possible starting material. Other ruthenium substrates could also be tested, such as $[RuCl_2(benzene)]_2$.

^{1}H NMR, IR AND MASS SPECTROMETRY DATA FOR THE COMPOUNDS OF CHAPTER THREE

compounds	Chemical shift on ^{1}H NMR spectra / ppm	N-H stretch on IR spectra / cm^{-1}	Molecular ion peak on mass spectrum
$[RuCl_2(NH_3)(\eta^6\text{–cymene})]$	5.522, 5.449; 5.291, 5.272	3346, 3298, 3236, 3154	
$[RuCl(NH_3)_2(\eta^6\text{–cymene})](PF_6)$	5.764, 5.741; 5.584, 5.561	3381, 3337, 3250, 3195	
$[Ru(NH_3)_3(\eta^6\text{–cymene})](PF_6)_2$	6.008, 5.985; 5.732, 5.709	3388, 3335	
$[RuCl(NH_2)(\eta^6\text{–cymene})]_2$	5.047, 5.024; 4.904, 4.883	3339, 3259	577

CHAPTER FOUR EXPERIMENTAL

4.1.General

Material The $[RuCl_2(cymene)]_2$ dimer was prepared according to the literature method [101]. All the solvents were distilled and dried by common procedures before use.

Method Elemental analysis were done by the Campbell Microanalytical Laboratory, University of Otago, New Zealand. ^1H NMR spectra were obtained on a M270 Spectrometer. IR spectra were obtained on Perkin Elmer Spectrometer. Data of X-ray crystallography were obtained at the Laboratory of X-ray Crystallography, University of Auckland, New Zealand. Positive ion FAB mass spectra were obtained at the Mass Spectrometry Laboratory of Massey University. Electrospray mass spectra were obtained at the mass spectrometry facility at Diary Research Institute, New Zealand. Cyclic voltammetry were measured in N_2 saturated MeCN solutions using $^tBu_4NPF_6$ as supporting electrolyte, ferracene as internal reference, carbon microelectrode as working electrode, Pt electrode as counter electrode and Ag/AgCl electrode as reference electrode. TLC were obtained in various solvents in different experiments using normal silica gel TLC sheets. Column separation used normal silica gel. The autoclave used is a normal autoclave with highest pressure of 100 Psi.

All operations, unless otherwise stated, were performed under an atmosphere of nitrogen using standard Schlenk techniques.

4.2. Preparation of arene ruthenium sulfur clusters $[Ru_3S_2(cymene)_3](PF_6)_2$, $[Ru_5S_4(cymene)_4](PF_6)_2$ and $[Ru_4S_2(SO)(cymene)_4](PF_6)_2$

A solution of Na_2S (157 mg, 0.653 mmol) in 5 ml MeOH (prepared using ultra sound bath) was added dropwise to a stirred solution of $[RuCl_2(cymene)]_2$ (200 mg, 0.326 mmol) in 10 ml of MeOH. There was a rapid colour change from orange-brown to very dark brown. The solution was stirred for 1 hour, and then solid NH_4PF_6 (375 mg, 2.5 mmol) was added. After further 30 minute stirring, the solvent was removed in vacuo. The

dark brown solid was extracted into 10 ml of solvent in the ratio of CH_2Cl_2 : $CHCl_3$: acetone : MeOH = 20 : 10 : 5 : 1 that is also the solvent used in next step. The dark brown solution was separated using a column filled with normal silica gel into three parts by three different colors of orange-brown part, red-brown part and purple-brown part, which indicated the $[Ru_3S_2(cymene)_3](PF_6)_2$ cluster, the $[Ru_5S_4(cymene)_4](PF_6)_2$ cluster and the unknown big cluster (Ru_{10} ?) or the $[Ru_4S_2(SO)(cymene)_4](PF_6)_2$ cluster, respectively.

$[Ru_3S_2(cymene)_3](PF_6)_2$: To orange-brown part, was added about 1 ml CH_2Cl_2, followed by addition of Et_2O producing orange-brown solid that was dried in vacuo. Recrystallization of the resulting solid from CH_2Cl_2/Et_2O using isobestic technique gave orange brown crystals of the product, yield 12 mg (5.2 %). Analytical calculation (from the work of Rauchfuss et.al.) for $C_{30}H_{42}F_{12}P_2Ru_3S_2$: C, 33.99%; H, 3.99%; S, 6.05%. Required: C, 33.95%; H, 3.91%; S, 5.99% [5]. (Isobestic technique: two vials were used: the little vial containing CH_2Cl_2 solution was put into the big vial with some Et_2O in it. Two drops of Et_2O was added into the little vial before a lid was used on the top of the big vial.)

$[Ru_5S_4(cymene)_4](PF_6)_2$: To red-brown part, was added about 2 ml CH_2Cl_2, followed by addition of Et_2O producing dark red-brown solid that was dried in vacuo. Recrystallisation of the resulting solid from CH_2Cl_2/Et_2O using isobestic technique (see preparation of $[Ru_3S_2(cymene)_3](PF_6)_2$ about isobestic technique) gave dark brown or red-brown crystals of the product, yield 25 mg (13.1 %). Elemental analysis gave $C_{40}H_{56}F_{12}P_2Ru_5S_4$: H, 3.56 %, C, 32.70 %. Required: H, 3.80%, C, 32.81%.

The big cluster (Ru_{10} ?) or $[Ru_4S_2(SO)(cymene)_4](PF_6)_2$: To purple brown part, was added about 3 ml acetone, followed by addition of Et_2O producing very dark brown solid, which was dried in vacuo. Recrystallisation of the resulting solid from acetone/ (Et_2O and $^iPr_2O$) or acetone/ $CHCl_3$ using isobestic technique (see preparation of $[Ru_3S_2(cymene)_3](PF_6)_2$ about isobestic technique) gave dark brown crystals of the product, yield 67 mg (26.9%). Elemental analysis for the dark brown crystals: H, 2.52 %, C, 18.97 %. Required for $C_{40}H_{56}F_{12}OP_2Ru_4S_3$: H, 4.59%; C, 39.09%.

Reactions of arene-ruthenium-sulfur clusters with H_2 and N_2

The crystals of the clusters were dissolved in D_6-acetone in a little vial with a lid that had some holes on the top of it. Then the vial was put into an autoclave followed by the screw tightened. H_2 gas with pressure of 100 Psi was filled in and then released, same operation was done for three or four times to get rid of the air in the autoclave. Then keep the autoclave under that pressure of H_2 for some time and then got the sample out to run NMR.

Similar experiment was done under N_2 with the reductants. $LiAlH_4$ was added in the solution immediately followed by putting the little vial into the autoclave. When Mg powder was used, it must be washed in acetone by ultra sound bath before it was put into the solution.

4.3. Preparation of arene-ruthenium-nitrogen complexes

4.3.1. Preparation of $[RuCl(NH_3)_2(\eta^6\text{–cymene})]PF_6$

$[RuCl_2(\eta^6\text{–cymene})]_2$ 500 mg (0.82mmol) was added to 20 ml dichloromethane saturated with NH_3 gas. After stirring for a few minutes, a yellow precipitate appeared. After removing of the solvent on the rotating evaporator, the product was dissolved in ethanol. containing NH_4PF_6 266 mg (one equivalent). Then the volume was reduced to half by evaporation and stored in the fridge. Yellow crystals of $[RuCl(NH_3)_2(\eta^6\text{–cymene})]PF_6$ 607 mg (yield 82.6%) was obtained.

4.3.2. Preparation of $[RuCl_2(NH_3)(\eta^6\text{–cymene})]$

$[RuCl_2(\eta^6\text{–cymene})]_2$ 250 mg (0.41 mmol) was added into 10 ml dichloromethane saturated with NH_3 gas with stirring for 5 minutes. All the solvent was removed at the rotating evaporator, and then 10 ml dichloromethane was added to dissolve the yellow

solid. The mixture was heated to 90^0C under N_2 gas for one hour. The solvent was removed from the red-brown solution and then a small quantity of acetone was added. Red-brown crystals was obtained by storing the solution in fridge over night, yield 240 mg (90.9%). C H N elemental analysis gave $C_{10}Cl_2H_{17}NRu$: C, 36.88%; H, 5.47%; N, 4.21%. Required: C, 37.16%; H, 5.30%; N, 4.33%.

4.3.3. Preparation of $[Ru(NH_3)_3(\eta^6\text{–cymene})](PF_6)_2$

$[RuCl_2(\eta^6\text{–cymene})]_2$ 200 mg (0.33 mmol) was added into 10 ml distilled methanol saturated with NH_3 gas refluxing at 60^0C for one hour. A solution of 213 mg NH_4PF_6 in a little methanol was added to the solution. Evaporation until half of the volume left, yield 249 mg (66.1%).

4.3.4. Preparation of $[RuCl(NH_2)(\eta^6\text{–cymene})]_2$

$[RuCl(NH_3)_2(\eta^6\text{–cymene})]PF_6$ 250 mg (0.55mmol) and 0.15 ml (1.10 mmol) DBU were added into 25 ml distilled and degassed dichloromethane. The mixture was heated to 60^0C for five hours. The solvent was removed by rotary-evaporator from the resulting red-brown solution and then a little acetone was added to dissolve the red-brown oil. Then the solution was put into the fridge over night. 48 mg (30.1% yield) bright orange crystals were obtained. Elemental analysis for $C_{20}H_{32}Cl_2N_2Ru_2$: C, 41.85%; H, 5.56 %; N, 4.64 %. Required: C, 41.6%; H, 5.58%; N, 4.88%.

4.5. Reactions of the new amide dimer

With [Ru(acetonitrile)$_3$(cymene)]$^{2+}$ [Ru(acetonitrile)$_3$(cymene)]$^{2+}$ was made by putting the solution of [RuCl$_2$(cymene)]$_2$ dimer 100mg in 10 ml acetonitrile with a little $AgNO_3$ into ultrasound bath for half of an hour at room temperature. Solvent was removed using rotary-evaporator giving some orange oil.

Solution of [RuCl(NH$_2$)(cymene)]$_2$ 30 mg (0.05 mmol) in 10 ml dichloromethane was added into the solution of orange oil in 10 ml dichloromethane and heated to 55^{0}C for two hours under N_2. Then the solvent was removed and ^{1}H NMR was run for the mixture of the reaction in $CDCl_3$.

With [Ru(acetone)$_3$(cymene)]$^{2+}$ [Ru(acetone)$_3$(cymene)]$^{2+}$ was made in similar way to that of [Ru(acetonitrile)$_3$(cymene)]$^{2+}$. The solvent was removed giving red-brown oil.

Solution of [RuCl(NH$_2$)(cymene)]$_2$ 30 mg (0.05 mmol) in 10 ml dichloromethane was added into the solution of mixture of above reaction in 10 ml dichloromethane and heated to 90^{0}C for two hours under N_2. Then the solvent was removed and ^{1}H NMR was run for the mixture of the reaction in $CDCl_3$.

Reaction with DBU [RuCl(NH$_2$)(cymene)]$_2$ 30 mg (0.05 mmol) and 0.02 ml (0.15 mmol) DBU were added into 10 ml degassed dichloromethane with stirring for 4 hours at room temperature. Then the solvent was removed using rotary evaporator and ^{1}H NMR was run in $CDCl_3$ for the resulting dark brown oil. A little $CHCl_3$ was added and the solution was put into the fridge overnight.

REFERENCES

1. Ozaki, A.; Aika, K. *Catal. Sci. Technol.* 3, 87, **1981**.

2. Evans, W. J.; Kociok-Kohn, G.; Ziller, J. W. *Angew. Chem. Int. Ed. Engl.* **1992**, 31, No.1

3. Seigbahn, P. E. M.; Westerberg, J.; Svensson, M.; Crabtree, R. H. *J. Phys. Chem.* B **1998**, 102, 1616-1623.

3. Gould, R. O.; Jones, C. L.; Roberston, D. R,; Stephenson, T. A. *J. Chem. Soc., Chem. Commun.*, **1977**, 2225.

5. Lockemeyer, J. R.; Rauchfuss, T. B.; Rheingold, A. L. *J. Am. Chem. Soc.* **1989**, 111, 5733-5738.

6. Taber, D. F.; Silverbery, L. J. *Tetrahedron Lett.*, 32 (**1991**) 3101.

7. Kitamura,M.; Tokunaga, M.; Ohcuma, T.; Noyori, R. *Tetrahedron Lett.*, 32 (**1991**) 4163.

8. Christner, J. A. et.al. *J. Am. Chem. Soc.* 106, 6786 (**1984**).

   Crane, B. R.; Siegel, L. M.; Getzoff, E. D. *Science* 270, 59 (**1995**).

9. Ragscale, S. W.; Kumar, M. *Chem. Rev.* 96, 2515 (1996); Hu, Z. et.al. *J. Am. Chem. Soc.* 118, 830 (**1996**).

10. Beinert, H.; Holm, R. H.; Munck, E. *Science*, vol. 277, 1, Aug, **1997**.

11. Beinert, H.; Kennedy, M. C.; Stont, C. D. *Chem. Rev.* 96, 2335 (**1996**).

12. Duff, J. L. C.; Breton, L. J.; Butt, J. N; Armstrong, F. A.; Thomson, A. J. *J. Am. Chem. Soc.* 118, 8593 (**1996**).

13. Spiro, T. G. Ed., *Iron-Sulfur Proteins*, Wiley-Inter Science, New York, 1982; Cammack, R. Adv. Inorg. Chem. 38, 281 (**1992**).

14. Crouse, B. R.; Meyer, J.; Johnson, M. K. *Ibid.* 117, 9612 (**1995**).

15. Papaefthymiou, V.; Girerd, J. –J.; Moura, I.; Moura, J. J. G.; Munck, E. *J. Am. Chem. Soc.* 109, 4703 (**1987**).

16. Buchner, W.; Schliebs, R.; Winter, G.; Buchel, K. H. *Industrial Inorganic Chemistry*, VCH press, Germany.

17. Ozaki, A.; Aika, K.; Furuta, A.; Okagami, A.,US patent, 3, 770, 658 (**1973**).

18. Aika, K.; Hori, A.; Ozaki, A. *J. Catal.* 27, 424, (**1972**).

19. Menon, P. G. *Appl. Catal.* A93, N16 (**1993**).

20. Izumi, Y.; Aika, K. –I. *J. Phys. Chem.* **1995**, 99, 10336-10345.

21. Izumi, Y.; Chihara, T.; Yamazaki, H; Iwasawa, Y. *J. Phys. Chem.* **1994**, 98, 594.

22. Izumi, Y.; Chihara, T.; Yamazaki, H,; Iwasawa, Y. *J. Am. Chem. Soc.* **1993**, 115, 6462.

23. Grange, P. *Catal. Rev.-Sci. Eng.* **1980**, 21, 135.

24. Topoe, H.; Clansen, B. S. *Catal.Rev-Sci. Eng.* **1984**, 26, 395.

25. Bianchini, C.; Meli, A. *J. Chem. Soc., Dalton Trans.*, **1996**, 801-814.

26. (a) Seminar of Sir John Mureg Thomas at the Department of Chemistry, Massey University, New Zealand, Feb. **1998**. (b) Bennett, M. A.; Smith, A. K. *J. Chem. Soc. Dalton Trans.* (**1975**) 233.

27. Smith, P. D.; Wright, A. H. *J. Organ. Chem.* 559, 141-147, **1998**.

28. Bennett, M. A.; Smith, A. K. *J. Chem. Soc. Dalton Trans.* (**1975**) 233.

30. Cabeza, J. A.; Nutton, A.; Mann, B. E.; Brevard, C.; Maitlis, P. M., *Inorg. Chim. Acta* **1986**, 115, L47.

31. Bodensieck, U.; Meister, A.; Meister, G.; Rheinwald, G.; Stoeckli-Evans, H.; Suss-Fink, G. *Chimia* 47 (**1993**) 189-191.

32. Hegedus, L. L.; McCabe, R. W. *Catalyst Poisoning*; Marcel Dekker: New York, **1984**.

33. Weisser, O.; Landa, S. *Sulfide Catalysts, Their Properties and Applications*; Pergamon Press: New York, 197334. Dubois, M. R. *Chem. Rev.* 89, 1-9, **1989**.

34. Kadowaki, Y.; Aika, K. *J. Catal.* **1996**, 161, 178-185.

35. Harmer, M. A.; Halbert, T. R.; Pan, W. H.; Coyle, C. L.; Cohen, S. A.; Stiefel, E. I. *Polyhedron*, **1986**, 5, 341.

36. (a) Sanchez-Delgado, R. A.; Herrera, V.; Rinco, L.; Andriollo, A.; Martin, G. *Organometallics*, **1994**, 13, 553. (b) Baralt, E.; Smith, S. J.; Hurwitz, I.; Horvath, I. T.; Fish, R. H. *J. Am. Chem. Soc.*, **1992**, 114, 5187.

37. (a) Rees, D. C.; Chan, M. K.; Kim, J. *Adv. Inorg. Chem.* **1993**, 40, 89-119. (b) Zhong, S.-J.; Liu, C.-W. *Polyhedron* **1997**, 16, 653-661. (c) Dance, I. G. *Aust. J. Chem.* **1994**, 47, 97-990. (d) Dance, I, G. *Transition Metal Sulfur Chemistry*; Stiefel, E. I., Matsumoto, K., Eds.; AVS Smposium Series 653; American Chemical Society: Washington, DC, **1996**. (e) Dance, I. G. *Chem. Commun.* **1997**, 165-166. (f) Dance, I. G. *Chem. Commun.* **1998**, 523-530.

38. Nishibayashi, Y.; Iwai, S.; Hidai, M. *J. Am. Chem. Soc.* **1998**, 120, 10559-10560.

39. Malinak, S. M.; Simeonov, A. M.; Mosier, P. E.; McKenna, C. E.; Coucouvanis, D. *J. Am. Chem. Soc.* **1997**, 119, 1662-1667.

40. Houser, E. J.; Rauchfuss, T. B.; Wilson, S. R. *Inorg. Chem.* **1993**, 32, 4069-4076.

41. Itoh,; Nagano, T.; Hirobe, M. *Tetrahedron, Lett.* **1980**, 21, 1343.

42. Bodensieck, U.; Stoeckli-Evans, H.; Suss-Fink, *Angew. Chem. Int. Ed. Engl.* 30 (**1991**) No.9, 1126.

43. (a) Adams, R. D.; Babin, J. E.; Tasi, M. *Organometallics* **1987**, 6, 2247. (b) Adams, R. D.; Babin, J. E.; Tasi, M.;Wang, J. G. *Ibid.* **1988**, 7, 755.

44. Startsev, A. *Catal. Rev. Sci. Eng.*, 1995, 37, 353; *ACS Symp. Ser.* **1990**, 429; Prins, R.; De Beer, V. H. J.; Somorjai, G. A. *Catal. Rev. Sci. Eng.*, **1989**, 31, 1; Satterfield, C. N. *Heterogeneous Catalysis in Industrial Practice*, McGraw-Hill, New York, **1980**; McCulloch, *Applied Industrial Catalysis*, ed. B. E. Leach, Academic Press, New York, **1983**, vol. 1, 69.

45. Pecorato, T. A.; Chianelli, R. R. *J. Catal.*, **1981**, 67, 430.

Harris, S.; Chianelli, R. R. *J. Catal.*, **1984**, 86, 400.

46. (a) Massoth, F. E. *Adv. Catal.*, 1978, 27, 265. (b) Grange, P. *Catal. Rev. –Sci. Eng.*, **1980**, 21(1), 135. (c) Massoth, F. E.; Murali Dhar, G. *Proceeding of the International Conference on Chemistry and Uses of Molybdnum*, 4 th, **1982**, 343.

47. Riaz, U.; Curnow, O.; Curtis, M. D. *J. Am. Chem. Soc.* **1994**, 116, 4357.

48. Harris, S. *Polyhedron* 16, 18, 3219-3233, **1997**.

49. Riaz, U.; Curnow, O.; Curtis, M. D. *J. Am. Chem. Soc.* **1991**, 113, 1416.

50. Curtis, M. D.; Riaz, U.; Curnow, O. J.; Kampf, J. W.; Rheingold, A. L.; Haggerty, B. S. *Organometallics* **1995**, 14, 5337.

51. Bianchini, C.; Meli,A. *J. Chem. Soc., Dalton Trans.*, **1996**, 801-814.

52. Bianchi, C.; Herrera, V.; Jimenez, M. V.; Meli, A.; Sanchez-Delgado, R. A.; Vizza, F. *J. Am. Chem. Soc.*, **1995**, 117, 8567.

53. Herrera, V.; Sanchez-Delgado, R. A.; Bianchini, C.; Meli, A. XV Reunion Del Grupo Especializado de Quimica Organometalica, Sevilla, **1995**, P121.

54. (a) Sanchez-Delgado, R. A.; Herrera, V.; Rincon, L; Andriollo, A.; Martin, G. *Organometallics*, **1994**, 13, 553. (b) Sanchez-Delgado, R. A. *Advances in Catalyst Design*, eds. M. Graziani and C. N. R. Rao, World Scientific Publishing Co., Singapore

55. (a) Fish, R. H.; Baralt, E.; Smith, S. J.; Hurwitz, I.; Horvath, I. T.; Fish, R. H. *J. Am. Chem. Soc.*, **1992**, 114, 5187. (b) Fish, R. H.; Baralt, E.; Smith, S. J. *Organometallics*, **1991**, 10, 54.

56. Sanchez-Delgado, R. A,; Gonzalez, E. *Polyhedron*, **1989**, 8, 1431.

57. Pecoraro, T. A.; Chianelli, R. R. *J. Catal.*, **1981**, 67, 430; Harris, S.; Chianelli, R. R. *J. Catal.*, **1984**, 86, 400.

58. (a) Girgis, M. J.; Gates, B. C. *Ind. Eng. Chem. Res.*, **1991**, 30, 2021. (b) Wiegand, B. C.; Friend, C. M. *Chem. Rev.*, **1992**, 92, 491. (c) Benson, J. W.; Schrader, G. L.; Angelici, R. J. *J. Mol. Catal.*, **1995**, 96, 283.

59. Arce, A. J.; Arrojo, P.; Deeming, A. J.; De Sanctis, Y. *J. Chem. Soc., Dalton Trans.*, **1992**, 2423.

60. Arce, A. J.; De Sanctis, Y.; Karam, A.; Deeming, A. J. *Angew. Chem., Int. Ed. Engl.*, **1994**, 33, 1381.

61. Riaz, U.; Curnow, O. J.; Curtis, M. D. *J. Am. Chem. Soc.*, **1991**, 113, 1416.

62. Riaz, U.; Curnow, O. J.; Curtis, M. D. *J. Am. Chem. Soc.*, **1995**, 117, 6366.

63. Luo, S.; Ogilvy, A. E.; Rauchfuss, T. B.; Rheingold, A. L.; Wilson, S. R. *Organometallics,* **1991**, 10, 1002.

64. Chen, J.; Daniels, L. M.; Angelici, R. J. *J. Am. Chem. Soc.*, **1991**, 113 2544.

65. Arce, A. J.; Arrojo, P.; Deeming, A. J.; De Sanctis, Y. *J. Chem. Soc., Dalton Trans.*, **1992**, 2423.

66. Bianchini, C.; Jimenez, M. V.; Meli, A.; Moneti, S.; Vizza, F.; Herrera, V.; Sanchez-Delgado, R. A. *Organometallics*, **1995**, 14, 2342.

67. Bazhenova,T. A.;Shilov, A. E. *Coord. Chem. Rev.* 144 (**1995**) 69-145.

68. Knoth, W. H. *J. Am. Chem. Soc.* 94, 104 (**1972**).

69. Fishel, C. T.; Davis, R. J.; Carces, J. M. *J. Catal.* 163, 148-157 (**1996**).

70. Manriquez, J. M.; Snner, R. D.; Marsh, R. E.; Bercaw, J. E. *J. Am. Chem. Soc.* 98 (**1976**) 8351.

71. Churchill, M. R.; Li, Y.-J. *J. Organmet. Chem.* 301 (**1986**) 49.

72. Nishibayashi, Y.; Iwai, S.; Hidai, M. *Science* **1998** Vol. 279, 540-542.

73. Luneva, N. P.; Mironova, S. A.; Shilov, A. E.; Antipin, M. Yu.; Struchkov, Yu. T. *Angew. Chem., Int. Ed. Engl.*, 32, **1993**, 1178.

74. (a) Schworer, B.; Tauer, R. K. *Arch. Microbiol.* **1991**, 155, 459. (b) Ma, K.; Zirngibl, C.; Linder, D.; Stetter, K. O.; Thauer, R. K. *Arch. Microbil.* **1991**, 156, 43. (c) Von Bunau, R.; Zirngibl, C.; Thauer, R. K.; Klein, . *Eur. J. Biochem.* **1991**, 202, 1205.

75. Thauer, R. K.; Klein, A. R.; Hurtmann, G. C. *Chem. Rev.* **1996**, 96, 3031-3042.

76. Albracht, S. P.J.; Graf, E. G.; Thauer, R. K. *FEBS Lett.* **1982**, 140, 311.

77. (a) Berlier, Y.; Lespinat, P. A.; Dimon, B. *Anal. Biochem.* **1990**, 188, 427. (b) Roberts, L. M.; Lindahl, P. A. *J. Am. Chem. Soc.* **1995**, 117, 2565.

78. Sellmann, D.; Gottschalk-Gaudig, T.; Heinemann, F. W. *Inorg. Chem.* **1998**, 37, 3982-3988.

79. Sellmann, D.; Rackelmann, G. H.; Heinemann, F. W. *Chem. Eur. J.* **1997**, 3, 2071.

80. Houser, E. J.; Rauchfuss, T. B. And Wilson, S. R. *Inorg. Chem.* **1993**, 32, 4069.

81. Tang, Z.; Nomura, Y.; Kuwata, S.; Ishii, Y.; Mizobe, Y. And Hidai, M. *Inorg. Chem.* **1998**, 37, 4909-4920.

82. Marko, L.; Marko-Monostory, B.; Madoch, T.; Vahrekamp, H. *Angew. Chem., Int. Ed. Engl.* **1980**, 19, 226.

83. Arulsamy, K. S.; Pandly, K. K.; Agarwala, U. C. *Inorg. Chim. Acta* **1981**, 54, L51.

84. Hofler, M.; Baitz, A. *Chem. Ber.* **1976**, 109, 3147.

85. Kolle, U; Kossakowski, J; Klaff, N.; Wesemann, L.; Englert, U.; Heberich, G. E. *Angew. Chem., Int. Ed. Engl.* **1991**, 30, 690; *Angew. Chem.* **1991**, 103, 732.

86. Kuwata, S.; Andou, M.; Hashizume, K.; Mizobe, Y. And Hidai, M. *Organometallics* **1998**, 17, 3429-3436.

87. Smith, B. E.; Eady, R. R. *Eur. J. Biochem.*, 205 (**1992**) 1.

88. Sivakumaran, S. **1995**, *Synthetic Pathways to Organometallic Carbohydrate Complexes; Synthesis and Characterization of 6-arene Ruthenium (2) complexes of surgars*. Dip. Sci. manuscript, held Chemistry Department, Massey University, Palmerston North, New Zealand.

89. Sellmann, D. In *Molybdenum Enzymes, Cofactors and Model Systems*; Stiefel, E. I., Coucouvanis, D., Newton, W. E., Eds.,; ACS Symposium Series 535; American Chemical Society: Washington, DC, **1993**; pp 332-345.

90. Gomez-Sal, P.; Martin, A.; Mena, M.; Yelamos, C. *J. Chem. Soc., Chem. Commun.* **1995**, 2185.

91. Abernethy, C. D.; Bottomley, F.; Decken, A.; Cameron, T. S. *Organometallics* **1996**, 15, 1758-1759.

92. Dehnicke, K.; Strahle, J. *Angew. Chem., Int. Ed. Engl.*, **1992**, 31, 995.

93. (a) Banaszak Holl, M. M.; Kersting, M.; Pendley, B. D.; Wolczanski, P. T. *Inorg. Chem.*, **1990**, 29, 1518. (b) Roesky, H. W.; Bai, Y.; Noltemeyer, M. *Angew. Chem., Int. Ed. Engl.*, **1989**, 28, 754. (c) Banaszak Holl, M. M.; Wolczanski, P. T. *J. Am. Chem. Soc.*, **1992**, 114, 3854.

94. Bates, R. S. *Arene Ruthenium Chemistry*. Ph. D Sci., **1992**. Held University of Nottingham, Nottingham, U. K.

95. Allen, A. D.; Senoff, C. V.; *Chem. Commun.* **1965**, 621-622

96. Mccormick , F. B.; Gleason, W. B., *Acta. Cryst.* Section C, **1988**, 44, 603.

97. Foulds, G. A. *J. Organomet. Chem.*, **1985**, 269, 147.

98. (a) Tang, Z.; Nomura, Y.; Ishii, Y.; Mizobe, Y.; Hidai, M. *Organometallics* **1997**, 16, 151. (b) Tang, Z.; Nomura, Y.; Ishii, Y.; Mizobe, Y.; Hidai, M. *Inorg. Chim. Acta* **1998**, 267, 73.

99. Marco, L.; Marco-Monostory, B.; Madach, T.; Vahrenkamp, H. *Angew. Chem. Int. Ed. Engl.* 19 (**1980**) No. 3 226-227.

100. Calculations done by Dr. A. H. Wright, Massey University, New Zealand

101. Bowyer, W. J.; Geiger, W. E. *Organometallics* 1989, 8, 191. Bowyer, W. J.; Geiger, W. E. *J. Electroanal. Chem.* **1988**, 239, 253.

102. Finke, R. G.; Voegeli, R. H.; Laganis, E. D.; Boekelheide, V. *Organometallics* **1983**, 2, 347.

103. Kharas, K. C. C.; Dahl, L. F.; *Adv. Chem. Phys.* **1988**, 70,1. Johnson, D. C.; Benfield, R. E.; Edward, P. P.; Nelson, W. J.H.; Vargas, M. D.; *Nature* **1985**, 314, 231. Teo, B. K.; Disalvo, F. J.; Waszczak, J. V.; Longoni, G.; Ceriotti, A. *Inorg. Chem.* **1986**, 25, 2265

104. Mingos, D. M. P.; May, A. S. In *The Chemistry of Metal Cluster Complexes*; Shriver, D. F.; Kaesz, H. D.; Adams, R. D., Eds.; VCH: New York, **1990**; Chapter 2.

105. Bennett, M. A.; Matheson, T. W.; Roberston, G. W.; Smith, A. K.; Tucker, P. A. *Inorg. Chem.* **1980**, 19, 1014.

106. Baraga, D.; Grepioni, F.; Johnson, B. F. G.; Chen, H.; Lewis, J. *J. Chem. Soc., Dalton Trans.* **1991**, 1559.

107. (a) Kane-Maguire, L. A. P.; Honig, E. D.; Sweigart, D. A. *Chem. Rev.*, 84 (**1984**) 525. (b) Pauson, P. L. In *J. Falbe (ed), Methoden der organischen Chemie* (Houben-Weyl), Vol. E18, Georg Thieme, Stuttgart, **1986**, Ch. II.

108. (a) Djukic, J. P.; Roe-Munch, F.; Rose, E.; Simon, F. *Organometallics*, 14 (**1995**) 2027. (b) Sollidie-Cavallo, A.; *Polyhedron*, 4 (**1985**) 901.

109. Gomez-Sal, M. P.; Johnson, B. F. G.; Lewis, J.; Raithby, P. R.; Wright, A. H. *J. Chem. Soc., Chem. Commun.* **1985**, 1682.

110. Adams, R. D.; Wu, W. *Polyhedron* **1992**, 21,23.

111. (a) Gallop, M. A.; Johnson, B. F. G.; Lewis, J.; Wright, A. H. *J. Chem. Soc., Dalton Trans.*, **1989**, 481. (b) Edwards, A. J.; Gallop, M. A.; Johnson, B. F. G.; Kohler, J. U.; Lewis, J.; Raithby, P. R. *Angew. Chem.* 106, **1994**, 1166; *Angew. Chem., Int. Ed. Engl.*, 33, **1994**, 1093.

112. (a) Wadepohl, H. *Angew. Chem.*, 104, **1992**, 253; *Angew. Chem., Int. Ed. Engl.*, 31, **1992**, 247. (b) Wadepohl, H.; Buchner, K.; Herrmann, M.; Pritzkow, H. *Organometallics*, 10, **1991**, 861.

113. Wood, S. L. *Pathway to Ruthenium Arene nitrogen cluster* Dip. Sci. **1996**, Held in Department of Chemistry, Massey University, New Zealand.

114. (a) Adams, H.; Bailey, N. A.; Gay, S. R.; Gill, L. J.; Hamilton, T.; Morris, M. J. *J. Chem. Soc., Dalton Trans.*, **1996**, 2403-2407. (b) Hoferkamp, L. A.; Rheinwald, G.; Stoeckli-Evans, H.; Suss-Fink, G. *Organometallics* **1995**, 15, 1122-1127. (c) Bodensieck, U.; Stoeckli-Evans, H.; Suss-Fink, G. *Angew. Chem. Int. Ed. Engl.* 30 (**1991**) No. 9, 1126.

115. Gowex-Sal, P. P.; Johnson, B. F. G.; Lewis, J.; Raithby, P. R.; Wright, A. H. *Chem. Commun* (**1985**) 1682.

116. Sellmann, D.; Wemple, M. W.; Donaubauer, W.; Heinemann, F. W. *Inorg. Chem.* **1997**, 36, 1397-1402.

117. Sellmann, D. et al. *Inorg. Chim. Acta* 269, **1998**, 63-72.

118. Ho, E. N-. M.; Wong, W-. T. *J. Chem. Soc. Dalton Trans.* **1998**, 4215-4228.

119. Meister, G.; Rheinwald, G.; Stoeckli-Evans, H.; Suss-Fink, G. *J. Chem. Soc. Dalton Trans.* **1994**, 3215-3223.

120. (a) Nugent, W. A.; Mayer, J. M. *Metal-Ligand Multiple Bonds*; Wiley-Interscience: New York, **1988**. (b) Dobbs, D. A.; Bergman, R. G. *Inorg. Chem.* **1994**, 33, 5329. (c) Liang, H. –C.; Shapley, P. A. *Organometallics* **1996**, 15, 1331.